The Pennsylvania State University

The Graduate School

College of Engineering

EXAMINATION OF BIOELECTROCHEMICAL SYSTEMS WITH DIFFERENT CONFIGURATIONS FOR WASTEWATER TREATMENT

A Dissertation in

Environmental Engineering

by

Lijiao Ren

Submitted in Partial Fulfillment
of the Requirements
for the Degreee of

Doctor of Philosophy

May 2014

The dissertation of Lijiao Ren has been reviewed and approved* by the following:

Bruce E. Logan
Kappe Professor of Environmental Engineering
Evan Pugh Professor
Chair of committee
Dissertation Advisor

John M. Regan
Professor of Environmental Engineering

William D. Burgos
Professor of Environmental Engineering
Chair of Graduate Program

Li Li
Assistant Professor of Energy and Mineral Engineering

*Signatures are on file in the Graduate School

Abstract

Bioelectrochemical systems (BESs) are emerging technologies that use microorganisms to convert the chemical energy stored in biodegradable substrates, such as wastewater, to direct electrical current or energy storage chemicals. BESs have undergone tremendous development resulting in substantial advances in performance during the past decade, in terms of increases in energy output, feasibility of scaling-up the reactors, and reduction in system costs. However, optimization of system operation and the development of evaluation methods are needed to facilitate commercialization of BESs for wastewater treatment. The research findings reported here addressed several different aspects of BES operation and performance for wastewater treatment: examination of what factors affected power production of multi-electrode microbial fuel cells (MFCs) with hydraulic and electrical connections; investigation of how substrate competition between exoelectrogens and other microorganisms affected coulombic efficiencies (CEs) and chemical oxygen demand (COD) removals in MFCs; development of an energy-efficient, high-quality wastewater treatment system that combined MFCs with a secondary treatment system; and the use of a high-throughput screening method to evaluate chemical effects and wastewater treatability.

The power production of four hydraulically connected MFCs was compared with the reactors wired using individual electrical circuits to that obtained when the anodes and the cathodes were wired together. Based on the polarization tests, the same power was produced by the combined and individual circuit MFCs when operated in fed-batch mode. In continuous flow mode, where the acetate concentration significantly affected MFC performance, slightly lower power was produced by the MFCs containing the electrodes wired together compared to those with individual circuits. Parasitic current flow between adjacent MFCs showed no appreciable impact on reactor performance. These results demonstrated that the acetate concentration

differences had more of an effect on the performance of multi-electrode systems than parasitic current, and thus that there was no need for electrolyte isolation between adjacent reactors.

The competition for acetate through current generation by exoelectrogens and aerobic microbial respiration was examined in single-chamber air-cathode MFCs by measuring COD removals at different current densities. COD removal was always first-order with respect to COD concentration, even under open circuit conditions. As a result, the COD lost to non-exoelectrogenic processes was not constant over time, but instead decreased with COD concentration. With current generation, substrate was consumed at a faster rate, reducing the bulk COD concentration faster and therefore reducing the rate that COD was lost to aerobic respiration. Thus, the COD degradation rates and CEs improved with increases in current densities due to the greater substrate uptake by exoelectrogens. This demonstrated that exoelectrogens could outcompete aerobic heterotrophs for acetate at high current densities, resulting in increased COD removal rates and CEs that were achieved by operating the MFCs at lower resistances.

A two-stage laboratory-scale treatment process, consisting of multiple MFCs followed by an anaerobic fluidized bed membrane bioreactor (AFMBR), was examined for the treatment of domestic wastewater at ambient temperatures. Four multi-electrode MFCs were separated into two flow lines, with two MFCs connected hydraulically in series, avoiding large COD changes in each reactor that has been shown to adversely affect power generation. The MFC-AFMBR produced a high-quality effluent (COD, 16 mg/L; TSS, < 1mg/L), with no need for membrane cleaning even after 50 d of operation, at a high flux of 16 $L/m^2/h$. The energy produced by the MFCs (0.0197 kWh/m^3) was theoretically sufficient to meet the energy demands (0.0186 kWh/m^3) for the system operation. These results showed that a two-stage MFC-AFMBR system could be used to effectively treat domestic wastewater at ambient temperatures, with a low energy requirement.

Mini-microbial electrolysis cells (mini-MECs) were tested as a high-throughput method to examine the effects of different chemicals on current production and the treatability of different

wastewaters. Amorphous ferric hydroxide [$Fe(OH)_3$] addition increased current densities for both mixed cultures and pure culture of *Geobacter sulfurreducens* in a bicarbonate buffer. Scanning electron microscopic images and electrochemical tests showed that this improved performance resulted from formation of a highly porous structure on the cathode surface, which reduced the cathode overpotential and its diffusion resistance. Tween 80 did not increase the current in MECs, although it has previously been shown to improve power production in MFCs. The addition of DNA also did not improve MEC performance.

Various refinery wastewater samples, with appreciably different solution characteristics, resulted in large differences in current production and treatability in mini-MECs. All de-oiled wastewater samples showed good performance, with one sample producing results comparable to those obtained using domestic wastewater. The other refinery wastewater samples produced less current or even failed to generate any current, due to low biodegradability or high initial pH. The most successful approach for starting up MECs was pre-acclimation with domestic wastewater, as this improved electricity production, treatability, and reduced start-up time. These results showed the feasibility of using MECs as a treatment or pre-treatment method for certain types of refinery wastewaters.

Table of Contents

List of Figures

List of Tables

Acknowledgment

There are numerous people who have advised, mentored and helped me during the process of my PhD study, and I would like to gratefully acknowledge all of them. It is hard to imagine that I could finish this dissertation without any of you.

First and foremost, I want to recognize my advisor, Dr. Bruce Logan, for his continual guidance, instruction and patience. His generous support and mentorship, especially after my pregnancy, helped me immensely in my confidence and strength to complete my graduate career. His dedication to his students and perspective of the academic field will have a lasting impact on my life. I also wish to thank Dr. John Regan for his interest, support and inspirational passion on my study. Special thanks to my dissertation committee members Dr. Willam Burgos and Dr. Li Li for their time and advices on my research.

I am appreciative of all the lab mates in Bruce and John's lab for making my four year graduate study a more colorful journey. It has been my pleasure to work with all of you, my knowledgeable and friendly colleagues. I would specifically like to thank David Jones, Xiuping Zhu, Douglas Call, Matthew Yates and Yongtae Ahn for their help in my research projects.

The financial support of the Award KUS-I1-003-13 from the King Abdullah University of Science and Technology (KAUST) is gratefully acknowledged.

I am grateful for the brothers and sisters in State College Chinese Alliance Church. Their unconditional love and prayers have accompanied me through the highs and lows.

I would like to give my grateful thanks to my parents, Bing and Yabing. I could not step on the journey of my PhD education without the consistent support from you. The deepest gratitude is for my husband, the love of my life, Xing. None of the words in the world can express the importance of his understanding, compassion and support that have kept me moving forward. May our Lord Jesus Christ keep blessing our family and especially to our soon-to-be-born son.

Chapter 1

Introduction

1.1 Energy crisis and climate change

The current energy crisis facing the world is the gap between the enormous increase in energy demand, especially for liquid fuels, and the shrinking resources of fossil fuels. The world energy consumption increased by 46% in the past 40 years, from 4672 Mtoe (million tons of oil equivalent) in 1973 to 8677 Mtoe in 2010 (IEA 2012). This consumption will grow even faster by 56% between 2010 and 2040, as a result of the economic development and population growth (EIA 2013). Fossil fuels such as coal, oil and natural gas are the primary energy supply worldwide, accounting for more than 85% in the past decades and continuing to almost 80% of the world energy use through 2040 (EIA 2013). About half of the accessible oil supply had been used in 150 years since the beginning of the nineteenth century, while it took hundreds of millions of years for nature to build up this supply (Goodstein and Intriligator 2012). With increasing consumption, oil supplies are assumed to be depleted in 50 – 150 years (Lewis and Nocera 2006), and the other two forms of fossil fuels will be run out as well by the end of this century (Goodstein and Intriligator 2012). Improvements in energy efficiencies make it possible to slow down the growth of the consumption, but in the long term, a gap between the demand and the availability of fossil fuels will become unavoidable (Müller et al. 2013). The use of alternative energy resources is necessary to fill this gap, and for now, the fastest growing energy sources are renewables and nuclear power (EIA 2013).

Environmental problems associated with the use of fossil fuels have further stimulated the use of renewable and sustainable sources such as solar energy, wind, geothermal heat, tides, and biomass (Du and Eisenberg 2012). Since the beginning of the Industrial Revolution, emission of greenhouse gas, most notably carbon dioxide, has dramatically increased as a result of burning fossil fuels (Metz et al. 2007). The increased levels of these gases in the atmosphere have caused

and accelerated many of the observed climate changes, such as rising temperatures, rainfall pattern shifts, and more extreme climate events (EPA 2012). These changes can bring about disruptions in ecosystems by affecting plant and animal life cycles, populations, communities, and biodiversity. Thus, climate changes will also affect human society, such as residential settlements, farming, and businesses (EPA 2012, WDRs 2010). With these important environmental, economic, and social concerns, the future energy supply should come from green, sustainable, and efficient conversions of clean and renewable energy sources (Yang et al. 2012).

1.2 Sustainable wastewater treatment and wastewater energy nexus

Sustainable wastewater treatment has been an increasing issue over the past two decades since the first international conference "Ecological engineering for wastewater treatment", that addressed sustainable wastewater treatment systems focusing on resource recycling and energy aspects (Etnier and Guterstam 1991). Growing energy concerns, increasing environmental challenges, and diminishing important resources have heightened the urgency of this issue (Chung et al. 2008, Muga and Mihelcic 2008, O'Riordan et al. 2008). The concept of "sustainability" includes ecological, economic, and sociological aspects performing on local, regional, and global stages (Jenssen et al. 2007). Therefore, identifying sustainable solutions for wastewater treatment requires the simultaneous consideration of economic, ecological, and social goals (Balkema et al. 2002, Ching 2010, Foley et al. 2010, Guest et al. 2009). The primary goals for sustainable wastewater treatment processes are to reduce pollution discharge, increase nutrients recirculation, and optimize energy consumption (Long and Cudney 2012, Palme et al. 2005). Wastewater is now not only considered as a waste stream to be disposed of appropriately, but also as a source of valuable chemicals and energy (Cornel and Schaum 2009, McCarty et al. 2011, Verstraete and Vlaeminck 2011).

Substantial amounts of plant nutrients, such as nitrogen and phosphorus, are present in wastewaters from household and food processing industries (Jenssen and Skjelhaugen 1994).

Theoretically, the nutrients in domestic wastewater are nearly sufficient to fertilize crops to feed the world population (Jenssen and Skjelhaugen 1994). Recycling nutrients from wastewaters cannot replace mineral fertilizers entirely, but it can reduce pollution and simultaneously save excessive use of the chemical fertilizers (Jenssen et al. 2007). For example, more than 40% of the chemical fertilizers could, theoretically, be substituted with nutrients from wastewaters in most developing countries, while at least 15% substituted in developed countries (Gardner 1997). In terms of nutrient recirculation, mechanical or chemical precipitation of nitrogen and phosphorus, such as struvite, are proposed to be more economical and efficient (Jenssen et al. 2007). Due to the composition ($NH_4MgPO_4 \cdot 6H_2O$) and fertilizing properties of struvite, its precipitation from wastewater can reduce ammonia and phosphorus levels in the effluent, while simultaneously producing a valuable byproduct (Cornel and Schaum 2009). Controlled struvite recovery from wastewater is usually achieved by chemical base addition, carbon dioxide stripping, or water electrolysis. Recently, bioelectrochemical systems (BESs), such as microbial fuel cells (MFCs) and microbial electrolysis cells (MECs), have been explored for struvite recovery with less energy and chemical consumptions (Cusick and Logan 2012, Ichihashi and Hirooka 2012, Kuntke et al. 2012).

Wastewater should be considered not only as a source of nutrients, but also as organic constituents, which is a potential energy source. Sustainable wastewater treatment requires the application of more energy-conscious choices in the construction of new facilities, and the maintenance or upgrade of existing plants (Long and Cudney 2012). Wastewater facilities are among the largest energy-intensive systems, accounting for approximately 30 – 50% of the municipal energy use (McCarty et al. 2011). Treatment of wastewater currently consumes about 3% of the electrical power produced in the United States (McCarty et al. 2011), while in the United Kingdom, 3 – 5% of the national electricity consumption goes for wastewater treatment (Oh et al. 2010). A considerable energy reduction potential (20 – 50%) has been demonstrated in existing plants, through process optimization and the use of innovative energy-efficient

technologies (Lazarova et al. 2012, Lindtner et al. 2008, Wett et al. 2007). Moreover, there is substantial energy potential in the organic matter in wastewater. For example, domestic, industrial, and animal wastewaters together present an energy power of ~17 GW, theoretically sufficient for the current consumption ~15 GW by wastewater treatment (Logan 2004, Logan and Rabaey 2012). Energy self-sufficiency for wastewater treatment is a feasible goal, if part of this energy currently wasted or lost in the treatment processes could be captured using cost-effective, reliable, easy to operate, and environmental-friendly techniques (Lazarova et al. 2012). A few methods have been established to recover energy from wastewater treatment processes, including thermochemical, physicochemical, and biochemical processes (Appels et al. 2011). Sludge combustion, gasification, and pyrolysis to generate heat or combined heat and power (CHP) are mostly deployed in European counties (Oh et al. 2010). Biofuels and hydrogen from fermentation, and methane from anaerobic digestion can be used for energy generation through combustion (Juang et al. 2011, Ren et al. 2011). Recent evolving examples of bioenergy recovery include hydrogen production and electricity harvesting using BESs (Logan et al. 2006, Wang et al. 2012).

1.3 Bioenergy production from wastewater

Biochemical conversion processes are more economical and advantageous to recover energy from waste biomass sources containing high water levels (>40%), such as wastewaters, compared to the physicochemical and thermochemical processes (Ward et al. 2008). Methane production from anaerobic digestions, biohydrogen production by fermentation, and electricity or biogas (hydrogen or methane) productions in BESs are the primary biochemical processes for energy harvesting from wastewaters.

Methanogenic anaerobic digestion is a traditional bioconversion process that has been used for over a century and widely applied in full-scale facilities (Appels et al. 2011, Bouallagui et al. 2005, Pavan et al. 2000, Zhang et al. 2005). Four steps, hydrolysis, acidification, acetogenesis, and methanogenesis, take place in an anaerobic digester to convert the complex organic matter in

the wastewater into the main end products of methane and carbon dioxide. In hydrolysis step, complex organic matter is converted into smaller molecules that are soluble in water. During acidification, these hydrolyzed products are converted into simple molecules such as volatile fatty acids. The products of the acidification are converted into acetic acids, hydrogen, and carbon dioxide during acetogenesis. Finally, fermentation products (the combination of hydrolysis, acidification, and acetogenesis) are converted into methane and carbon dioxide (Stafford et al. 1980). This multi-step, microbial methanogenic process requires complicated system designs and strict process control to achieve an optimum performance for high methane production (Buffiere et al. 2008, Schnurer et al. 1999). In terms of system configurations, there are one-stage and two-stage anaerobic digestion processes (Li and Yu 2011). Substrates are converted into methane through the four steps in a single reactor in the one-stage process (Sterling et al. 2001). In comparison, the two-stage process separates the fermentation and the methanogenesis into two sequentially connected reactors that may have different operational conditions, such as temperature and retention times (Demirer and Chen 2005). Two temperature ranges are usually used for the anaerobic digestion: mesophilic (95 – 98 ^{o}F, 35 – 37 ^{o}C) and thermophilic (122 – 135 ^{o}F, 50 – 57 ^{o}C). Mesophilic temperatures are more prevalent as they require less energy and put less stress on the concrete tanks (WEF). Various types of waste biomass are suitable for anaerobic digestion, from solid wastes, such as agricultural waste and sewage sludge (Appels et al. 2011), to wastewaters including dairy, food processing, palm oil mill, and acid whey wastewater (Li and Yu 2011).

Hydrogen has been considered as a more desirable energy carrier than methane due to its higher energy content (Lee et al. 2010). Biological hydrogen production represents a renewable, more sustainable, and cost-effective option, compared with other chemical hydrogen production processes (Brentner et al. 2010). There are four different biohydrogen production mechanisms: biophotolysis, indirect biophotolysis, photofermentation, and dark fermentation (Das and Veziroglu 2008). However, hydrogen can only be produced from waste biomass using dark

fermentation and photofermentation. In dark fermentation, microorganisms anaerobically break down complex substrates into volatile fatty acids and alcohols, releasing hydrogen and carbon dioxide (Brentner et al. 2010), through the first three steps (hydrolysis, acidification, and acetogenesis) in methanogenic anaerobic digestion. The smaller organic acids produced from hydrolysis and acidification can be utilized by photoheterotrophs under anaerobic conditions to produce hydrogen and carbon dioxide in photofermentation (Brentner et al. 2010). Methanogenic hydrogen consumers must be eliminated from the system in order to produce hydrogen gas in bulk, which can be achieved in suspended growth reactors by using a shorter retention time (Chen et al. 2002, Chong et al. 2009). These two mechanisms can be used independently in a one-stage hydrogen production system. Dark fermentation has higher (2 – 4 orders of magnitude) production rates than photofermentation, but a lower substrate conversion efficiency. Photofermentation outperforms the dark fermentation in substrate conversion efficiency and waste stream qualities as the organic compounds are fully converted to hydrogen and carbon dioxide (Brentner et al. 2010). A two-stage dark and photofermentation system has thus been developed to increase hydrogen yield and substrate conversion efficiency, as well to reduce the organic concentrations in the effluent (Chen et al. 2008, Tao et al. 2007). The waste biomass materials that can be potential sources for the biohydrogen generation are similar to those used for methanogenic anaerobic digestion, such as food waste, dairy waste, palm oil mill effluent, and molasses (Chong et al. 2009, Ren et al. 2011). Although the biohydrogen production process has been advanced significantly over the past two decades by identifying efficient microorganisms, developing new bioreactors, and optimizing system operations, this biotechnology has not yet to be utilized on a scale large enough to replace fossil fuels.

Bioelectrochemical systems (BESs) are emerging bioconversion technologies to produce energy from wastewaters, which have only been intensively studied and advanced in the past decade (Wang et al. 2013). BESs use microorganisms to oxidize biodegradable substrates, such as waste biomass, and convert the chemical energy stored in these fuels to direct electrical current or

energy storage chemicals like hydrogen and methane (Logan 2008). The strength of BESs is that the bioenergy conversion can take place at lower substrate concentrations and under a wide range of temperatures, compared to the anaerobic digestion that requires more concentrated waste streams (>3 kg/m^3 organic matter) and high temperatures (>30 ^oC) to be economical (Pham et al. 2006). These merits also make BESs a better option to replace the current energy-intensive aerobic biological wastewater treatment processes, such as the activated sludge (Logan and Rabaey 2012). As a nascent platform, BESs face many opportunities and challenges to overcome the limitations of low energy output and high system costs for successful applications, which can be achieved by increasing research efforts as done for other incipient techniques.

1.4 Introduction to bioelectrochemical systems (BESs)

In a bioelectrochemical system (BES), organic matter is oxidized by microorganisms using the anode as an electron acceptor, with electrons transferred through an external circuit to the cathode for final reduction of various chemical species. BESs associate the production of current with microbial catabolism, which open up a multidisciplinary field integrating microbiology, electrochemistry and engineering (Logan 2012, Wang et al. 2013).

The first report of electrical current generation by bacteria was over one hundred years ago in 1911 by Potter (Potter 1911), but very few developments were achieved until the end of the twentieth century (Allen and Bennetto 1993, Lewis 1966). With the recognition of mediator-less BESs in 1999 (Kim et al. 1999a, Kim et al. 1999b), research interests in this field have blossomed, mostly in increasing power generation of microbial fuel cells (MFCs) (Logan 2012). Most recently, the BESs have been developed with a great variety of functions, such as microbial electrolysis cells (MECs) and microbial electrosynthesis (MES) for chemical production, microbial desalination cells (MDCs) for water desalination, and microbial reverse electrodialysis cells (MRCs) that can be used to increase voltage and power output (Harnisch and Schroder 2010,

Logan and Rabaey 2012, Pant et al. 2012, Wang et al. 2013). Here, I focus on the two most basic types of BESs: MFCs with power generation and MECs with hydrogen production.

MFCs and MECs share the common principle that in the anode chamber, a biofilm oxidizes the organic substrate anaerobically to produce electrons, protons, and carbon dioxides (Fig. 1-1). The electrons are donated by the biofilm to the anode, and then travel through an external electric circuit to the cathode with the generation of electrical current. The protons are released into the aqueous solution. Charged ions migrate between the anode region and the cathode region to balance the negative change of the electrons. The electrons and protons are subsequently used by the cathode in the reduction of the final electron acceptors (Logan and Regan 2006b, Zhou et al. 2013). Exoelectrogens, being the functional group on the bioanodes of BESs, are microorganisms that are capable of generating and transferring electrons outside the cell membrane (Logan and Regan 2006a). A wide range of microorganisms have been shown to be able to transfer electrons exocellularly to or from the electrodes (Logan 2009, Logan and Regan 2006a, Logan and Regan 2006b, Zhou et al. 2013). Only the strains, those can generate substantial current without exogenous electron mediators, are considered as exoelectrogens of primary interest today (Logan 2012).

The major differences between MFCs and MECs are the cathode configurations and reduction reactions. In MFCs, oxygen is usually reduced on the cathode using the electrons and protons to form water (Fig. 1-1a). Other terminal electron acceptors have also been used, such as ferricyanide, permanganate, and nitrate (Logan 2008, Logan et al. 2006). In contrast, the cathode chamber of an MEC is kept anaerobic by omitting the aforementioned electron acceptors. With the supply of an additional voltage (>0.25 V), protons are reduced on the cathode to produce hydrogen gas (Fig. 1-1b) (Call and Logan 2008, Logan 2008). Although the coupled redox reaction in MECs is thermodynamically unfavorable, less power is needed for this process than in water electrolysis that in practice requires an applied voltage of >1.8 V. The lower power requirement of MECs is due to the fact that bacterial electrolysis of organic matter is exothermic,

providing part of the energy needed to form hydrogen gas (Logan et al. 2008, Logan and Regan 2006a, Zhou et al. 2013).

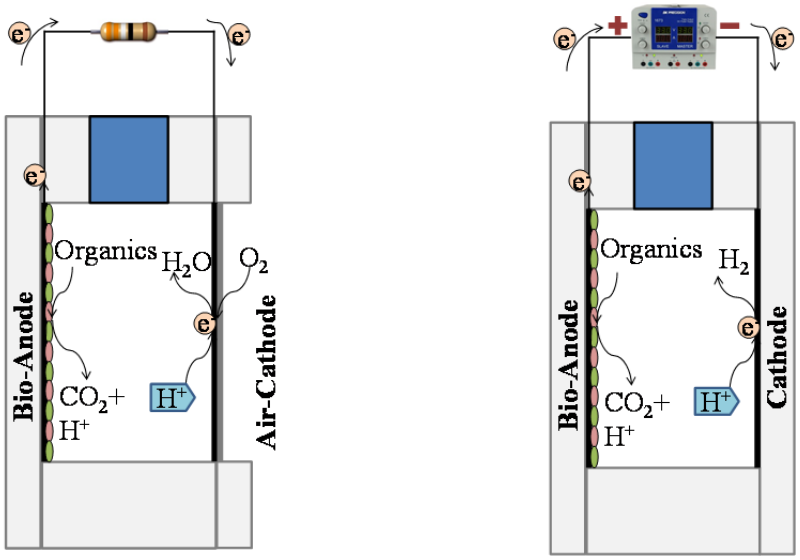

(a) Single-chamber air-cathode MFC (b) Single-chamber hydrogen evolution MEC

Figure 1-1 Schematics of microbial fuel cell (MFC) and microbial electrolysis cell (MEC).

A series of measures have been established for the characterization and evaluation of the MFCs and MECs. The electrode packing density (surface area of the electrode per volume of reactor) is one of the most important factors for a new design, besides the reactor configuration and electrode materials. The cell voltage of an MFC is the potential difference between the cathode and the anode, which is measured using a multimeter (Bard and Faulkner 2001). Current is calculated using Ohm's law ($I = U/R$; A), and power is calculated as $P = IU$ (W), where U is the measured voltage (V), and R the external resistance (Ω) (Hong et al. 2011). Current densities and power densities are used to compare electricity production of different systems. Current densities are usually normalized to the projected area of an electrode or the membrane, while power densities are reported in two characteristics of the reactor, per projected area and per total volume (Logan 2008, Logan 2012, Logan et al. 2006). A power curve describes the power (density) as the function of the current (density). The power increases with current from the open circuit point to a maximum power point, and then drops due to the increasing ohmic losses and electrode overpotentials (Logan et al. 2006). Coulombic efficiency (CE), defined as the ratio of

the total coulombs recovered as electrical current to that available in the substrate removal (Logan 2008), is used to evaluate the substrate conversion efficiency. In terms of wastewater treatment, the removal of chemical oxygen demand (COD) is a common measure, although biochemical oxygen demand (BOD) is also used. The COD removal efficiency is calculated as the ratio between the removed and the influent CODs (Logan et al. 2006).

Most of these electrical and chemical measures can be applied in the evaluation of MECs, such as the current (density), coulombic efficiency, and COD removal. The applied voltage, hydrogen yield, and hydrogen production rate are the additional metrics used to describe the operation and performance of MECs (Logan et al. 2008). The hydrogen yield (Y; kg-H_2/kg-COD) is the ratio of the total mass of hydrogen produced to that of the substrate consumed (Call and Logan 2008, Logan et al. 2008). The hydrogen production rate (Q; m^3-H_2/m^3/d) is calculated as the volume of hydrogen produced per reactor volume per day (Tenca et al. 2013), with the maximum hydrogen production rate (Q_{max}) directly proportional to the current (Call and Logan 2008, Logan et al. 2008).

With the exponentially increasing number of studies in the past decade, the performance of BESs has been advanced tremendously, in terms of energy output, substrate conversion efficiency, and construction costs. However, optimizations in system operations and developments in evaluation methods are needed to speed up the commercialization of these processes for wastewater treatment.

1.5 Dissertation objectives and outline

My PhD dissertation focuses on understanding of the operational factors affecting system performance, developing an energy-efficient high-quality wastewater treatment system, and evaluating of a high-throughput screening method, based on different BES configurations. The objectives of this dissertation were:

1. Examine the factors affecting power production of multi-electrode MFCs with hydraulic and electrical connections in both fed-batch and continuous flow conditions.
2. Characterize the substrate competition between exoelectrogens and other microorganisms which affects the CEs and COD removals of MFCs.
3. Develop a high-efficient and low-energy-cost wastewater treatment system by combining MFCs with anaerobic fluidized bed membrane bioreactor (AFMBR).
4. Evaluate the effects of different chemicals on current generation and the treatability of various wastewater sources using high-throughput mini-MECs.

The dissertation contains five chapters that addressed the stated objectives following the introduction (**Chapter 1**) and literature review (**Chapter 2**), with a final chapter on future work (**Chapter 8**).

Chapter 3 presents the comparisons of the power production of four hydraulically connected MFCs with individual electrical circuits and when the anodes and the cathodes were wired together, in both fed-batch operations and continuous flow conditions. This work was summarized in a paper by Ren, L. J., Ahn, Y., Hou, H. J., Zhang, F., and Logan, B. E., titled "Electrochemical study of multi-electrode microbial fuel cells under fed-batch and continuous flow conditions", and it was accepted for publication in the *Journal of Power Sources*. Dr. Yongtae Ahn helped with the design of the reactors, and Dr. Huijie Hou and Dr. Fang Zhang gave me useful suggestions on data analysis. I performed all the experiments, analyzed all the results, and prepared the first draft of the manuscript. All the co-authors contributed to the revision of the paper.

Chapter 4 presents an examination of the competition for substrate through current generation by exoelectrogens with microbial aerobic respiration in single-chamber, air-cathode MFCs, and its effect on the CEs and COD removal rates. This work was summarized in a paper by Ren, L. J., Zhang, X. Y., He, W. H., and Logan, B. E., titled "High current densities enable

exoelectrogens to outcompete aerobic heterotrophs for substrate", that has been submitted for publication. Dr. Xiaoyuan Zhang and Mr. Weihua He provided some useful suggestions for the experiments. I performed all the experiments, analyzed all the results, and prepared the first draft of the manuscript. All the co-authors contributed to the revisions of the paper.

Chapter 5 presents the investigation of the treatment efficiencies, energy balance, and membrane fouling of a two-stage MFC-AFMBR system, treating domestic wastewater at ambient temperatures. This work was summarized in a paper by Ren, L. J., Ahn, Y., and Logan, B. E., titled "Domestic wastewater treatment with a two-stage microbial fuel cell and anaerobic fluidized bed membrane bioreactor (MFC-AFMBR) system", that has been submitted for publication. Dr. Yongtae Ahn helped with the design and assembly of the membrane module. I performed all the experiments, analyzed all the results, and prepared the first draft of the manuscript. All the co-authors contributed to the revision of the paper.

Chapter 6 presents the examination of the effects of amorphous ferric hydroxide, Tween 80, and DNA on current production for both mixed cultures and a pure culture of *Geobacter sulfurreducens*, using high-throughput mini-MECs. This work was published as a paper by Ren, L. J., Tokash, J. C., Regan, J. M., and Logan, B. E., titled "Current generation in microbial electrolysis cells with addition of amorphous ferric hydroxide, Tween 80, or DNA", in the *International Journal of Hydrogen Energy*. Dr. Justin C. Tokash helped with analyzing the cyclic voltammetry (CV) and electrochemical impedance spectroscopy (EIS) data. I performed all the experiments, analyzed all the results including those of CV and EIS, and prepared the first draft of the manuscript. All the co-authors contributed to the revision of the paper.

Chapter 7 presents the evaluation of the treatability of many different refinery wastewater samples all having appreciably different characteristics, using high-throughput mini-MECs. This work was published as a paper by Ren, L. J., Siegert, M., Ivanov, I., Pisciotta, J. M., and Logan, B. E., titled "Treatability studies on different refinery wastewater samples using high-throughput microbial electrolysis cells (MECs)", in the *Bioresource Technology*. Dr. John M. Pisciotta

helped with the assembly of the reactors. Dr. Michael Siegert and Dr. Ivan Ivanov helped to maintain the reactors. I performed the main experiments including reactor assembly and maintenance, analyzed all the results, and prepared the first draft of the manuscript. All the co-authors contributed to the revision of the paper.

Chapter 2

Literature Review

2.1 BESs for bioenergy production and wastewater treatment

Bioelectrochemical systems (BESs) can extract bioenergy from various types of organic matter, ranging from simple compounds, such as acetate, to complex biomass wastes. The substrate is one of the most important biological factors affecting bioenergy production and organic removals in BESs (Liu et al. 2009). In general, the bioenergy production potential of BESs depends on the chemical characteristics and concentrations of the components that can be used as fuels (Angenent and Wrenn 2008). For example, MFCs will produce higher maximum power densities using simple substrates that are readily biodegradable and at high concentrations, compared to those with a complex composition and at low concentrations. In single-chamber air-cathode MFCs, 506 mW/m^2 was produced with 800 mg/L acetate, and 305 mW/m^2 with 1000 mg/L butyrate (Liu et al. 2005). In similar reactors, only 261 mW/m^2 was produced using swine wastewater at a concentration of 4470 mg/L COD (Min et al. 2005), and 146 mW/m^2 was generated using domestic wastewater (200 – 300 mg/L COD) (Liu and Logan 2004).

BESs are promising and attractive bioenergy production techniques because they can utilize biomass in wastewaters, which is otherwise wasted (Zhou et al. 2013). BESs have several advantages for bioenergy production and simultaneous wastewater treatment compared to traditional techniques. First, BESs can potentially be more economical than aerobic biological wastewater treatment processes, as they are able to convert the biomass in low strength wastewater (<3 kg/L organic matter per m^3) to bioenergy at a relatively good energy efficiency (Logan and Rabaey 2012). Second, the use of an anode as the electron acceptor in BESs, coupled to the passive oxygen transfer in MFCs or hydrogen production in MECs, can avoid energy intensive processes such as aeration to provide dissolved oxygen in activated sludge wastewater treatment processes (Cusick et al. 2010). Aeration is the predominant energy consuming process

in a wastewater treatment plant (30 – 55% of the total treatment energy demand) (Oh et al. 2010). In addition, the lower sludge production in BESs compared with aerobic treatment could further reduce the costs and challenges associated with sludge handling and treatment (Rabaey and Verstraete 2005). Therefore, using BESs to treat wastewater and recover energy from low-degrade biomass could achieve significant energy savings and meet the concept of sustainable wastewater treatment.

2.1.1 Electricity production by MFCs

In the past decade, numerous studies have been reported on increasing power output and organic removals in MFCs used for wastewater treatment, by exploring promising wastewater sources, optimizing reactor configurations, and developing new electrodes with improved surface properties. Many types of wastewaters have been used as substrates in MFCs for electricity generation, and a comprehensive list has been provided in a previous review (Pant et al. 2010). Most recent studies have been focused on the treatment of recalcitrant compounds such as azo dyes (Murali et al. 2013), nutrient removal and recovery (Haddadi et al. 2013, Yan and Regan 2013, Zhu et al. 2013a), and *in situ* remediation (Sajana et al. 2013).

In terms of electricity production, the most promising substrates are domestic, brewery, and food processing wastewaters (Pant et al. 2010). Brewery wastewater is a suitable substrate in MFCs as the organic matter components are derived from food with low concentrations of inhibitors, such as ammonia in animal wastewaters (Feng et al. 2008). The moderate strength of brewery wastewater, with a typical COD concentration in the range of 3000 – 5000 mg/L, has made it more favorable than many other types of wastewaters (Vijayaraghavan et al. 2006). Food processing wastewater is an energy-rich resource, due to the simple chemical composition and relatively high concentrations of carbohydrates (2300 – 3500 mg/L) (Jin et al. 1998, Lu et al. 2009). Domestic wastewater has been shown repeatedly to be a good substrate for power production in MFCs, with good organics removals. Therefore, this type of wastewater has been

used as a typical complex substrate to examine the performance of an MFC with a new reactor configuration or electrode design, or as a positive control to evaluate the treatability of other wastewater sources.

Single-chamber membrane-less MFCs with high surface area electrodes tightly packed together are favored for wastewater treatment to maximize power densities, by allowing an adequate interactions between microorganisms and the wastewater (He et al. 2005, Logan and Rabaey 2012). Using swine wastewater, a much higher maximum power density of 261 mW/m^2 was produced by a single-chamber air-cathode MFC than the 45 mW/m^2 produced using a H-shaped two-chamber MFC with an aqueous cathode, as a result of the decreased internal resistance of the single-chamber system (Min et al. 2005). In a single-chamber, air-cathode MFC used to treat domestic wastewater, 28 mW/m^2 was produced with a polymeric cation exchange membrane (CEM) bonded directly onto the solution side of the cathode, while 146 mW/m^2 was obtained when the CEM was removed, due to the increased cathode potential (Liu and Logan 2004). Although the coulombic efficiency (CE) decreased from 28% to 20% without the CEM, this would not be disadvantageous from the perspective of energy production from wastewater, as the primary goals are power output and removal efficiencies of organic matter. Performance was compared between two different MFC configurations, a separator electrode assembly (SEA) and a spaced electrode (SPA), in smaller laboratory scale (14 mL) and larger bench scale (130 mL) reactors treating domestic wastewater (Ahn et al. 2014, Zhang et al. 2014). The SEA MFCs showed higher maximum power densities (14 mL, 360 mW/m^2 versus 310 mW/m^2; and 130 mL, 328 mW/m^2 versus 282 mW/m^2) and CEs (14 mL, 30 – 49% versus 17 – 34%; and 130 mL, 9 – 31% versus 2 – 23%), but slower organics removals (Ahn et al. 2014, Zhang et al. 2014). The increased power density was due to the decreased internal resistance obtained using the SEA configuration, as a result of minimized electrode spacing. The higher CEs and slower removals in SEA MFCs were achieved by the separators reducing oxygen intrusion. Therefore, trade-offs need to be made between energy capture and treatment efficiency before choosing the optimal

configuration. However, all these tests were conducted in fed-batch conditions, and thus more studies are needed to make these comparisons in continuous flow conditions. The results obtained in continuous flow tests could provide more insight to optimize the reactor configuration for wastewater treatment, as our goal should be using MFCs to treat wastewater continuously.

Improvements in electrode materials, configurations and surface characteristics can also increase electricity generation in MFCs treating domestic wastewater. Packing granular activated carbon in an anode chamber produced 127 mW/m^2 (5 W/m^3) in a single-chamber cylindrical MFC with an air-cathode (Jiang and Li 2009). In comparison, 146 mW/m^2 (7.3 W/m^3) was obtained using a carbon paper anode in a single-chamber air-cathode MFC (Liu and Logan 2004). A higher power density of 334 mW/m^2 (16.7 W/m^3) was produced in an air-cathode MFC with a similar configuration by using carbon brush anode (Ahn and Logan 2010). In the SEA configuration, the use of brush anodes produced a higher maximum power density of 240 mW/m^2 than carbon mesh anodes (<45 mW/m^2), and a higher COD removal (80% versus 58%), with similar CEs (Hays et al. 2011). Anode surface modifications, including ammonia gas treatment, heat treatment, carbon nanotube coating, and neutral red coating, increased the power densities of MFCs , to an extent that depended on the specific reactor configurations (Cheng and Logan 2007, Feng et al. 2010, Tsai et al. 2009, Wang et al. 2011d).

The use of inexpensive electrode materials is crucial for the commercialization of MFCs, as this will enable cost-effective systems at larger scales. The use of activated carbon as a replacement for the platinum catalyst in a cathode, stainless steel mesh instead of carbon cloth, and an inexpensive poly(dimethylsiloxane) (PDMS) coating as the diffusion layer on the air-cathode can substantially reduce costs, as the air-cathode materials account for 47% of the MFC capital costs (Zhang et al. 2009). The use of a separator on the solution side of an air-cathode showed benefits to performance by slowing down cathode degradation due to fouling by its direct exposure to the wastewater (Zhang et al. 2014). Biocathodes, mainly composed of carbon-based materials with no inorganic oxygen reduction catalyst, have the advantages of relatively low cost

and multiple functions for wastewater treatment (Wei et al. 2011). However, the performance and stability of biocathodes require further improvements to be practical for wastewater applications (Xia et al. 2013).

2.1.2 Hydrogen and methane production by MECs

MEC and MFC systems share many similar features, and thus most methods to increase electricity production in MFCs can be used to increase hydrogen generation in MECs. For example, a maximum hydrogen yield of 0.0125 mg-H_2/mg-COD (applied voltage of 0.5 V) was obtained in a two-chamber MEC fed domestic wastewater with packed graphite granules anode (Ditzig et al. 2007). When the domestic wastewater from the same source was tested in a single-chamber MEC with a carbon brush anode, the hydrogen yield increased to 0.05 kg-H_2/kg-COD (applied voltage of 0.9 V) with a higher CE of 64% (compared to 26%) (Lalaurette et al. 2009). This improvement was partly due to better anode performance and improved reactor configurations, but also to the higher applied voltage. In general, the performance of MECs, such as current density and hydrogen recovery, will increase with the applied voltage, in the range of 0.2 – 1.0 V (Logan et al. 2008).

Wastewater characteristics also have significant effects on the performance of MECs. Appreciable differences in biogas production and COD removals were observed with two wastewater sources that had large differences in composition: a food processing wastewater, with high concentrations of complex carbohydrates; and a chemical manufacturing wastewater, that had a lower concentration of biodegradable organic matter and a high concentration of methanol. The chemical manufacturing wastewater had higher biogas production and COD removals than the food processing wastewater, resulting in a positive energy recovery, but there was a net energy input for the food processing wastewater (Tenca et al. 2013).

The major differences between MEC and MFC systems, such as the cathode reactions, require additional studies targeted specially at improving the performance or lowering the costs of

MECs. In MECs, the hydrogen evolution reaction takes place on the cathode, instead of the oxygen reduction in MFCs, leading to the exploration of different cathode materials. Although platinum showed a superior catalytic effect for both the oxygen reduction and hydrogen evolution reactions, different alternative catalysts have been used for MFCs and MECs. Activated carbon is a promising cathode catalyst in MFCs, whereas metals and their alloys have been proposed for MECs, such as stainless steel (SS), molybdenum disulfide (MoS_2), and nickel (Selembo et al. 2009, Tokash and Logan 2011). MoS_2 cathodes were shown to perform better than SS cathodes using both food processing and chemical manufacturing wastewaters, in terms of biogas production, current density, and COD removals (Tenca et al. 2013).

Methane production in MECs has usually been taken as a nuisance that needs to be eliminated or inhibited due to the higher specific energy content of hydrogen (Wagner et al. 2009, Wang et al. 2009). However, methane is also an energy source and thus might not be problematic in terms of recovering energy from wastewaters. Electrochemical production of just methane at the cathode of a MEC is being considered as an attractive option to hydrogen gas production as a biofuel (Pant et al. 2012). It was shown that methane could be produced at an overall energy efficiency of 80% in MECs by a process called electromethanogenesis, using a biocathode to reduce carbon dioxide at an applied cell voltage of >0.8 V (Cheng et al. 2009). Future research in this area should test the feasibility of this process using complex organic matter as the substrate for the anode, instead of acetate, to evaluate its efficiency for energy recovery from wastewater through methane production in comparison with the hydrogen producing MECs.

2.1.3 Comparison between MFCs and MECs

Few studies have made side-by-side comparisons of MFCs and MECs in terms of treatment efficiencies or energy recoveries. Organic removals were shown to be higher in MFCs, while higher CEs and current densities were obtained in MECs fed winery or domestic wastewater (Cusick et al. 2010). Oxygen leakage through the air-cathode was shown to be responsible for the

higher COD removals and lower CEs in MFCs, compared to the anaerobic cathode used in MECs that avoids oxygen intrusion. In terms of values of the different energy products in MFCs and MECs, different wastewater sources showed different results, although the energy recoveries were higher for MFCs with both wastewaters. For winery wastewater, the MFCs were found to be more economical than the MECs as the overall value obtained was $0.10/kg-COD, compared to $0.06/kg-COD for the MECs. In contrast, MECs were found to be more economical for domestic wastewater treatment, due to the higher value of $0.19/kg-COD (Cusick et al. 2010). This finding indicated that MFCs are superior for organic removals compared to MECs, but detailed evaluations are needed to decide which type of BESs is more beneficial for a specific wastewater source.

Comparisons of the developments of MFCs and MECs have shown that MFCs still need to be improved considerably to be economical for practical applications. Improvements are suggested to be made by decreasing internal resistances and through the production of high-value products. MECs have been found to be closer for real applications than MFCs due to the higher product revenue of the gas produced (Sleutels et al. 2012). However, this analysis was based on the internal resistances and current densities produced mostly in acetate-fed systems, which might not be applicable to actual wastewaters.

In practical application of the BESs for wastewater treatment and energy recovery, large scale reactors should be operated in continuous flow conditions. In terms of scale-up, MECs may be more advantageous than MFCs, as the completely sealed system configuration avoids the need for exposing the cathode to air. An MEC reactor can be designed by simply placing the anodes and cathodes appropriately in any commercially available large scale anaerobic reactors or even a tightly sealed tank. Oxygen reducing cathodes are always the most difficult component to design for larger scale MFCs. Air-cathodes with passive oxygen transfer are favorable for MFC design from the perspective of energy requirements and chemical consumption. However, improvements

in materials and manufacturing processes are important to make large air-cathodes strong, stable, and watertight.

2.2 Scaling-up BESs

The design of BESs have advanced impressively in the past decade, from the original H-shaped bottles made of expensive materials with low performance, to scalable cost-effective designs with higher energy output. Most of the progress, including the improved current densities, the use of non-precious metal electrode materials, and compact configurations, has been addressed in laboratory studies (Logan 2010). However, studies of larger scale BESs are needed before any practical applications are possible (Ter Heijne et al. 2011). Larger systems, on the scale of liters or more, will be useful for a better understanding of the factors affecting volumetric power densities, such as reactor architecture, electrode packing density, and electrode spacing (Cheng and Logan 2011). Pilot studies at the cubic meter scale are needed to evaluate the performance of the materials at larger scales, and these devices need to be operated over time to understand variations in operational conditions on performance, such as wastewater composition, environmental temperature, and maintenance requirements (Logan 2010).

In order to enlarge the reactor capacity of BESs, three approaches (or their combination) are usually explored. The first, and the most simple way, is to increase the electrode and reactor sizes (i.e. larger electrodes in larger tanks) to build larger systems up to several liters in volume (Li et al. 2008, Liu et al. 2008). Second is the use of many smaller BES units hydraulically-coupled or constructed in stacks to achieve a larger total capacity (Ieropoulos et al. 2008, Ledezma et al. 2012). Finally, multiple small electrodes can be aligned in a reactor with increased size (i.e. several electrodes in larger tanks) (Ahn and Logan 2012, Rader and Logan 2010). These approaches each have their advantages and limitations, depending on the purpose of the tests and operational conditions. Reactors at liter scale can be built using any one of the three approaches, while the pilot scale systems need to exploit a combination of them.

2.2.1 Larger Systems

Studies on scaling up MFCs by increasing electrode and reactor sizes have shown the importance of increasing electrode packing density to improve volumetric power production. It has been shown that power (16 W/m^3) produced in a larger MFC (LMFC, 520 mL) seemed to be consistent with power generated (14 W/m^3) in a smaller one (SMFC, 28 mL) as long as the cathode packing density was relatively unchanged (31 m^2/m^3 in the LMFC compared to 25 m^2/m^3 in the SMFC) (Liu et al. 2008). However, not all the construction factors were the same. Compared to the SMFC, the LMFC had smaller average electrode spacing (2.6 cm versus 4.0 cm), higher anode packing density (150 m^2/m^3 versus 25 m^2/m^3) (Liu et al. 2008). Further increases in the anode surface area were shown to be relatively insignificant for boosting power production. Therefore, it was proposed that the cathode surface area limited the power production. This hypothesis was verified by showing that the volumetric power density increased as a function of cathode packing density using a series of single-chamber, air-cathode MFCs with different sized cathodes (Cheng and Logan 2011). When the packing density was increased for both the anode and cathode, even higher volumetric power could be produced. A 1.5 L MFC produced 2.0 W/m^3, which was almost four times higher than the 0.58 W/m^3 produced by a 0.45 L smaller system, and the electrode packing density (21 m^2/m^3) of the former was also four times higher than that (5.6 m^2/m^3) of the later. In these two systems, there was comparable power densities per electrode surface area (94 mW/m^2 in the larger versus 104 mW/m^2 in the smaller) (Li et al. 2008). It seems that power could be improved by increasing the electrode packing density as long as the power density per electrode surface area was not significantly altered. However, power density normalized to the electrode of interest (either anodes or cathodes) has been shown to decrease with an increase in electrode surface area (Dewan et al. 2008). Therefore, power will increase more and more slowly as the electrode area increases, even becoming constant when the electrode gets large enough (Oh and Logan 2006). As a result, it is currently not possible to build very large

pilot-scale BESs with the same performance as the smaller ones by simply enlarging the electrode and reactor sizes.

A series of liter-scale, tubular-shaped MFCs were tested for continuous domestic wastewater treatment. However, the volumetric power produced in these systems was relatively small even with high cathode packing densities, due to the dramatic decrease in power densities as the surface area of the cathodes increased. Cathode surface area was assumed to limit the power production as carbon brushes were used as the anodes in these MFCs, which had very high surface areas (130 m^2 surface area based on fibers/m^2 projected surface area) (Ahn and Logan 2012). These tubular MFC reactors were all constructed by wrapping a whole piece of carbon cloth on a membrane tube that served as the cathode, and placing the membrane cathode outside a large brush anode and inside a PVC-tube sleeve with holes throughout (Zhang et al. 2013a, Zhang et al. 2013b, Zhang et al. 2013c). A power density of 0.4 W/m^3 was produced when a 2.0 L MFC with 80 m^2/m^3 cathode packing density was tested *in situ* by submerging it in an aeration tank in a water reclamation facility (Zhang et al. 2013b). The COD removals (<53%) achieved using this MFC were also relatively low (Zhang et al. 2013b). When it was tested *ex situ*, there were increased power densities (2.3 W/m^3) and COD removals (65 – 70%) compared to *in situ* tests, due to the better operational conditions and shortened HRT (11 h to 5.5 h) (Zhang et al. 2013b, Zhang et al. 2013c). These two long-term studies (400 and 450 days) showed that MFCs could handle fluctuations in water levels, HRTs and temperatures.

Further improvement in a similar tubular MFC (2.4 L) was made in a separate study, by using spiral spacers around the anode brush to create a helical flow path (Zhang et al. 2013a). This was shown to improve electricity generation in both laboratory (acetate solution, 4.0 W/m^3 to 8.2 W/m^3) and on-site tests (domestic wastewater, 0.34 W/m^3 to 1.2 W/m^3) (Zhang et al. 2013a). Although the cathode packing density reached 57 m^2/m^3, the volumetric power density (8.2 W/m^3) produced in this MFC was only one third of the 24 W/m^3 obtained in a 130 mL reactor with 27 m^2/m^3 cathode packing density, when 1 g/L acetate solution was fed continuously

at a HRT of 8 h in both studies (Ahn and Logan 2012, Zhang et al. 2013a). The lower power production in the tubular MFC could be primarily result from the lower power density (144 mW/m^2) achieved using the large cathode (1400 cm^2) compared to the 888 mW/m^2 produced by the small cathode (35 cm^2) in the 130 mL MFC (Ahn and Logan 2012, Zhang et al. 2013a).

2.2.2 Unit stacking

Combining multiple reactors together may be a more practical and useful approach for scaling up BESs than enlarging single reactors, as power densities have always been higher in smaller reactors than in larger systems due to the increase in the volume dependent internal resistance (Dekker et al. 2009, Ledezma et al. 2013). The first paper on stacked MFCs was aimed at continuous electricity generation at high voltages and currents. In this study, six identical two-chamber MFC units (156 mL) were constructed using graphite granules as electrode materials, and operated continuously by pumping the acetate solution into each of the anode chambers, and hexacyanoferrate solution into each of the cathode chambers (Aelterman et al. 2006). By connecting the units electrically in series or in parallel, increased voltage (2.0 V at 228 W/m^3) and current (255 mA at 248 W/m^3) were observed for a short time (<1 h), while voltage reversal happened at high current with series connection (Aelterman et al. 2006). Since then, many studies have been reported on stacking MFCs of various sizes, using fed-batch operation or continuous flow conditions.

It was shown that higher power densities (0.4 W/m^3) were produced in smaller MFCs (6.3 mL and 30 mL) compared to the 0.2 W/m^3 by a larger MFC (650 mL), where these different sized reactors had similar configuration and the same electrode packing density (900 m^2/m^3) (Ieropoulos et al. 2008). Therefore, the idea was suggested that scaling up MFCs could be better achieved by connecting multiple small-sized units rather than increasing the size of an individual unit. This idea was shown to be possible to achieve increased power output by the stacked small units compared to that of a large one, based on the preserved power density (0.4 W/m^3) produced

by the 10 stacked small MFCs (Ieropoulos et al. 2008). Similar results were obtained using domestic wastewater or urine as fuels in multiple systems operated in fed-batch mode (Ieropoulos et al. 2010, Ieropoulos et al. 2013).

The approach of building large BESs by unit stacking was also tested in continuous flow conditions. The largest MFC system built by unit stacking had a total working volume of 20 L, which was constructed from four two-chamber units connected using three bipolar plates (Dekker et al. 2009). The electrode packing density of this MFC stack was 300 m^2/m^3 (Dekker et al. 2009). When acetate was fed continuously to the four anode chambers, 11 W/m^3 was produced initially due to the low oxygen reduction rate of the aqueous cathode and cell reversal, but the power increased to 144 W/m^3 by decreasing the pH, purging with pure oxygen, and increasing the flow rate in the cathode chamber (Dekker et al. 2009). A continuous flow stacked MFC system (72 mL) was constructed as a vertical cascade by 6 identical units with an electrode packing density of 1200 m^2/m^3. It was tested with different electrical connections. With the acetate solution flowing sequentially through each units, 7.5 W/m^3 were obtained in a parallel electrical connection despite substrate imbalances (Ledezma et al. 2013). The stacked MFC could produce 9.3 W/m^3 using a series electrical connection with fluidic and electrical isolation that seemed to avoid voltage reversal (Ledezma et al. 2013). Continuous treatment of real swine wastewater was shown using a tubular air-cathode MFC stack (0.3 L liquid volume). This MFC stack consisted of 5 units constructed by enveloping a graphite felt anode in a porous polyvinylchloride (PVC) plastic tube wrapped with a hot-pressed membrane cathode (packing density of 64 m^2/m^3) (Zhuang et al. 2012). Higher maximum power of 11 W/m^3 was produced when the units were connected electrically in parallel compared to the 4.3 W/m^3 produced in the series connection. COD removals of 77 – 83% and ammonia removals of 80 – 90% were achieved using this tubular MFC stack (Zhuang et al. 2012).

A cassette architecture has been used in several studies for stacking air-cathode MFCs or MECs, because this stacking configuration requires a separate gas chamber. A 1 L MFC

consisting of 12 cassette electrodes was tested using a synthetic wastewater containing starch, peptone, and fish extract (Shimoyama et al. 2008). Each box-shaped cassette had two flat air-cathodes sandwiched in between two proton-exchange membranes, and two graphite-felt anodes on both sides of a plastic frame, achieving an electrode packing density of 137 m^2/m^3 (Shimoyama et al. 2008). The maximum power was stable at 129 W/m^3, with a high COD removal (93 – 95%) (Shimoyama et al. 2008). A similar designed single-chamber stacked MFC with air-cathodes was tested with different electrical connections using acetate. It showed that higher power (23 W/m^3) was produced in a parallel electrical connection than the 15 W/m^3 obtained in a series connection (Wang and Han 2009). The lower power production achieved in this cassette MFC compared to the former one was most likely due to the less compact cassette assembly with an electrode packing density of 15 m^2/m^3.

For MECs, fewer studies have been carried out in terms of system scale-up. A stacked MEC was developed by placing six identical cassettes into a 120 L reactor tank (Heidrich et al. 2013). In each cassette, a stainless steel wire wool cathode was set in a 2.6 L cathode chamber, separated on each side by membrane with a carbon felt anode sandwiched between two stainless steel mesh current collectors (Heidrich et al. 2013). At a loading rate (0.14 kg-COD/m^3/d) comparable to the activated sludge process (0.2 – 2 kg-COD/m^3/d), the energy cost of 2.3 kJ/g-COD was lower (versus 2.5 – 7.2 kJ/g-COD), when it was tested to treat raw domestic wastewater at ambient temperatures (Heidrich et al. 2013). Gas production was 0.015 L-H_2/L/d, at a high purity (100 ± 6.4 %), resulting in ~70% of the electrical energy input recovered with a coulombic efficiency of 55% (Heidrich et al. 2013). The cassette electrodes should be a highly scalable design that can be applied conveniently for wastewater treatment due to their high flexibility and easy installation.

In general, these BESs scaled-up by combining multiple units together showed better performance, such as volumetric power densities, than those large single reactors. The primary reasons for the improved power production in these stacked BESs should be the higher electrode

packing densities achieved by units stacking, and the higher power densities preserved using the relative smaller electrodes, compared to the systems with enlarged electrodes set in large tanks.

2.2.3 Multi-electrode systems

Placing multiple smaller electrodes in a larger reactor tank, instead of a single larger electrode, is an alternative approach to build large BESs without losses in volumetric power, as that avoids the need to use large electrodes. A 130 mL multi-electrode MFC reactor was designed to have a separator electrode assembly (SEA), with two layers of textile separators sandwiched in between multiple graphite brush anodes and a single air-cathode (Ahn and Logan 2012). The cathode packing density was 27 m^2/m^3, and that of the anodes was 20 m^2/m^3 based on the projected surface or 2600 m^2/m^3 based on individual fibers (Ahn and Logan 2012). Using acetate as fuel, this multi-electrode MFC produced 30 W/m^3 in fed-batch operation, and 24 W/m^3 at an HRT of 8 h in continuous flow (Ahn and Logan 2012). When domestic wastewater was fed into this reactor, 3.2 W/m^3 was produced in fed-batch operation with a good COD removal (>90%), and 1.5 W/m^3 was obtained in continuous flow condition (HRT = 8 h) with lower COD removals (50 – 60%) (Ahn and Logan 2013). The power production by this multi-electrode MFC was much higher than the 8.2 W/m^3 produced in a 2.4 L tubular MFC with a single large brush anode and air-cathode using acetate (Zhang et al. 2013a). In contrast, comparable power outputs were obtained (1.5 W/m^3 versus 1.2 W/m^3) by these two MFCs treating domestic wastewater, which could be resulted from the higher electrode packing density (cathode, 57 m^2/m^3; anode, 50 m^2/m^3) in the tubular MFC than in this multi-electrode system (Ahn and Logan 2013, Zhang et al. 2013a). However, the power densities (cathode, 57 mW/m^2; anode, 75 mW/m^2) produced by the multi-electrode MFC was higher than those (cathode, 21 mW/m^2; anode, 24 mW/m^2) by the tubular one, due to the use of smaller electrodes in the former compared to that in the later.

Recently, there have been several studies using multiple anodes, which shows the importance of the electrode arrangement on the performance of MFCs. Single and multiple brush

anodes were shown to produce similar power in typical air-cathode MFCs (28 mL), as long as the anode projected area could fully cover the cathode (Lanas and Logan 2013). The performance of three large brush anodes versus eight small brushes was compared in a larger MFC (130 mL), both in fed-batch mode and continuous operation. When the brush core was set at the same distance from the cathode, large brushes produced higher power (Lanas et al. 2014). However, the small ones performed better once moved closer to the cathode, which resulted in a more compact electrode packing (Lanas et al. 2014). A two-chamber MFC (1.87 L) was developed that consisted of 225 graphite rod anodes divided into 9 segments, with the same number of rods connected together as a single cathode, in order to optimize the design of multiple anodes (Zhang et al. 2013d). High current output, low ohmic resistance, and more biomass production were observed for the anode segments closer to the cathode, indicating equidistant electrode spacing was necessary for a larger MFC design (Zhang et al. 2013d). Improvement in uneven current distributions was achieved by increasing the COD concentration or the anolyte conductivity (Zhang et al. 2013d). Comparison between staggered array (MFC-S) and inline array (MFC-I) anode designs showed that the MFC-S design was superior, with faster start-up, and higher maximum power densities (Zhu et al. 2013b). However, neither array arrangement could eliminate uneven anodic current distributions (Zhu et al. 2013b).

Electrical connections and flow patterns are importance issues in multi-unit and multi-electrode MFCs, especially under continuous flow conditions. To connect multiple units or electrodes electrically in series, electric apertures such as DC-DC power conversion systems (Kim et al. 2011b) or adaptive control systems (Andersen et al. 2013) have been used to avoid losses in power or damage to the bioanodes by voltage reversal (Kim et al. 2012a, Oh and Logan 2007). Wiring multiple units or electrodes in parallel was shown to adversely affect power production, due to the ionic connection between these units (Zhuang and Zhou 2009). To address this issue, reactors were designed to severe the direct fluidic flow among the individual units (Ledezma et al. 2013) or to create very high ionic resistances in the flow path (Zhuang and Zhou

2009) by using relatively complicated architectures. By dividing flow up into individual units (hydraulically in parallel), direct flow connections can be avoided between the units, but a large substrate gradient caused by the requirement of a low effluent COD concentration will decrease power production (Ahn and Logan 2012, Ahn and Logan 2013). In contrast, series flow sequentially through all units can minimize the substrate concentration change in each unit, which at the same time making it easier to design and provide a larger treatment capacity (Pinto et al. 2010). However, it is not possible to completely avoid electrolyte connection between multiple units or electrodes hydraulically connected in series. Such considerations of the electrical and flow connections for larger scale multi-unit and multi-electrode MFCs, require additional research to improve our understanding for a better system design, in terms of reactor configuration and system operation.

A 2.5 L MEC was designed using this multi-electrode approach, which had eight separate electrode pairs consisting of graphite brush anodes and stainless steel mesh cathodes (Rader and Logan 2010). With a cathode packing density of 64 m^2/m^3, this multi-electrode MEC produced a volumetric current of 74 A/m^3 and maximum hydrogen production of 0.53 L/L/d, consistent with that expected based on the projected cathode surface area using similar materials in small reactors (28 mL) (Rader and Logan 2010). These results indicated that using multiple smaller electrodes to build larger BESs was able to achieve comparable performance as the smaller reactors, which avoids the losses in power densities caused by the use of large electrodes.

2.2.4 Pilot-scale demonstrations

The first demonstration of pilot MFCs was based on benthic-types of MFC (BMFC), which were used to power a remote meteorological buoy. The first design consisted of 7 subunits containing graphite plate anodes and cathodes, with a mass of 230 kg, and a volume of 1.3 m^3. This BMFC produced a sustained power of 24 mW when deployed in the Potomac River in Washington, DC, USA. A second type of unit was made of 12 graphite plate anodes arranged

vertically in an array that was affixed to the underside of a fiberglass top plate. It had a 1-m long graphite brush cathode positioned in overlying water. This type of BMFC was smaller (16 kg, 0.03 m^3) and less costly than the previous design, and it produced more power (36 mW) (Tender et al. 2008).

The first above ground pilot-scale MFC test was conducted at Foster's brewery in Yatala, Queensland (Australia), by the Advanced Water Management Center at the University of Queensland. The MFC system consisted of 12 modules, each 3 m high, with a total volume of approximately 1 m^3. Each tubular module contained carbon brush anodes inside the reactor, and similar brush cathodes outside of the tube, with flow up through the inside and out over the top, flowing over the outside cathodes (Logan 2010). Another type of pilot-scale MFC was conducted by researchers at the University of Connecticut and their collaborators (Fuss & O'Neill, and Hydroqual Inc.) at a wastewater treatment facility in upstate New York (USA) (Cooper 2009). The reactors contained granular graphite as anode, with Pt-catalyzed carbon cloth cathodes. They could remove up to 80% COD at 300 – 600 mg/L (Logan 2010). Little else is known about the performance of these two MFCs at these sites, as there have been no published reports, only material from the internet.

The first demonstration of a pilot-scale MEC was conducted at the Napa Wine Company, in Oakville, CA, USA, by Penn State researchers with engineering services by Brown and Caldwell (Walnut Creek, CA, USA). The reactor contained 24 modules, each consisting six pairs of carbon brush anodes and stainless steel cathodes, in a tank approximately 1 m^3 in total volume. Fed with winery wastewater, the maximum current reached 7.4 A/m^3, with a soluble COD removal of 62 % at a hydraulic retention time of 1 day (applied voltage of 0.9 V). Gas production reached a maximum of 0.19 L/L/day, primarily in the form of methane (86 %) (Cusick et al. 2011).

The first commercial BES system is the EcoVolt, launched by Cambrian Innovation, Boston, MA, USA. EcoVolt is used to enhance performance through electromethanogenesis, by applying electrical power to the electrodes in the reactor (CAMBRIAN 2013c). The single reactor volume

is 20,000 gal (76 m^3), with a flow rate of 13,300 – 40,000 gal/day (50 – 150 m^3/day) (CAMBRIAN 2013b). The reactor was tested at the Clos du Bois Winery, located in California's Napa Wine Country. Over a period of 15 months, the EcoVolt treated up to 10% of the total wastewater flow, with 80 – 90% BOD removal, while simultaneously generated high-quality methane. Using this technology, the winery was able to reduce energy used by their aeration pump and the methane produced could be used for further energy recovery (CAMBRIAN 2013a).

2.3 Combined system for improved performance

Combining different BESs together or with other treatment technologies can enhance the overall system performance, promote sustainability, and fulfill specific treatment requirements such as high effluent quality. Combined systems can be developed by coupling different BES systems together, such as using MFCs to power MECs for hydrogen production, or integrating them with other biological, physical, or chemical processes (Zhou et al. 2013).

To make MECs a green and sustainable technology, electricity from renewable energy sources such as solar, wind, or salinity gradients is preferred instead of electrical grid energy (Mehanna et al. 2010, Nam et al. 2012). The use of MFCs to power MECs has been proposed due to the advantages of generating hydrogen from waste biomass without the consumption of electrical grid energy while treating wastewater (Sun et al. 2009, Sun et al. 2008, Wang et al. 2011a, Zhao et al. 2012). This idea was first demonstrated by using a single MFC to power a two-chamber MEC, with a maximum hydrogen production of 0.015 m^3/m^3/day (Sun et al. 2008). However, the hydrogen production was significantly less than that obtained using a power supply with an applied voltage of 0.8 V (>4 m^3/m^3/day) (Tartakovsky et al. 2009). This dramatic difference was due to the low voltage applied by the MFC, resulting in an unstable coupled system that reduced hydrogen production (Hatzell et al. 2013). Connecting multiple MFCs in series or in parallel did not improve hydrogen production relative to a single MFC, even though the applied voltage was increased to 0.8 V with three MFCs connected in series (Sun et al. 2009,

Wang et al. 2011a). The use of a capacitor based energy storage system to boost the applied voltage was shown to increase hydrogen production to 0.72 m^3/m^3/day, providing a promising approach for integrating MFCs to MECs for renewable hydrogen production (Hatzell et al. 2013).

Another approach to improve system performance is to integrate the MFC cathodes with other processes. In a hybrid MFC and fuel cell (FC) system (M2FC), Fe^{2+} and Fe^{3+} were recirculated between the MFC cathode and the FC anode, with dissolved oxygen reduction at the FC cathode (Eom et al. 2011). The M2FC produced an average power density of 0.65 W/m^2, which was approximately six times higher than that of the corresponding MFC system (Eom et al. 2011), likely due to the reduced oxygen intrusion into the MFC anode. A sediment MFC was constructed with two cathodes, one in the rice rhizosphere and the other at the air-water interface, to demonstrate that the excreted oxygen from the rice rhizosphere could improve the efficiency of the biocathode to be comparable with an air-cathode (Chen et al. 2012). One advantage of this biocathode was that it could be placed closer to the anode in the soil, to increase MFC performance by reducing the internal resistance. By combining an oxic-biocathode MFC (O-MFC) with an anoxic-biocathode MFC (A-MFC), the combined MFC system was capable of simultaneous carbon (98%) and nitrogen removal (97%) (Xie et al. 2011). COD was mostly removed in the two anode chambers, and ammonium was removed by being oxidized to nitrate first in O-MFC's cathode chamber, and then fed into the A-MFC's cathode chamber for denitrification (Xie et al. 2011). Carbon neutral MFCs were achieved by utilizing photosynthetic algae in a cathode chamber for CO_2 sequestration. With the presence of light, the CO_2 generated on the anode could be fed into the catholyte and converted into biomass by suspended or immobilized microalgae (*C. vulgaris*), while oxygen was generated to serve as the electron acceptor for the cathode (Wang et al. 2010, Zhou et al. 2012).

In the past year, there were several studies on combining the MFC with a membrane bioreactor (MBR) to enhance overall COD removal compared to that of the MFC alone, or to improve the overall energy efficiency for wastewater treatment. A membrane bioelectrochemical

reactor (MBER) was developed by integrating hollow-fiber ultrafiltration membranes into a single-chamber tubular MFC, accomplishing 90% COD removal and reducing the effluent turbidity to <1 NTU with domestic wastewater (Ge et al. 2013). Energy self-sufficiency was possible with an acetate solution, but not with domestic wastewater, due to serious membrane fouling (Ge et al. 2013). Low membrane fouling was observed by using non-woven cloth as both the cathode separator and the filter in a electrochemical membrane bioreactor (EMBR) (Wang et al. 2013). This EMBR achieved high removal efficiencies (COD, 91%; ammonia, 97%; total nitrogen 55%; and effluent turbidity, ~3 NTU) and a net energy production (0.0361 kWh/m^3) at an optimal HRT of 9 h with acetate (Wang et al. 2013). An anaerobic membrane bioelectrochemical reactor (AnMBER), was developed by installing hollow-fiber ultrafiltration membranes inside a stainless steel cassette, nitrate reduction cathode in a two-chamber MFC (Tian et al. 2014). The AnMBER produced a maximum power density of 1.2 W/m^3 and efficiently removed nutrients (COD, 92%; and nitrate, 95%) with minimized membrane fouling (Tian et al. 2014), but no energy balance was presented. Other studies have shown that membrane fouling can be mitigated when combining an MFC with an MBR, because the electric field established by the electrodes would produce a negatively charged membrane surface that would repel particles and enhance the degradability of surplus biomass solids (Liu et al. 2013, Song et al. 2013, Su et al. 2013). However, to my knowledge, there was no report of such combined MFC-MBR system that could achieve high treatment efficiencies and be energy self-sufficient with real wastewaters. This gap was most likely due to the low energy production of wastewaters compared to acetate, and the high energy costs of membrane processes. To fulfill the gap, more studies are needed to improve the design of current systems and investigate the operational factors limiting the overall energy balance.

2.4 High-throughput BESs

Application of BESs for energy recovery from wastewater not only requires studies on scaling up the system with high performance, but also needs investigations on high-throughput BES devices that could be used for fast, cost-effective screenings for various purposes. These BESs should be easy to fabricate with reduced reactor volume and low costs.

Microliter-MFC (μMFC) arrays with independent fluidic access to individual units are emerging as a promising platform for high-throughput screenings (ElMekawy et al. 2013). The first μMFC array was constructed using 1 mL pipette tips and contained 9 anode chambers (500 μL) with a common cathode chamber (Biffinger et al. 2009). A plate-shaped μMFC array was fabricated using photolithography, that consisted of 8 single-chamber air-cathode units (25 μL) (Chen et al. 2011). The most high-throughput micro-fabricated μMFC array was developed to enable 24-well parallel screening and analysis (Han et al. 2013). The first design of this μMFC array had 24 conventional two-chamber MFCs (~600 μL) with ferricyanide cathodes (Hou et al. 2009). This 24-well μMFC array was further developed by using air-cathodes (Hou et al. 2011). Microfluidic control was used to replenish the anolyte and catholyte in the second design, enabling long-term multiplexed analyses using this μMFC array (Hou et al. 2012). However, these μMFC arrays were not able to be used for long-term analysis, or did not avoid contamination among chambers due to the lack of independent fluidic access to the individual units. To solve this problem, a 6-well μMFC array was developed using independent fluidic compartment for each unit (Mukherjee et al. 2013). There was small deviation (1.4%) among the units due to the design of spatially distinct wells (Mukherjee et al. 2013).

These multi-well μMFC arrays are all based on an MFC configuration, and some require expensive materials and access to state of the art micro-fabrication technologies (Han et al. 2013, Mukherjee et al. 2013). To enable more wide spread experimentation, a simple and inexpensive (ca. $1.50) mini-MEC was built using a small crimp top serum bottle (5 mL), with a graphite plate anode and a stainless steel (SS) mesh cathode (Call and Logan 2011b). In μMFC arrays,

gold was used as the anode material that caused a high internal resistance due to the poor attachment of bacteria to the electrode surface (Ye et al. 2013). While carbon-based anodes showed the best performance and stability in macroscopic BESs, due to their large surface area and those functional groups favoring cell vitality (Logan 2008, Richter et al. 2008). Caution is needed to extrapolate the screening results obtained in μMFC arrays with gold anodes to larger systems with carbon-based electrodes. For example, *S. oneidensis* produced a higher current density (25 mA/m^2) than *G. sulfurreducens* (18 mA/m^2) in a μMFC with gold electrodes (Li et al. 2011), but the opposite was observed using the mini-MECs with graphite plate anodes (Call and Logan 2011a).

For now, the utility of these high-throughput BESs was only demonstrated by screening bacterial exoelectrogenic activity, and through characterization of exoelectrogenic strains (Mukherjee et al. 2013, Wang et al. 2011c). Additional research should extend their functionality for other applications, such as screening the chemical factors which have the potential to increase the performance of BESs, or evaluating the treatability of different wastewater sources as candidate fuels for BESs.

2.5 Outlook

Energy savings and environmental benefits may be achieved using BESs through production of electricity or chemicals from waste renewable sources, thus reducing our energy dependence on fossil fuels for wastewater treatment. The energy output of BESs should not be expected to be better than that possible using chemical fuel cells, especially if the fuel is organic matter in wastewater. The above review has shown that BESs have undergone dramatic development and advances in the past decade, in terms of performance improvement, feasibility for scaling-up the reactors, and expansion of products possible from these systems. However, BESs still face many challenges before large scale systems with high performance and efficiency can be implemented for real world applications. A better understanding of the issues associated with system scale-up

and demonstration of new test methods could facilitate any further development and application of the BESs aimed at enhancing overall system performance and energy efficiencies. With a sustained pace in research in BESs, it is reasonable to envision that BESs will be applied for additional commercial uses in the near future, providing a feasible method to address current energy and environmental problems associated with the water infrastructure.

Chapter 3

Electrochemical study of multi-electrode microbial fuel cells under fed-batch and continuous flow conditions

Abstract

Connecting multiple microbial fuel cells (MFCs) hydraulically and electrically together can reduce overall performance relative to that expected from the individual reactors, in ways that depend on the operational conditions. Power production of four hydraulically connected MFCs was compared when the reactors were operated with individual electrical circuits (individual), and when four anodes were wired together and connected to four cathodes all wired together (combined), in both fed-batch and continuous flow conditions. Comparisons of power produced under these different conditions could not be made based on a single resistance. Instead, polarization tests were needed to assess performance of individual reactors relative to the combined MFCs. Based on the power curves, power produced by the combined MFCs (2.12 ± 0.03 mW, 6.53 ± 0.04 mA, 200 Ω) was found to be essentially the same as the summed power (2.13 mW, 6.51 mA, 50 Ω) produced by the four individual reactors in fed-batch mode. When operated with continuous flow through the four MFCs, the maximum power (0.59 ± 0.01 mW) produced by the combined MFCs was slightly lower than the summed maximum power of the four individual reactors (0.68 ± 0.02 mW). There was a small parasitic current flow from adjacent anodes and cathodes, but overall performance was relatively unaffected. These findings demonstrate that optimal power production by reactors hydraulically and electrically connected can be anticipated based on performance of individual reactors.

3.1 Introduction

A microbial fuel cell (MFC) is a device that converts chemical energy from biodegradable substrates to electrical energy via microbially-catalyzed redox reactions (Du et al. 2007, Logan et

This chapter was accepted as: Ren, L. J., Ahn, Y, Hou, H. J., Zhang, F., and Logan, B. E. (2014). Electrochemical study of multi-electrode microbial fuel cells under fed-batch and continuous flow conditions. *Journal of Power Sources*.

al. 2006, Oh et al. 2010). MFCs have been used to produce electricity while simultaneously treating many different types of wastewaters (Erable et al. 2011, Logan 2009, Pham et al. 2009). Studies on the scale-up of MFCs containing multiple electrodes have shown the importance of optimization of electrode spacing and increasing specific surface area (surface area of the electrode per volume of reactor) to improve performance (Liu et al. 2008). Building larger reactors simply by increasing the electrode and reactor sizes (i.e. larger electrodes in larger tanks) can result in decreased volumetric power output compared to smaller bench scale reactors (Ieropoulos et al. 2008, Liu et al. 2008, Rader and Logan 2010). The use of many smaller electrodes in stacks of hydraulically-coupled reactors has therefore been proposed as a more effective method for scale up (Ahn and Logan 2012, Galvez et al. 2009, Ledezma et al. 2013, Winfield et al. 2011).

Multiple MFCs should not be electrically connected in series as this can substantially reduce power production. Electrically connecting fuel cells or batteries in series normally will increase the voltage in proportion to the number of individual units. However, connecting MFCs in series can produce voltage reversal, resulting in little voltage gains or even elimination of power production (Aelterman et al. 2006, Oh and Logan 2007). Factors that result in voltage reversal include different internal resistances between the units, or unequal voltage production due to differences in substrate concentrations (Ahn and Logan 2013, Kim et al. 2012a, Oh and Logan 2007). Instead of connecting the units electrically together in series to increase voltage, higher voltages can also be obtained by using DC-DC power conversion systems or by charging arrays of capacitors in parallel that are then discharged in series (Kim et al. 2011b).

Practical applications of MFCs will require operation under continuous flow conditions, but hydraulic flow through arrays of MFCs can adversely affect power production and COD removal relative to that expected from individual reactor performance (Pinto et al. 2010, Winfield et al. 2011, Zhuang et al. 2012). Wastewater can be processed through multiple MFCs in one of two ways: sequentially through all reactors (hydraulically connected in series) (Ahn and Logan 2012,

Wang and Han 2009); or divided up to flow through each individual MFC (hydraulically in parallel) (Aelterman et al. 2006). Series flow can minimize the substrate concentration change in each reactor (i.e. difference between inlet and outlet concentration) and this approach has been used in several studies (Ahn and Logan 2012, Fedorovich et al. 2009, Zhuang and Zhou 2009). Parallel flow will produce similar conditions in all reactors (Aelterman et al. 2006, Ieropoulos et al. 2008), but a low desired effluent COD concentration would result in a large substrate gradient in each MFC. This large change in COD, in a single reactor with multiple anodes wired together, has been shown to adversely affect power production (Ahn and Logan 2013). The same phenomenon occurs when multiple MFCs are wired together under conditions where there is an ionic connection between the electrodes (i.e., the electrodes of different units share the same fluid chamber) (Zhuang et al. 2012). To avoid ionic connections between adjacent electrodes, flow through a series of MFCs was arranged in one study so that the water cascaded (overflowed) from one MFC to another (Ledezma et al. 2013). This separation of the MFCs avoided direct fluid connections, and thus severed solution ionic connections. Alternatively, ionic separation can be achieved by using large constrictions in the flow path (creating very high ionic resistances between adjacent cells), or the cells can be widely separated (O'Hayre et al. 2003, Zhuang and Zhou 2009). The optimal condition is to have no electrolyte connection between these reactors (Kim et al. 2012a), but that would not be possible in larger MFCs that contain multiple anodes or cathodes as these electrodes all share the same electrolyte.

The aim of this study was to better understand the reasons why power production decreases when multiple anodes are wired together, under conditions where there are large substrate concentration changes. To study how substrate concentration changes might affect power production in a multi-electrode reactor, we hydraulically connected four MFCs in series to simulate the operation of single MFC containing multiple anodes and cathodes. The electrical connections between the reactors were either set with completely individual circuits between the paired anodes and cathodes, or they were combined into a single circuit with all four anodes

wired together and connected to four cathodes all wired together. Power production with this parallel electrical connection was compared to the summed power produced by the individually wired MFCs to determine how the electrical connections between the electrodes affected performance. These comparisons with the two different electrical connections were made using polarization data for MFCs operated in either fed-batch mode or in continuous flow conditions with hydraulic flow in series through the four reactors. Continuous flow operation produced conditions that resulted in large substrate concentration changes across the multiple electrodes, allowing examination to how substrate changes affect overall performance. The individual potentials of the electrodes were measured using reference electrodes and individual current using resistances on the different anodes and cathodes, allowing a more comprehensive characterization of the multi-electrode MFCs.

3.2 Materials and methods

3.2.1 Reactor construction

Single-chamber, air-cathode MFCs were made of cube-shaped Lexan blocks, each having a single cylindrical chamber with a volume of 14 mL (7 cm^2 cross sectional area) as previously described (Liu and Logan 2004). Windows (20 mm length × 6 mm width) were cut in the center on the left and right sides of the block to allow hydraulic flow between MFC reactors aligned side by side (Fig. 3-1). This hydraulic connection of the individual cells enabled simulation of a single multi-electrode system. The total liquid volume of the four connected MFC reactors was 58 mL. Anodes were non-waterproof carbon cloth (#CCP40, Fuel Cell Earth, USA) with a projected surface area of 7 cm^2. Air cathodes (7 cm^2) made of waterproof carbon cloth (30 wt.%, #CC640WP30, Fuel Cell Earth, USA) had a catalyst loading of 0.5 mg-Pt/cm^2 on the water side, and four PTFE diffusion layers on the air side (Cheng et al. 2006a). The electrode spacing was 2 cm (anode surface to cathode surface). The distance between the main liquid chambers of each MFC was 2 cm. A reference electrode [Ag/AgCl; +200 mV vs. standard hydrogen electrode

(SHE); BASi] was inserted into the middle of each of the four MFCs to determine the anode and cathode potentials (Fig. 3-1b). Additional tests were conducted with four MFCs connected hydraulically in series using very thin needles (21 G × 1, BD™ sterile hypodermic needle, BD, USA) to reduce ionic connections between the reactors.

A tracer test was conducted using abiotic reactors to determine whether there was flow short circuiting. A KCl solution (1 mol/L) was used as the conservative tracer, with an input of 1 h duration. The tracer concentration at the outlet was measured using a conductivity meter over a period of 34 h. The experimental data was modeled using both dispersion model and CSTRs in series model (Howe et al. 2012).

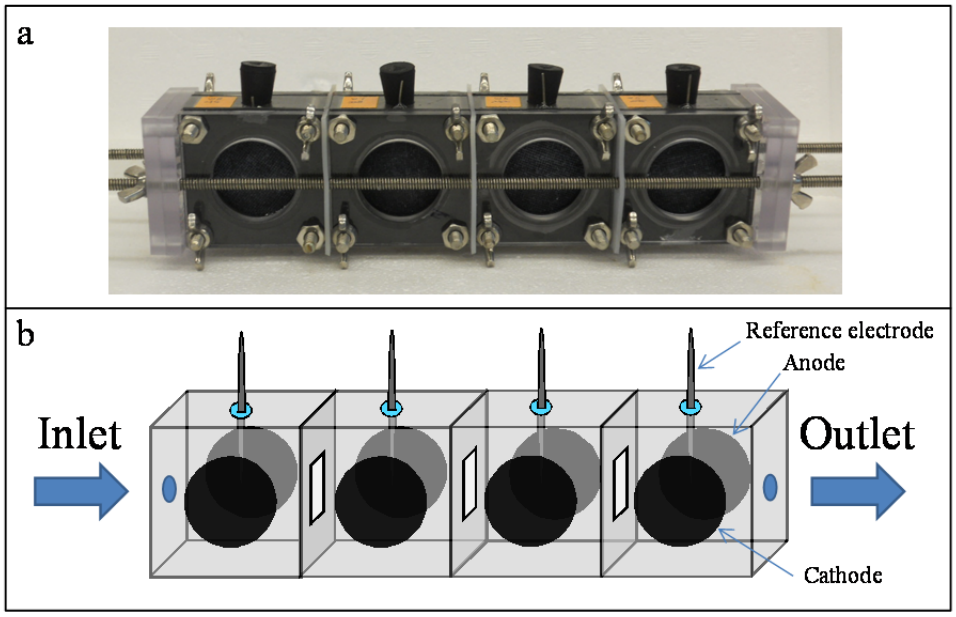

Figure 3-1 Configuration of the four hydraulically connected MFCs: (a) photo showing the outside structure and (b) schematic drawing showing the hydraulic connection.

3.2.2 Reactor operation

MFCs connected by individual circuits were compared to the four MFCs wired together (combined circuit) under fed-batch mode and continuous flow mode in terms of power production. For individual circuit connections, each MFC was connected through a separate external resistor (Appendix A, Scheme A-1a). For combined circuit connections, the four anodes were wired together using copper wires and then connected through a single external resistor to

all the cathodes similarly wired together with copper wires (Scheme A-1b). The four MFCs with individual electrical connections were designated as R1 to R4 (duplicates R5 to R8). For combined electrical connection, the MFC was designated as M1234 (duplicate M5678).

The MFCs were each initially acclimated using an individual circuit connection with a 1000 Ω external resistor in fed-batch mode, with the growth medium replaced when the voltage decreased to <0.05 V. Polarization and power data were obtained for both the individual connections and the combined connections after the MFC reactors exhibited stable performance, defined as reproducible voltage output over at least three consecutive cycles. Following batch tests, the MFCs were switched to continuous flow operation, with medium flowing sequentially through reactors R1 to R4 (Fig. A-1b). The hydraulic retention time (HRT) was set at 12 h using a flow rate of 0.08 mL/min. All the experiments were conducted in duplicate in a temperature controlled room at 30 °C.

The medium contained (per liter): 0.5 g CH_3COONa, 10 mL vitamins, and 10 mL minerals (Balch et al. 1979) in a 50 mM PBS buffer (0.31 g NH_4Cl, 2.45 g $NaH_2PO_4 \cdot H_2O$, 0.13 g KCl, 4.58 g Na_2HPO_4; pH = 7.1 ± 0.2, conductivity γ = 7.6 ± 0.2 mS/cm). The medium was autoclaved and then placed in an ice bucket during tests to avoid degradation prior to being fed into the reactors in continuous flow tests. The fluid warmed during transfer into the MFC, avoiding temperature differences between tests.

3.2.3 Chemical and electrochemical analysis

Soluble chemical oxygen demand (sCOD) was measured using standard methods (method 5220, HACH COD system, HACH Company, Loveland, CO) (APHA 1998). All samples for sCOD measurement were filtered through 0.45 μm pore diameter syringe filters (polyvinylidene difluoride, PVDF, 25 mm size, Restek Corporation, USA). Conductivity and pH were measured using a probe (SevenMulti, Mettler-Toledo International Inc.).

Voltage was recorded using a multimeter (model 2700; Keithley Instruments, Inc.) at 20 minute intervals, with the power calculated as $P = IU$, and the current calculated using Ohm's law ($I = U/R$), where U is the measured voltage (V), and R the external resistance (Ω) (Hong et al. 2011). For fed-batch tests, polarization data were obtained using the multiple-cycle method (two cycles each) by changing the external resistances from 4000 to 1000, 500, 200, 120, 80, and 40 Ω (individual connections), or from 1000 to 250, 125, 40, 30, 20, and 10 Ω (combined connections). In continuous flow tests, the external resistances were changed from 4000 to 2000, 1000, 500, and 300 Ω (individual connections), or from 1000 to 500, 250, 125, and 75 Ω (combined connections), with a single resistor used for a minimum of two days. All electrode potentials were reported versus the Ag/AgCl reference electrode. In some combined electrical connection experiments, an additional 10 Ω resistor was introduced in series with each anode and cathode in order to measure the current of each individual electrode.

3.3 Results

3.3.1 Power production

In fed-batch mode, the performance of the individual MFCs (R1 to R4) relative to each other was the same, based on power curves obtained from reactors after being fed with fresh medium, with a maximum power of 0.53 ± 0.03 mW at a current of 1.63 ± 0.01 mA (200 Ω) (Fig. 3-2a). The average power curve for the four reactors was therefore produced by averaging the current and power of the four individual MFCs at each external resistance. The maximum power that could be obtained from the four MFC reactors based on summation (i.e., four times the average) of the power of the individual reactors (2.12 ± 0.03 mW, 6.53 ± 0.04 mA, 200 Ω) was the same as that obtained with all electrodes wired together (2.13 mW, 6.51 mA, 50 Ω, M1234, Fig. 3-2b).

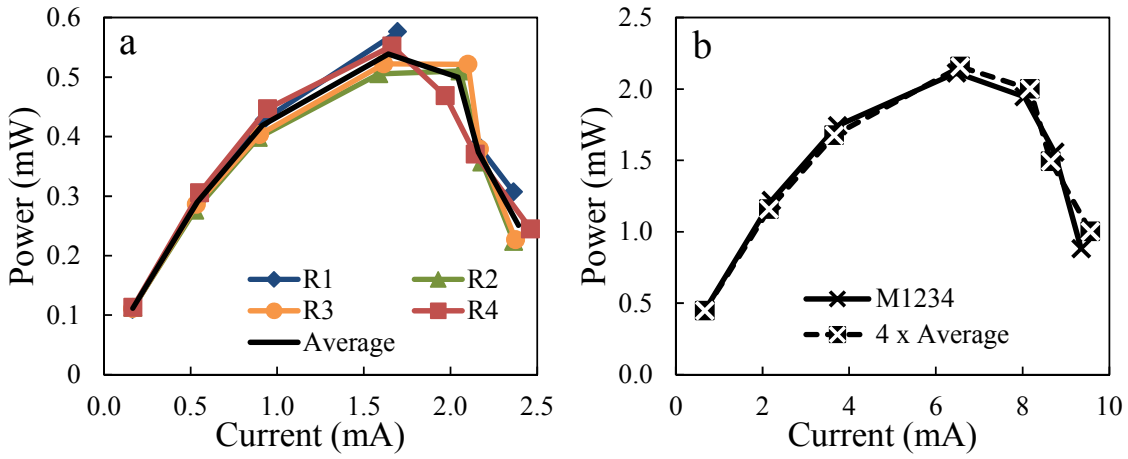

Figure 3-2 Power production of the MFC reactors in fed-batch mode. (a) Individual connection showing the identical performance of the four MFC reactors (R1 to R4). (b) Combined connection where the summed power of the four individual reactors (4 × Average) compared to that of the combined reactor (M1234). Results are shown for two separate sets of reactors (1-4, and duplicates 5-8 in Fig. A-2).

The power produced by the individual MFCs under continuous flow conditions relative to each other was quite different from that obtained in fed-batch tests, due to differences in substrate concentrations among the reactors. The power produced by the MFCs decreased from inlet to outlet, with a maximum power for the individually-wired MFCs of 0.23 mW (1000 Ω, R1), 0.20 mW (1000 Ω, R2), 0.16 mW (2000 Ω, R3), and 0.10 mW (4000 Ω, R4) (Fig. 3-3a). The sCOD concentrations measured in the direction of flow decreased from the inlet concentration of 363 mg/L, to outlet concentrations of 253 mg/L (R1), 168 mg/L (R2), 112 mg/L (R3), and 86 mg/L (R4) (1000 Ω external resistance for each MFC). The reduction in power due to the lower substrate concentration was expected based on previous studies using individual reactors (Liu et al. 2005, Wang and Han 2009). Tracer tests showed that the calculated HRTs using both models (16.5 h for CSTRs in series model and 15.2 h for dispersion model) were slightly larger than theoretical value of 12 h (Fig. A-1), indicating there was no flow short circuiting in the reactors. This lack of short circuiting is also supported by the large changes in COD along the direction of flow.

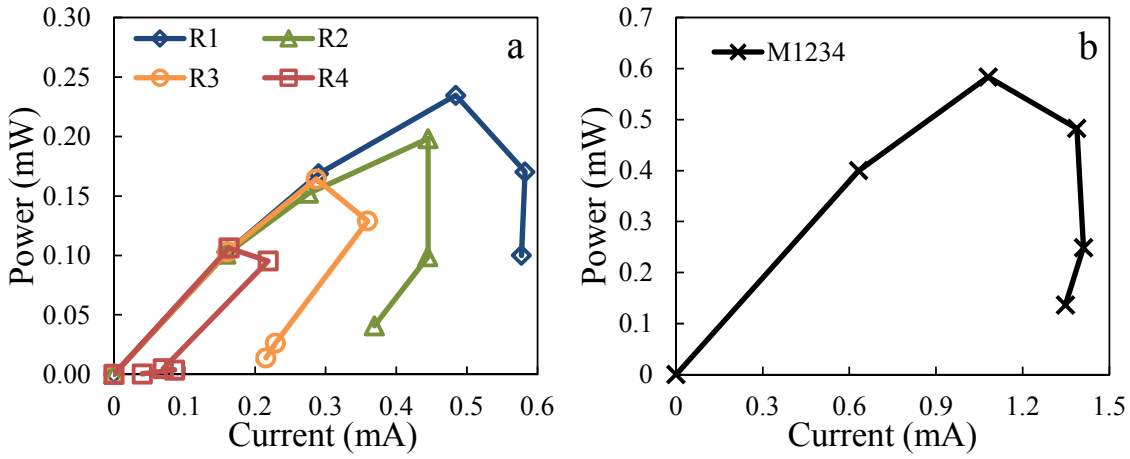

Figure 3-3 Power production of the MFC reactors operated in continuous flow with the flow from R1 to R4. (a) Individual connection showing the different performance of the four MFC reactors (R1 to R4). (b) Combined connection (M1234). Results are shown for two separate sets of reactors (1-4, and duplicates 5-8 in Fig. A-3).

Under continuous flow condition, a comparison was made between the summed maximum power produced by the four individual MFCs and that of the combined MFCs with the electrodes wired together, as no averaged power curve could be calculated due to the different performance of the individual reactors. The maximum power produced by each individually-wired MFC was summed as 0.68 ± 0.02 mW (the average of the maximum power of R1 to R4, and those for R5 to R8). This was slightly higher (15%) than the maximum power produced by the combined MFCs with the electrodes wired together (0.59 ± 0.01 mW, averaged for M1234 and M5678) at an external resistance of 500 Ω (Fig. 3-3b). Additional tests conducted using reactors connected hydraulically with needles to break the ionic connections between the reactors also showed similar reactor performance between the individual circuit connections and the combined circuit connections as that of the MFCs hydraulically connected by windows, even under continuous flow conditions. The summed maximum power produced by the individual MFCs in these tests was 0.64 ± 0.01 mW, also slightly higher than that produced by the combined MFCs (0.59 ± 0.01 mW, 500 Ω) (Fig. 3-4). The maximum power in continuous flow was lower than that obtained in fed-batch tests (2.13 ± 0.03 mW) due to the lower substrate concentrations in the MFCs at steady

state under continuous flow conditions, compared to that present in the reactors at the start of the fed-batch test (Ahn and Logan 2012).

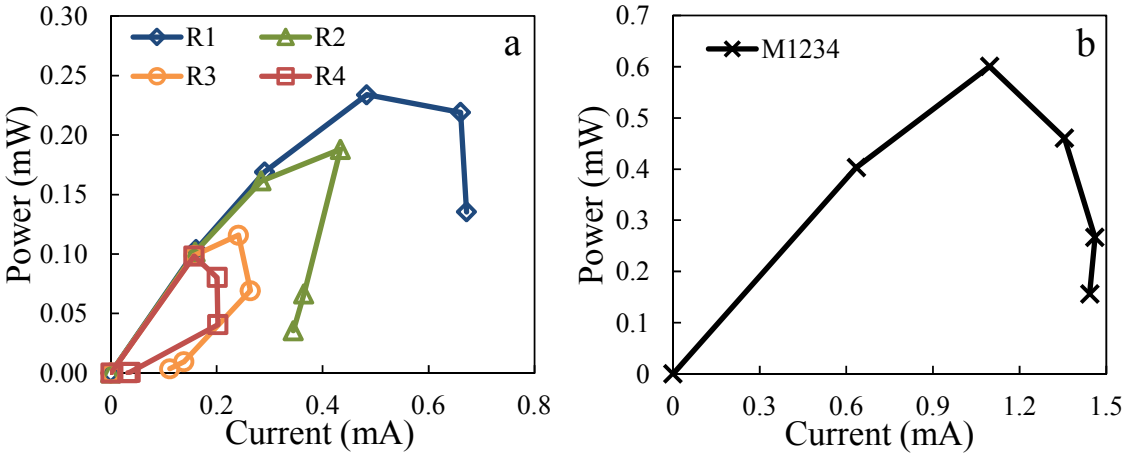

Figure 3-4 Power production of the MFC reactors hydraulically connected using needles in continuous flow with the flow from R1 to R4. (a) Individual connection showing the different performance of the four MFC reactors (R1 to R4). (b) Combined connection (M1234). Results are shown for two separate sets of reactors (1-4, and duplicates 5-8 in Fig. A-5).

3.3.2 Effect of external resistance

The external resistances used to compare the combined system with the individual MFCs are particularly important in terms of power production. When the anodes and cathodes of multiple MFCs were electrically connected together to form a single anode and cathode connection, it was determined that the external resistance had to be reduced compared to that used for individual connections in order to obtain the maximum power. In fed-batch operation, the four combined MFCs produced their maximum power at 50 Ω, compared to 200 Ω needed for the MFCs with separately wired anodes and cathodes (Fig. 3-2). Similarly, the maximum power produced by the combined MFCs under continuous flow conditions was obtained at an external resistance of 500 Ω, compared to those (1000 Ω, 2000 Ω and 4000 Ω) for the individual MFCs (Fig. 3-3).

These results on the maximum power at different resistances suggested that polarization and power curves should be conducted to compare the combined electrode system with the individual MFCs, instead of measuring the power production under a single resistance. For example, when a 2000 Ω resistance was used for the four MFC reactors electrically combined in one circuit, the

power was 0.24 ± 0.01 mW, compared to 0.65 ± 0.04 mW obtained by summation of the power produced by the four individual reactors at 2000 Ω (Fig. 3-5). However, when the resistance was decreased to 500 Ω, the power produced by the four combined MFCs increased to 0.64 ± 0.01 mW (Fig. 3-5). Additional examples at different external resistances in both fed-batch operation and continuous flow were provided in Appendix A (Fig. A-6 and A-7).

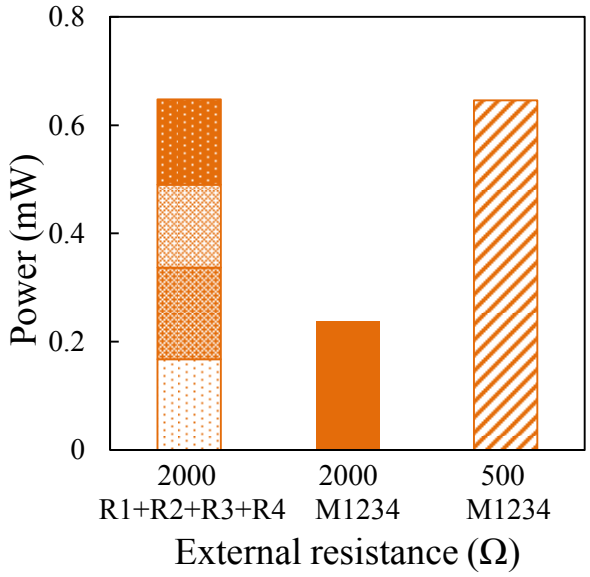

Figure 3-5 Power output of the MFC reactors at individual connection (R1 to R4, 2000 Ω external resistance) and combined connection (M1234, 2000 Ω and 500 Ω external resistance) in continuous flow. Results are shown for two separate sets of reactors (1-4, and duplicates 5-8 in Fig. A-7b).

The reduced external resistance used for the combined MFCs to achieve comparable power to that produced through summation of power of the individual MFCs, indicated a decrease in internal resistance for the combined MFCs. Theoretically, for *n* batteries with same electromotive force (Emf) and internal resistance, an external resistance used for the combined circuit to obtain the same power production to the summation of individual circuits should be 1/*n*, compared to that used in the individually-wired electrode, where *n* is the number of electrodes combined together. This rule can be applied for the multi-electrode MFCs operated in the fed-batch operation, because four reactors had the same performance. However, in continuous flow tests the four MFCs had different internal resistances (Fig. 3-3a) due to the large substrate gradient in the

direction of flow. When the four MFCs were combined to form one circuit, the apparent internal resistance also decreased, but the value was dependent on the individual Emfs and internal resistances.

3.3.3 Current profiles for combined electrodes

When multiple anodes or cathodes are connected together, parasitic current could affect the performance of an adjacent electrode. This parasitic current could arise from differences in potentials between adjacent electrodes that were produced, for example, by differing substrate concentrations among the electrodes. In continuous flow tests, the sCOD concentration was reduced during flow from R1 to R4. Thus, the anode potentials in the direction of flow increased from – 0.39 ± 0.01 V (R1) to – 0.32 ± 0.02 V (R2), – 0.23 ± 0.02 V (R3), and – 0.15 ± 0.01 V (R4) (results using a 125 Ω external resistance). Based on measurements of voltages from each anode and cathode (obtained using a small 10 Ω resistor in each electrical connection to monitor current), the R4 anode (R4A) produced very little current (0.014 mA), compared to the current flowing into the opposing R4 cathode (0.18 mA, R4C) (Fig. 3-6). This imbalanced current flow between the opposing electrodes indicated that there was an ionic current from the anode of the adjacent MFC (R3A) to the opposing cathode (R4C). Similarly, there was also ionic current from the R2 anode (R2A) to the R3 cathode (R3C) as indicated by an unbalanced current between R3A (0.24 mA) and R3C (0.37 mA). The parasitic current flow here was primarily due to the poor performance of the last anode (R4A), as it had very little current production likely due to the low effluent substrate concentration. As a result of the parasitic current flow, more current was produced by R2A (1.09 mA) and R1A (1.25 mA) than those by their opposing cathodes (R2C, 0.90 mA; R1C, 1.18 mA). As a result of this improved anode current flow compensating for the reduced anode current flow, overall reactor performance was not significantly affected.

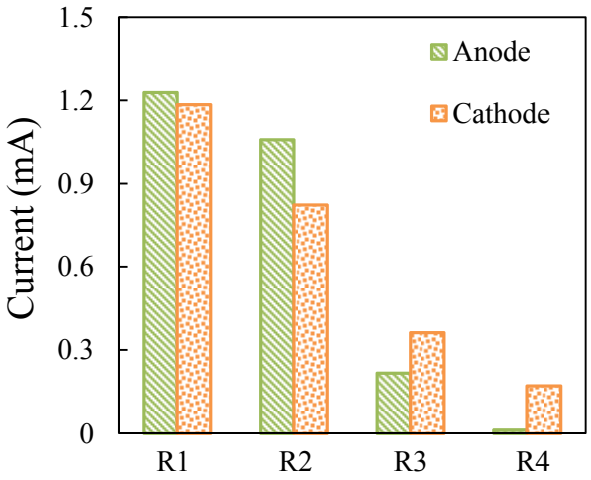

Figure 3-6 Current output of the anodes and cathodes at combined connection (M1234, 125 Ω external resistance) in continuous flow. Results are shown for two separate sets of reactors (1-4, and duplicates 5-8 in Fig. A-8).

The effect of low current generation by an anode was further examined by disconnecting anodes (R1 and R3) under non-substrate limiting conditions (1 g/L sodium acetate) in continuous flow tests (300 Ω external resistance). The four cathodes were always wired together during these tests, while either four working anodes or only two working anodes (R2 and R4) were wired together and connected to the cathodes. When one anode was connected to two cathodes (one opposed, and one adjacent), the current was 1.18 ± 0.01 mA (0.81 ± 0.02 mA by the opposed cathode and 0.37 ± 0.01 mA by the adjacent cathode). This current was slightly higher than obtained by the same anode with a working adjacent anode which produced 1.08 ± 0.01 mA. Parasitic current was also observed from the current producing anodes (R2A and R4A) to the adjacent cathodes (R1C and R3C) opposing the anodes with no current production, resulting in higher anode current production.

3.4. Discussion

These experiments with multiple reactors connected electrically in different ways revealed two important aspects of MFC operation. First, the performance of an electrode could not be properly assessed without conducting polarization tests on each individual electrode. If only a

single resistance was used for testing the power produced by the whole reactor or an individual electrode, the performance of that individual electrode connected separately from other electrodes would appear to be much better than it was when connected with other electrodes. This result was due to the different electrical loads on that electrode when the same resistance was applied for each individual electrode versus the combined electrodes from multiple reactors. Comparisons of power curves for individual versus combined electrodes here indicated that the resistance used for the combined MFCs should be lower than that used for the individual reactors to achieve comparable power production due to a decreased in internal resistance when the anodes and cathodes were connected electrically in parallel. Previously it was reported that anode performance was reduced when all anodes were connected together in a reactor containing a single cathode (Ahn and Logan 2013). However, this comparison was based on using the same external resistance (1000 Ω) for the individual electrodes and the combined electrodes. Our results here suggest that the resistor used for the combined anodes should have been much lower than the 1000 Ω used for the individual anodes. The best way to compare individual electrode performance is therefore to conduct polarization tests on each individual anode. It was shown here that a power curve based on the summed power produced by the four individual reactors was essentially identical to that of the MFC with the four anodes wired together and the four cathodes wired together in fed-batch operation (Fig. 3-2b). While in continuous flow, the summed maximum power from the power curves of the four individual MFCs was slightly higher (15%) than that from the power curve of the combined MFC (Fig. 3-3)

A second important finding was that the substrate concentration differences at the anodes, produced under continuous flow conditions, had more of an effect on the performance of multiple reactor systems than parasitic current between the electrodes. In continuous flow operation, the four individual MFCs can have different Emfs and internal resistances at the substrate concentration where they achieved their maximum power. A loss in maximum power could result when MFCs with different Emfs and internal resistances are combined into a single circuit

because of the differences in these systems. Therefore, there is no single external load that could be chosen that would allow all the individual reactors to produce their maximum power.

Parasitic current flow between adjacent electrodes, determined from individual electrode measurements and by disconnecting electrodes, did not appreciably affect the overall performance of the multi-electrode MFC, although it did alter the current produced by the individual electrodes. The anode near the exit of the flow from the MFC (R4) produced very little current when wired to other anodes. However, while the R4 anode (R4A) generated little current, the adjacent anode (R3A) generated a higher current as a result of an ionic flux supported by both its opposing cathode (R3C) and the adjacent cathode (R4C). This resulted in greater current generation by R3A than would be possible in the absence of R4C, as further shown in tests comparing performance of anodes with and without the adjacent anode electrically connected to the circuit. As a result of this improved anode current flow compensating for the reduced anode current flow, overall reactor performance was not affected.

Research by others suggested that completely separating reactors, so that there was no fluid connections between them, might further improve power production compared to the case here with all electrodes exposed to the same fluid (Aelterman et al. 2006, Kim et al. 2012a, Ledezma et al. 2013). However, additional tests using reactors connected hydraulically by very thin needles showed the same performance as those connected by windows, in terms of power production for different electrode connections (Fig. 3-3 and 3-4), although a very large solution resistance created by the needle bridge had reduced the parasitic current to a level below the detection limit ($<10^{-3}$ mA). This further suggested that parasitic current would not affect MFC performance when the electrodes sharing the same electrolyte were wired together, and thus completely separating reactors might not improve power production.

3.5. Conclusions

The best way to compare the performance between the combined MFCs and the individual reactors is to conduct polarization tests. Changes in substrate concentration with flow through the reactors can result in differences in internal resistance among the reactors, which can preclude accurate comparison based on a single external resistance. When compared on the basis of polarization data, the MFCs with the electrodes wired together showed no differences in power production from that obtained by summing power from the individually wired reactors in fed-batch operation. Even in continuous flow conditions, where the substrate concentration significantly affected the anode potentials and MFC performance, the maximum power of the combined MFC was only slightly lower than that summed of the four individual reactors. Parasitic current flow measured for MFCs hydraulically connected in series and electrically in parallel showed, no appreciable impact on reactor performance, and thus there was no need for electrolyte isolation between adjacent reactors under such flow conditions.

Chapter 4

High current densities enable exoelectrogens to outcompete aerobic heterotrophs for substrate in microbial fuel cells

Abstract

In mixed-culture microbial fuel cells (MFCs), exoelectrogens and other microorganisms compete for substrate. It has been assumed that coulombic efficiencies (CEs) increase with current densities due to shorter cycle times, and therefore less loss of substrate to microbial respiration using dissolved oxygen (DO). To better understand this competition for substrate through current generation or aerobic respiration, COD concentrations were measured over time in fed-batch, single-chamber, air-cathode MFCs at different current densities (external resistances). Reactors were sacrificially sampled during the cycle, with each reactor sampled only once to avoid oxygen contamination during sampling. COD degradation rates were all first order at the different conditions, and increased from 0.14 ± 0.01 h^{-1} (open circuit) to 0.33 ± 0.02 h^{-1} at a maximum current density of 3.43 A/m^2 (100 Ω). Increased COD removal rates resulted from a faster rate of COD consumption by exoelectrogens at lower resistances. Since COD removal in open circuit controls followed first order kinetics, less COD was lost to aerobic heterotrophs as substrate concentrations decreased more rapidly with current generation. Higher CEs were therefore due to greater rates of substrate uptake by exoelectrogens, and not just constant losses of substrate to DO. These results show that higher current densities (lower resistances) redirect a greater percentage of substrate into current generation, enabling an increase in CEs.

4.1 Introduction

A microbial fuel cell (MFC) is a device in which microorganisms oxidize organic matter and transfer electrons to the anode, generating a current through an external circuit to the cathode where typically oxygen is reduced (Du et al. 2007, Logan et al. 2006, Oh et al. 2010). In a mixed-

This chapter was submitted as: Ren, L. J., Zhang, X. Y., He, W. H., and Logan, B. E. High current densities enable exoelectrogens to outcompete aerobic heterotrophs for substrate.

culture MFC, exoelectrogens capable of electron transfer outside the cell membrane (Logan et al. 2006) compete for substrate with other microbial functional groups, such as fermenters, methanogens, and heterotrophs (Jung and Regan 2011). Only a few previous studies have focused specifically on this competition for electrons by microorganisms in MFCs (Freguia et al. 2007, Jung and Regan 2011). These studies have been conducted using two-chamber MFCs that have lower current densities and less oxygen diffusion into the anode chamber than single-chamber, air-cathode MFCs (Fan et al. 2007, Liu et al. 2008, Zhu et al. 2011). Thus, there is a need to better understand how competition between exoelectrogens and other microorganisms affects the extent of conversion of substrate into current, and the maximum current densities that can be produced in these single-chamber systems.

Coulombic efficiency (CE), defined as the ratio of the coulombs recovered as electrical current to that available in the substrate that is removed from solution (Logan 2008), is used to evaluate how much of the substrate is converted into electricity. The higher the value of the CE, the more of the electrons stored in the substrate are extracted as electricity energy. In single-chamber MFCs, lowering the external resistance increases the maximum and average current density, and increases the CE (Hays et al. 2011, Liu and Logan 2004, Zhang et al. 2010, Zhang et al. 2011c). The change in the CE is thought to be related primarily to a constant loss of substrate to heterotrophic substrate removal using oxygen that leaks into the anode solution through the air-cathode (Logan 2012). An increase in the current using a lower external resistance should decrease the required cycle time, resulting in a greater proportion of flow of electrons from the substrate to current compared to loss of substrate to aerobic heterotrophs. This explanation is based on the assumption that the two processes proceed independently, i.e. that the conversion of substrate into current is not intrinsically affected by the specific resistance used. However, anode potentials increase with current generation and exoelectrogens important for current generation, such as *Geobacter sulfurreducens,* express different cytochromes at different anode potentials (Inoue et al. 2010, Katuri et al. 2010, Wagner et al. 2010, Zhu et al. 2012). Therefore, changing

the resistance and current density could change the rate of electron transfer by the biofilm as well as the efficiency of energy conversion into biomass. It has also been observed that CEs can decrease at very high current densities in single-chamber air-cathode MFCs (Yang et al. 2013), making it difficult to conclude that the rate of substrate conversion into electrical current is independent of current density. CEs are usually calculated on the basis of the solution chemical oxygen demands (CODs) measured only at the beginning and end of a fed-batch cycle (Liu et al. 2005, Liu and Logan 2004, Logan et al. 2006). Typical COD removals are >90% in single-chamber, air-cathode MFCs with acetate as the sole substrate (Cheng et al. 2006a, Liu and Logan 2004, Pant et al. 2010). The rate of COD removal in an MFC, however, is not necessarily proportional to current generation. In some cases, high current densities were maintained even after the substrate had been reduced to low concentrations in the solution (Freguia et al. 2007). Therefore, COD removal cannot be simply calculated over a fed-batch cycle by assuming its removal in proportion to current. In order to calculate COD removal rates, the CODs must be measured over time.

The aim of this study was to better understand how current generation affects CEs in single-chamber MFCs by directly measuring substrate concentrations over time in order to determine substrate used by exoelectrogens versus loss of substrate to aerobic heterotrophic microorganisms. In order to evaluate substrate losses to aerobic heterotrophs, COD and dissolved oxygen (DO) concentrations were measured under open-circuit conditions in identical reactors. Oxygen mass transfer coefficients were calculated to estimate the rate of oxygen transfer through the cathode into the bulk solution under both open circuit conditions and with current generation, allowing calculation of the maximum possible substrate consumption by aerobic heterotrophs. Acetate was used as the substrate to avoid substrate losses to fermentative products, and methane production was assumed to be minimal in the air-cathode MFCs based on previous findings (Freguia et al. 2007, Jung and Regan 2011). Therefore, substrate was assumed to be consumed only by exoelectrogens or aerobic heterotrophs. CEs and COD removals were measured at

different current densities using two different criteria to identify the end of a cycle: voltage lower than a fixed value; or current below a fixed value. Comparison of these two different criteria allowed us to better evaluate the flow of COD into current compared to aerobic processes.

4.2 Materials and methods

4.2.1 Reactor and operation

Single-chamber, air-cathode MFCs were cube-shaped blocks made of Lexan, having cylindrical chambers with a volume of 14 mL (7 cm^2 cross sectional area) as previously described (Liu and Logan 2004). Anodes were made of non-waterproof carbon cloth (#CCP40, Fuel Cell Earth, USA) with a projected surface area of 7 cm^2. Air cathodes (7 cm^2) were made of waterproof carbon cloth (30 wt.%, #CC640WP30, Fuel Cell Earth, USA), with a catalyst loading of 0.5 mg-Pt/cm^2 on the water side, and four PTFE diffusion layers on the air side (Cheng et al. 2006a). The electrode spacing was 2 cm (anode surface to cathode surface). A reference electrode [Ag/AgCl; +200 mV vs. standard hydrogen electrode (SHE); BASi] was inserted into the middle of reactor to determine anode and cathode potentials. All electrode potentials were reported versus the Ag/AgCl reference electrode.

The MFCs were started and operated in fed-batch mode, with the growth medium replaced when the voltage decreased to 0.05 V, or the current decreased to 0.05 mA. The medium contained (per liter): 0.5 g CH_3COONa, 10 mL vitamins, and 10 mL minerals (Balch et al. 1979) in a 50 mM PBS buffer (0.31 g NH_4Cl, 2.45 g $NaH_2PO_4 \cdot H_2O$, 0.13 g KCl, 4.58 g Na_2HPO_4; pH = 7.1 ± 0.2, conductivity γ = 7.6 ± 0.2 mS/cm). Five MFC reactors were used, with tests duplicated. Error bars shown in the results are based on ±SE (standard error). All the experiments were conducted in a constant temperature room (30 °C). All the measurements were carried out after the MFC reactors exhibited stable performance, defined as reproducible voltage output over at least three consecutive cycles.

4.2.2 Chemical and electrochemical analysis

Soluble chemical oxygen demand (sCOD) was measured using a standard method (method 5220, HACH COD system, HACH Company, Loveland, CO) (APHA 1998). Samples were filtered using 0.45 μm pore diameter syringe filters (polyvinylidene difluoride, PVDF, 25 mm size, Restek Corporation, USA). sCOD removal was calculated for a complete cycle as $R_{sCOD} = [(sCOD_{in} - sCOD_{out})/sCOD_{in}] \times 100\%$, where *in* and *out* subscripts refer to sCODs at the beginning or end of the cycle. When sCOD concentrations were measured at different times within a fed-batch cycle, multiple MFC reactors were used. A reactor was sampled (2 mL) only once, and then that reactor was not sampled again. This sampling strategy avoided reusing a reactor that would have had air into the reactor, as the introduction of oxygen in air would have altered the results on COD utilization by exoelectrogens versus aerobic heterotrophs. sCOD degradation rates were modeled using a first order reaction, or $d(sCOD)/dt = -k_1\, sCOD$, where k_1 is the first order reaction rate constant (h^{-1}), and *sCOD* is measured at time *t*. The sCOD degradation rates were measure in MFCs with 1000 Ω, 300 Ω, or 100 Ω external resistances, or under open circuit conditions.

Oxygen transfer through the air-cathode into the bulk solution in an abiotic reactor was characterized using the oxygen mass transfer coefficient , $\boldsymbol{k}$ (cm/s), calculated as $\boldsymbol{k}\, t = -(v/A) \ln[(DO_s - DO)/DO_s]$, where *v* is the volume of the chamber (14 mL), *A* the cross sectional area (7 cm^2), *DO* the bulk oxygen concentration of the solution at time *t*, and DO_s the concentration at the air side of the cathode (assumed to be saturation, 7.7 mg/L) as previously described (Cheng et al. 2006a). The two-chamber reactor used in these oxygen transfer tests was constructed from two cube-shaped Lexan blocks each having the same configuration as that used for the MFC reactor, but separated by an anion exchange membrane (AMI-7001, Membrane International Inc., NJ) (Kim et al. 2007) (Fig. B-3). The anode and cathode were made of the same materials and sizes as those used in the MFCs. The anolyte was a 0.4 mol/L potassium ferrocyanide ($K_4[Fe(CN)_6]\cdot 3H_2O$) solution and the catholyte was 50 mM PBS buffer. A non-consumptive DO

probe (FOXY, Ocean Optics, Inc., USA) was inserted in the middle of the cathode chamber, between the air-cathode and the anion exchange membrane. This positioning method allowed measurement of the DO concentrations in the chamber due to oxygen in air diffusing through the air-cathode, which was occurring in the single-chamber MFCs. Oxygen transfer coefficients were calculated for two different conditions: open circuit; and a current density of 4.3 A/m^2 set using a potentiostat (VMP3 Multichannel Work-station, Biologic science instruments, USA). DO concentrations were also measured in MFCs at the same current densities (50 Ω external resistance) and at different positions in the reactor (anode side, middle of the chamber and cathode side). Conductivity and pH were measured using a probe (SevenMulti, Mettler-Toledo International Inc.).

A multimeter (model 2700; Keithley Instruments, Inc.) was used to record the voltage of the MFCs at 20 minute intervals, with the power calculated as $P = IU$, and the current calculated using Ohm's law ($I = U/R$), where U is the measured voltage (V), and R the external resistance (Ω) (Hong et al. 2011). Current density (j; A/m^2) was normalized to the cathode projected surface area of 7 cm^2. When a single current density is used to characterize the cycle at a fixed external resistance, it refers to the maximum current density produced at the beginning of the cycle. Columbic efficiency was calculated as $CE = C_t/C_{th} \times 100\%$, where C_t was the total coulombs calculated by integrating the current over time ($C_t = \Sigma\, I \cdot \Delta t$, where Δt was the time interval of 20 minutes), and C_{th} was the theoretical amount of coulombs available based on the sCOD removed in the MFC over time or in the complete fed-batch cycle. Polarization data were obtained using the multiple-cycle method (two cycles for each external resistance) by changing the external resistances from 1000, to 500, 200, 100, and 50 Ω.

4.3 Results

4.3.1 COD degradation at different current densities

Substrate concentrations decreased faster with lower resistances, producing higher current densities. At open circuit with no current flow, the solution sCOD concentration decreased much more slowly than when it did with current generation (Fig. 4-1a). After 9 hours, there was still 130 mg/L sCOD (33% of the original concentration) left in the solution without current production, compared to 44 – 48 mg/L sCOD (8 – 12% of the original concentration) when producing current (Fig. 4-1a). Although the sCOD final concentration was nearly the same with different external resistances and current densities, a detailed measurement of the sCOD concentration versus the time showed that sCOD decreased faster when the current densities increased from 0.77 A/m^2 to 3.43 A/m^2. For example, at 5 hours, the solution sCOD was 133 mg/L (32% of the original concentration) at a current density of 0.77 A/m^2 (1000 Ω), compared to 85 mg/L (23% of the original concentration) at 2.14 A/m^2 (300 Ω), and 77 mg/L (18% of the original concentration) at 3.43 A/m^2 (100 Ω) (Fig. 4-1).

The COD concentrations showed good agreement with the assumption of first order kinetics (Fig. 4-1a). The calculated reaction rate constants increased with current densities, indicating that substrate was consumed faster with higher current densities. The first order reaction rates increased from 0.14 ± 0.01 h^{-1} at open circuit, to 0.21 ± 0.01 h^{-1} (0.77 A/m^2 current density), 0.28 ± 0.01 h^{-1} at 2.14 A/m^2, and 0.33 ± 0.02 h^{-1} at 3.43 A/m^2. This result shows that the substrate removal rate under open circuit conditions (i.e. by microorganisms using oxygen) is reduced in proportion to the bulk substrate concentration. Therefore, when current is generated, and the substrate is removed faster, then the rate of loss of substrate to aerobic heterotrophs will decrease. Thus, the rate of substrate loss to aerobic processes is not constant when current is generated, as has previously been assumed.

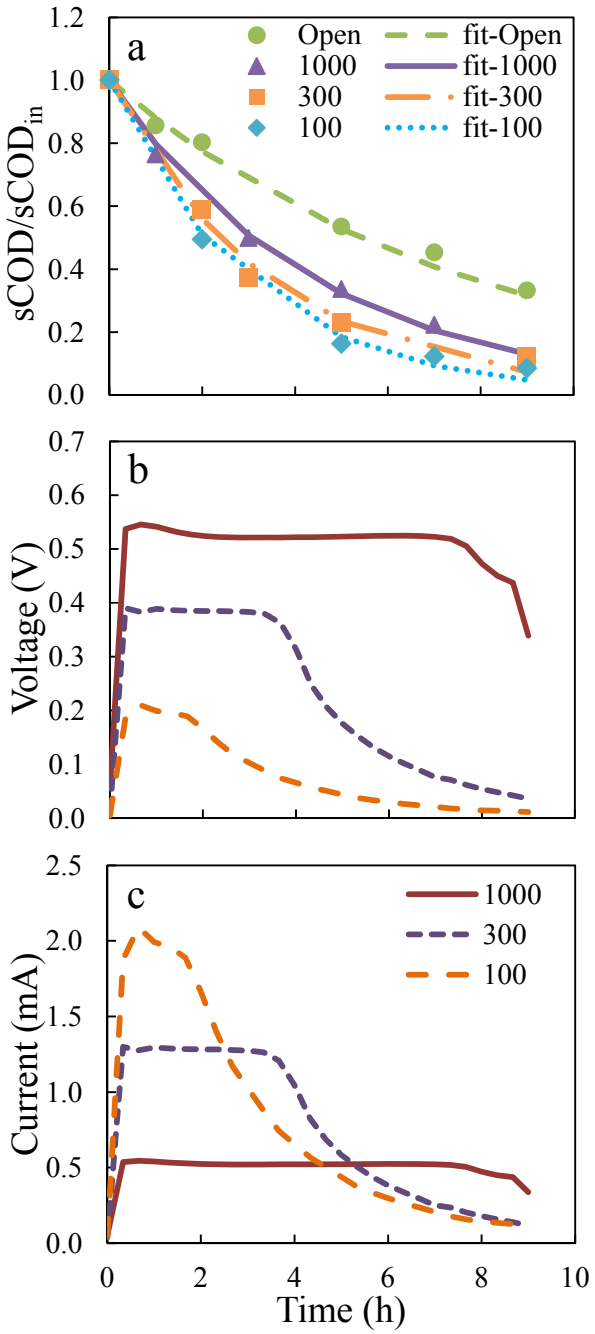

Figure 4-1 (a) sCOD concentrations over time in fed-batch cycles at different external resistances (1000, 300, and 100 Ω) and open circuit. The data were fitted assuming first-order kinetics, with sCOD concentrations normalized by the initial sCOD. Example data for a single cycle at different external resistances showing (b) voltage, and (c) current.

4.3.2 Oxygen transfer rate at different current densities

Current generation could also alter the amount of oxygen entering the reactor through the cathode, which could affect CEs. The oxygen mass transfer coefficient measured in abiotic

reactors through the air-cathode into the bulk solution decreased slightly (12%) when the current densities increased from zero at open circuit to 4.3 A/m^2 (Fig. 4-2). By the end of the measurement, the DO concentration in the bulk solution had increased to 5.8 mg/L with an open circuit, compared to 4.0 mg/L at a current density of 4.3 A/m^2 (Fig. 4-2a). The calculated oxygen transfer rates were 2.5 ± 0.1 × 10^{-3} cm/s for the open circuit reactor, compared to 2.2 ± 0.1 × 10^{-3} cm/s at 4.3 A/m^2 (Fig. 4-2b). The most likely reason for the net decrease in oxygen transfer into the solution was the oxygen utilization in the cathode for current generation.

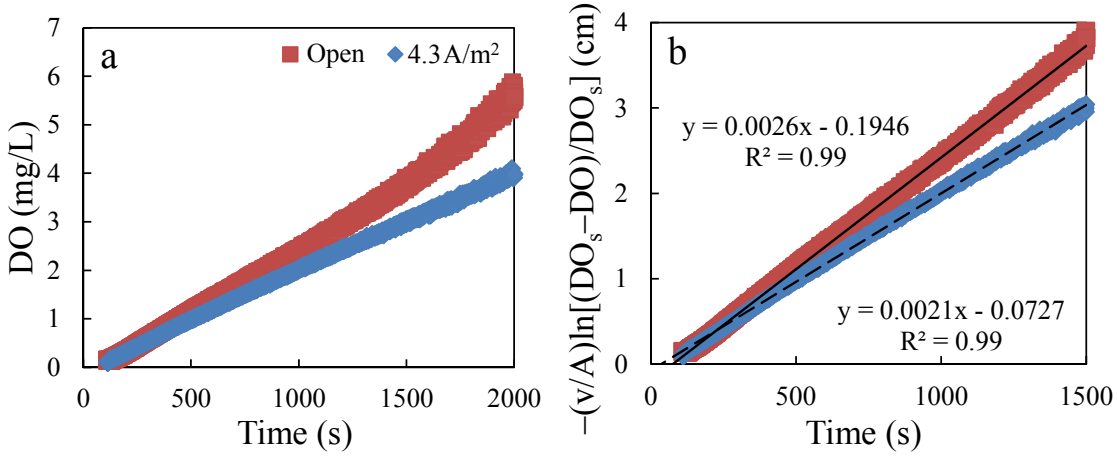

Figure 4-2 Oxygen transfer in the abiotic reactor at open circuit and current density of 4.3 A/m^2: (a) dissolved oxygen (DO) concentrations and (b) linearized DO data used to calculate oxygen mass transfer coefficient.

The DO concentrations measured in the MFCs at different current densities showed a different trend than the abiotic reactors in terms of the resulting DO concentrations in the presence and absence of current generation. The DO concentrations in these tests were all in the range of 0.93 – 0.96 mg/L, with no apparent correlation with open or closed circuit conditions and current densities. It was expected that under open circuit conditions that slightly more oxygen would be consumed by microorganisms than that with current production, based on the abiotic tests that showed more oxygen could be transferred into the reactors under open circuit conditions. The DO concentrations at different locations in the anode chamber were relatively homogeneous, with 0.96 ± 0.04 mg/L near the cathode, 0.94 ± 0.04 mg/L in the middle of the chamber, and 0.95

± 0.02 mg/L near the anode. This homogeneity of DO in the solution suggests that most oxygen that leaked into the MFC through the air-cathode was consumed by the cathode biofilm.

4.3.3 Measurements of COD removals and CEs

COD removals varied when different cycle termination criteria were used. When the cycles were ended at a voltage of <0.05 mV, COD removals decreased from 93% to 74% with increased current densities (Fig. 4-3a), mainly due to the shortened cycle length at higher current densities (Fig. 4-3c). For example, when a low voltage was used to end the cycle, 36% of the COD was left at 3.43 A/m^2 (3 h, 0.1 V voltage) compared to 19% at 2.14 A/m^2 (6 h, 0.1 V voltage) and less than 12% at 0.77 A/m^2 (9 h, 0.3 V voltage) (Fig. 4-1). Thus, the higher currents resulted in reaching the endpoint sooner due to the much lower voltages produced at the lower resistance. In contrast, COD removals all were consistently high (93 — 96%) at all current densities (Fig. 4-3a), when the cycles were stopped when the current decreased to <0.05 mA as the cycle length was all about the same (15 h) (Fig. 4-3d). As the COD concentrations in the solution always decreased to about the same low level after 9 h at different current densities (Fig. 4-1a), the COD concentrations measured at 15 h were not substantially different.

The CEs showed different trends with the increase of current densities when different cycle termination criteria were used. CEs increased from 40% to 59% when the current density increased from 0.77 A/m^2 to 3.04 A/m^2, independent of the criterion used to end the cycle (Fig. 4-3b). CEs measured overtime (based on data in Fig. 4-1) also showed this same trend that CEs increased with current density (Appendix B, Fig. B-1). However, at a higher current of 3.8 ± 0.3 A/m^2, the CE decreased to 44% when the fed-batch cycle was ended at a voltage <0.05 mV, but increased slightly to 61% when the cycle was ended at a current <0.05 mA (Fig. 4-3b). This decrease of CEs at high current density was also previously reported when a voltage <0.05 mV was used as the criterion for ending the fed-batch cycle (Yang et al. 2013)

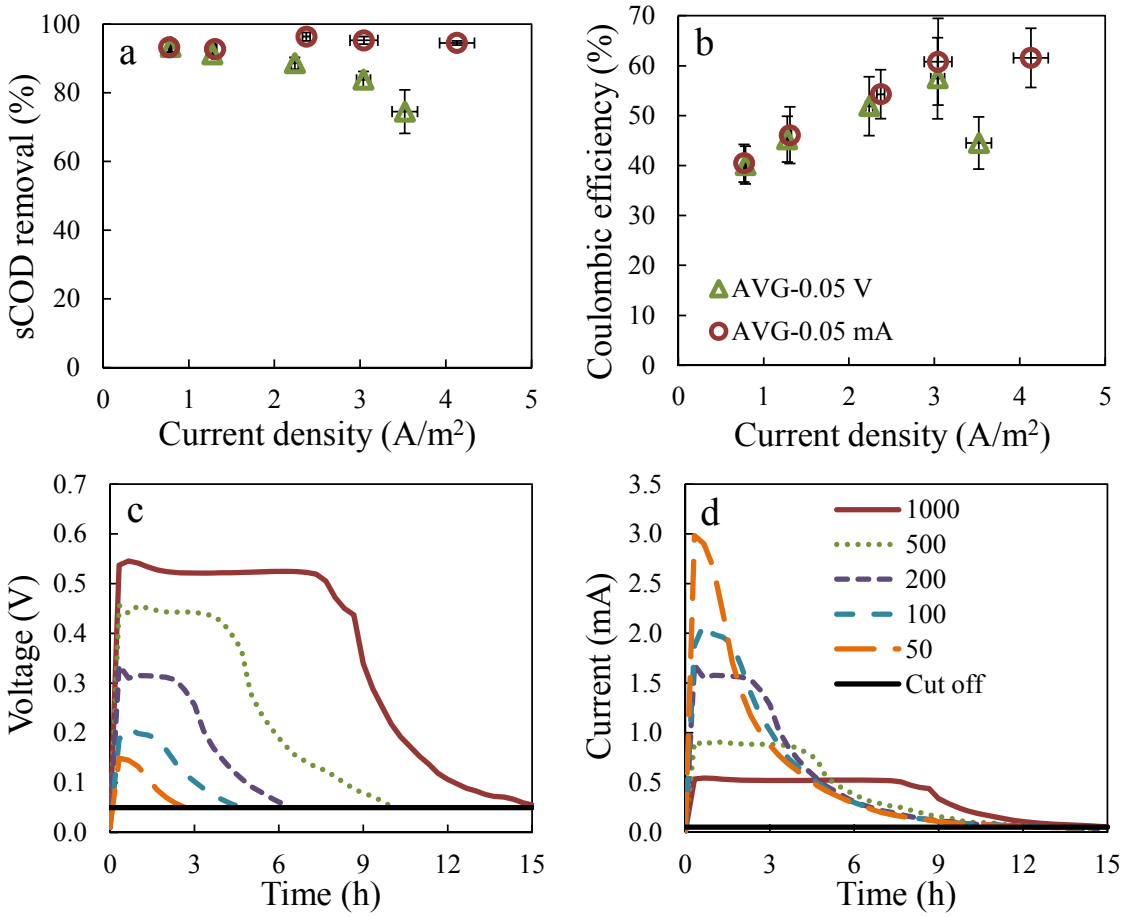

Figure 4-3 Coulombic efficiencies and sCOD removals measured using different final criteria (voltage <0.05 V, or current <0.05 mA): (a) sCOD removals and (b) CEs. Example data for a fed batch cycle at different external resistances (1000, 500, 200, 100, and 50 Ω): (c) cycles ended at voltage <0.05 V and (d) cycles ended at <0.05 mA.

4.4 Discussion

The results obtained in this study revealed two important aspects in MFC operation relative to competition for substrate and criteria used to end a fed-batch cycle. First, high current densities enabled exoelectrogens to obtain a greater proportion of the substrate compared to aerobic heterotrophs. The increased first-order rate constants showed that substrate was consumed faster with an increase in current density. This increased rate of substrate degradation was attributed to the increased consumption by exoelectrogens, as it was shown in abiotic reactors that less oxygen could be transferred into solution with current production compared to an open circuit. With an open circuit, 67% substrate in the biotic MFCs was used by heterotrophs after 9 h (assuming

exoelectrogens did not consume substrate without current generation) (Fig. 4-1a). When the current density was 2.14 A/m^2, ~35% was consumed by heterotrophs based on 88% COD removal and 53% of the substrate converted to electricity by exoelectrogens (based on the total coulombs transferred over the same period of time) (Fig. 4-1). Part of the reduction in substrate consumption by aerobic heterotrophs could be due to less oxygen transfer into the reactor. However, the abiotic tests results suggest that there would be only a 12% reduction in loss in substrate due to oxygen transfer into the reactor over a period of 9 h (detailed calculations are in Appendix B.1). Therefore, the main reason for the decrease in substrate used by heterotrophs was likely the faster depletion of the substrate that resulted with current generation, as it was shown that aerobic heterotrophic uptake of substrate (using open circuit tests) was first order with respect to COD. Therefore, a faster reduction in the COD concentration with current generation would reduce the rate of substrate consumed by aerobic heterotrophs. A similar conclusion regarding the importance of substrate reduction was found in two-chamber MFCs, where oxygen diffusion through the membrane into the anode chamber was much lower than that in single-chamber MFCs through the cathode (Jung and Regan 2011).

A second important finding here is that a low current, rather than a fixed voltage, was a better criterion for fed-batch cycle termination. When current was used to end the cycle, all reactors had a similar cycle length at the different external resistances (Fig. 4-3d), and the CEs all increased with current density (Fig. 4-3b). The increase in CEs at high current densities resulted from greater flow of substrate into current, due to exoelectrogens outcompeting heterotrophs for substrate. However, a decrease of CE at the highest current density was found here, as well as in a previous study (Yang et al. 2013) when voltage was used as the criterion to end the fed batch cycle. As the main goal in an MFC experiment is to fully reduce the COD concentration in the reactor, low current should be used in fed-batch tests as the criterion to terminate the cycle and not low voltage.

4.5 Conclusions

The COD degradation rate was increased with current generation due to the greater consumption of substrate by exoelectrogens compared to aerobic heterotrophs. Substrate removal rates could be described by first order kinetics at each different current density, with an increase in first order rate constants with lower external resistances (higher current densities). This increase in the rate constant, combined with oxygen transfer measurements, showed that less substrate was lost to aerobic heterotrophs with current production. Higher current densities therefore enabled exoelectrogens to outcompete aerobic heterotrophs for substrate in the single-chamber, air-cathode MFCs. This increased substrate uptake by exoelectrogens allowed for increased CEs at higher current densities, rather than greater losses of substrate by higher oxygen leakage into the reactor as the cycle length was constant under these conditions. Additional tests further showed that a minimum current, rather than a low voltage, was a better criterion for ending a fed-batch cycle as the cycle length with different external resistances was nearly constant and much longer than that needed for COD removal.

Chapter 5

Domestic wastewater treatment with a two-stage microbial fuel cell and anaerobic fluidized bed membrane bioreactor (MFC-AFMBR)

Abstract

Microbial fuel cells (MFCs) are a promising technology for energy-efficient domestic wastewater treatment, but the effluent quality has typically not been sufficient for discharge without further treatment. A two-stage laboratory-scale combined treatment process, consisting of microbial fuel cells and an anaerobic fluidized bed membrane bioreactor (MFC-AFMBR), was examined here to produce high quality effluent with minimal energy demands. The combined system was operated continuously for 50 days at room temperature (~25 °C) with domestic wastewater having a total chemical oxygen demand (tCOD) of 210 mg/L. At a combined hydraulic retention time (HRT) for both processes of 9 h, the effluent tCOD was reduced to 16 mg/L (92.5% removal), and there was nearly complete removal of total suspended solids (TSS; from 45 mg/L to <1 mg/L). The AFMBR was operated at a constant high permeate flux of 16 L/m2/h with no significant membrane fouling during the entire study, and no backwashing or chemical cleaning. Total electrical energy required for the operation of the MFC-AFMBR system was 0.0186 kWh/m3, which was slightly less than the electrical energy produced by the MFCs (0.0197 kWh/m3). The energy in the methane produced in the AFMBR was comparatively negligible (0.005 kWh/m3). These results show that a two-stage MFC-AFMBR system could be used to effectively treat domestic primary effluent at ambient temperatures, producing high effluent quality with low energy requirements.

This chapter was submitted as: Ren, L. J., Ahn, Y., and Logan, B. E. Domestic wastewater treatment with a two-stage microbial fuel cell and anaerobic fluidized bed membrane bioreactor (MFC-AFMBR) system.

5.1 Introduction

Growing concerns over the large energy requirements needed for effective wastewater treatment has stimulated interest in the use of wastewater as a source of renewable energy (Kim et al. 2011a). Microbial fuel cells (MFCs) are being developed as a sustainable energy technology, as they can directly produce electricity from wastewater allowing for energy recovery to offset the costs of wastewater treatment (He 2013, Logan and Rabaey 2012). In an air-cathode MFC, organic matter in wastewater is oxidized by microorganisms, and electrons discharged to the anode travel through an external circuit to the cathode where they combine with oxygen, forming water (Logan et al. 2008, Logan and Regan 2006a). Passive transfer of oxygen to the air-cathode avoids the need for energy intensive aeration of the wastewater that is currently required for typical activated sludge or aerobic membrane bioreactor processes. In addition, MFCs have lower sludge production than conventional aerobic treatment processes, which could reduce treatment costs and the challenges associated with sludge treatment and disposal (Rabaey and Verstraete 2005).

MFCs fed domestic wastewaters have shown good performance in terms of electricity generation and simultaneous wastewater treatment (Liu and Logan 2004, Min and Logan 2004, You et al. 2006), and there continue to be improvements in MFC designs that have produced configurations more suitable for scaling up to larger systems (Ahn and Logan 2013, Du et al. 2007, Hays et al. 2011, Zhang et al. 2013c, Zhuang et al. 2012). Capital costs of the materials used in MFCs are also being reduced, for example, by using cathode catalysts such as inexpensive activated carbon (Zhang et al. 2009, Zhang et al. 2011b). One operational aspect of using MFCs for wastewater treatment that has not been sufficiently addressed is the need to meet stringent effluent quality requirements. Effluent chemical oxygen demand (COD) concentrations with domestic wastewater in MFCs have ranged from 23 – 164 mg/L in fed-batch tests, and 60 – 220 mg/L in continuous flow tests, depending on influent COD concentrations, reactor configurations, and cycle time or hydraulic retention time (HRT) (Ahn and Logan 2013, Hays et

al. 2011, Min and Logan 2004). One of the reasons for these high effluent CODs is likely inefficient removal of particulate organics (Huang and Logan 2008), as biofilm reactors such as MFCs and trickling filters are more effective for soluble than particulate COD removal. Thus, post-treatment or integrated processes are needed to further improve the quality of the treated wastewater to meet discharge limits.

One approach to improve the overall extent of wastewater treatment has been to integrate the MFC with a membrane-based process in a single reactor. This approach has been referred to either as a membrane bioelectrochemical reactor (MBER) (Ge et al. 2013) or an electrochemical membrane bioreactor (EMBR) (Wang et al. 2013). Although higher treatment efficiencies have been obtained for both acetate solutions and domestic wastewater in tests with this approach, energy consumption has only been balanced with electrical energy production when acetate was used as the substrate. One main challenges with domestic wastewater treatment is aligning the optimal HRT to minimize energy consumption with the control of membrane fouling (Ge et al. 2013). Using a shorter HRT can optimize treatment efficiency (less reactor volume) but a longer HRT may reduce membrane fouling (Ge et al. 2013). Membrane fouling remains the biggest challenge in the use of membranes in anaerobic systems. In previous studies, membranes inside MFCs have fouled over time, requiring cleaning and treatment. The high maintenance cost of cleaning processes could limit applications of integrated MFC and membrane bioreactor processes.

A new approach to obtain high quality effluent with low energy requirements is proposed here based on using a second stage anaerobic fluidized bed membrane bioreactor (AFMBR) following wastewater treatment in the MFCs. The AFMBR has recently been shown to be an effective approach for achieving high quality effluent when used as a post-treatment method for an anaerobic fluidized bioreactor (AFBR) (Kim et al. 2011a, Yoo et al. 2012). In the AFMBR, membrane fouling is controlled by using granular activated carbon (GAC) as the fluidized particles, as these particles can scour the membrane and minimize fouling (Kim et al. 2011a, Yoo

et al. 2012). The properties of particles used in the fluidized bed are important, as spherical plastic particles have been shown to not be as effective as GAC (Kim et al. 2012b). The use of an MFC as the primary treatment process, as opposed to the AFBR, may be useful for several reasons. First, electrical energy is directly produced in the MFC, whereas in the AFBR electricity would have to be produced in a separate process from biogas that must be cleaned and purified. Second, methane can accumulate to concentrations above saturation, so removing the methane from treated water is important to avoid its release into the atmosphere, as methane is a potent greenhouse gas (Reddy et al. 2013, Yoo et al. 2012). Third, the MFC can be effective over a wide range of temperatures, while the temperature range for effective treatment by methanogenesis can be limited (Li and Yu 2011, Logan and Rabaey 2012).

In this study we examined domestic wastewater treatment using a two-stage MFC-AFMBR system, containing four MFCs and one AFMBR, at ambient temperature. There were two separate flow lines into the AFMBR, with two MFCs connected hydraulically in series (with separate electrical circuits) to avoid large changes in COD concentrations in each reactor that have been shown to adversely affect current generation (Ahn and Logan 2012, Ahn and Logan 2013). Each pair of MFCs had a different electrode configuration: either a separator electrode assembly (SEA), where the electrodes were sandwiched together and a separator was placed between them to prevent short circuiting and reduce oxygen crossover from the cathode; or a spaced electrode assembly (SPA), where the electrodes were kept close to each other, but without contact (no separator was used). It has recently been shown that the SPA design can reduce treatment time, although less energy maybe recovered due to the loss of organic matter to aerobic processes rather than current generation (Ahn et al. 2014). Treatment efficiency was evaluated in terms of COD and total suspended solid (TSS) removals, and energy efficiency was quantified for both processes in terms of production and demands, under continuous flow conditions.

5.2 Materials and methods

5.2.1 Reactors and operation

The two-stage MFC-AFMBR system consisted of four MFC reactors and one AFMBR reactor. The four MFC reactors were arranged in two groups, each group having two MFC reactors with the same electrode configuration that were hydraulically connected in series (Fig. 5-1). Single-chamber, air-cathode MFCs (130 mL) were constructed as previously described (Ahn and Logan 2012). Each reactor contained three brush anodes connected together externally with copper wire, and a single air-cathode. The anodes were graphite fiber brushes (25 mm diameter by 35 mm length) (Mill-Rose, Mentor, OH) heat treated at 450°C for 30 min. The cathode (35 cm^2 projected surface area) was made of wet-proofed carbon cloth (30 wt.%, #CC640WP30, Fuel Cell Earth, USA), with a platinum catalyst (0.5 mg/cm^2) on the water side and four PTFE diffusion layers on the air side (Cheng et al. 2006a).

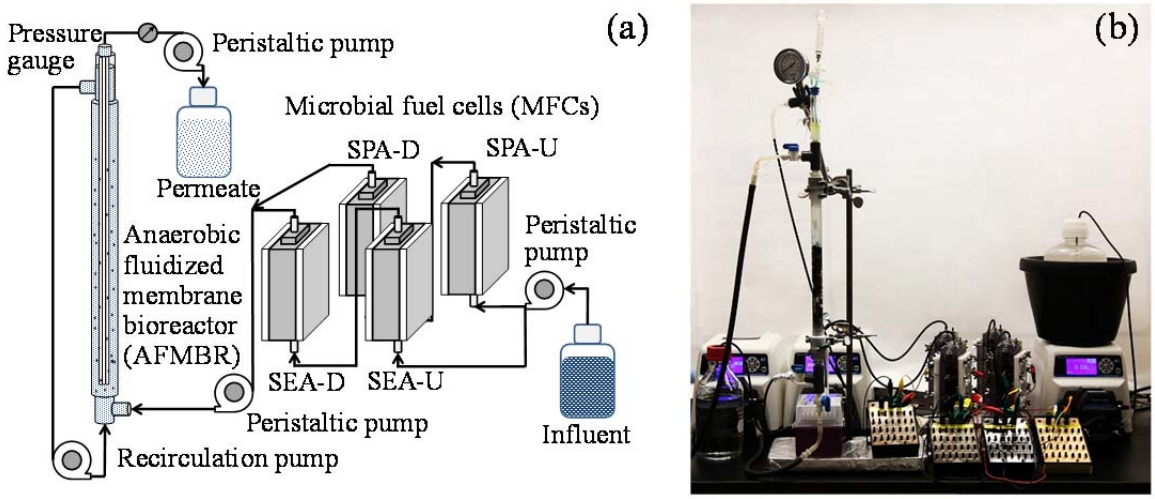

Figure 5-1 Schematic diagram (a) and photo (b) of the two-stage MFC-AFMBR system.

For the SEA MFCs, the brush anodes were trimmed in half to prevent contact by the bristles with the cathode through the separator, as both electrodes were pressed against the separator. Two layers of textile separator (46% cellulose and 54% polyester, 0.3 mm thickness, Amplitude Prozorb, Contec Inc., USA) were used in the SEA reactors to prevent short-circuiting and to

minimize oxygen crossover. The SPA MFCs did not contain separators, so the edge of the brush anodes were set 0.8 cm from the surface of the cathode.

The AFMBR (65 mL) consisted of a 300 mm long by 16 mm diameter clear polyvinyl chloride (PVC) tube (U.S. Plastic Corp.) containing 10 g (wet weight) of GAC (DARCO® MRX, Norit activated carbon) as the fluidized bed medium and support for bacterial growth. The GAC was washed with deionized water for three times prior to use to remove any residuals. The AFMBR contained a submerged membrane module with eight 200 mm long polyvinylidenefluoride (PVDF) hollow fiber membranes (2.0 mm outside diameter, 0.8 mm inside diameter, 0.1 μm pore size, Kolon Inc., South Korea), having a total membrane surface area of 0.004 m^2. An anaerobic tube (10 mL, Bellco Glass, Inc., USA) with the bottom cut off was glued onto the top of the PVC tube and sealed with blue rubber stopper, for biogas collection and measurement.

The MFCs were inoculated and fed with domestic wastewater collected from the primary clarifier of the Pennsylvania State University Wastewater Treatment Plant, and operated in continuous flow mode at an HRT of 4 h. The primary clarifier effluent was collected weekly and stored in a refrigerator (4 ^oC) to minimize COD changes over time. During tests, a container of wastewater was placed in an ice bucket to keep it cool in order to minimize degradation prior to being fed into the MFCs. The wastewater warmed in the tube when it was transferred into the bottom of the reactors using a peristaltic pump (Model NO. 7523-90, Masterflex, USA) at a flow rate of 780 mL/d. The effluent from the top of the upstream MFC reactor flowed into the bottom of the downstream MFC due to the hydraulic pressure. The effluent from the two MFCs series was delivered to the AFMBR using another peristaltic pump (as above), and the flow rate was adjusted at 1560 mL/d to obtain an HRT of 1 h. The top of the membrane module was connected to the same peristaltic pump, to maintain a constant permeate flux of 16 $L/m^2/h$ (LMH) from the AFMBR. The pump was operated with 10 min on and 1 min off cycle time, as it was previous shown that periodic relaxation of the membrane reduced trans-membrane pressure (TMP) (Yoo et

al. 2012). TMP was monitored continuously using a vacuum pressure gauge (Type1490, Ashcroft, USA). Fluidization of GAC was maintained with a peristaltic pump (Model NO. 7523-80) at the desired flow rate of 170 mL/min, resulting in bed expansion of 70 – 80 % to a height of 210 – 240 mm. The combined MFC-AFMBR system was operated at room temperature (~25 °C).

5.2.2 Measurements and chemical analyses

The voltage across an external resistor for the MFC circuit was measured every 20 min using a multimeter (Model 2700; Keithley Instruments, Inc.). Current was calculated using Ohm's law ($I = U/R$), with power calculated as $P = IU$, where U is the measured voltage (V), and R the external resistance (Ω) (Hong et al. 2011). Polarization and power curves were obtained by changing the external resistances from open circuit to 1600, 800, 400, 200, and 100 Ω, with one day at each resistance (six HRTs). Columbic efficiency (CE) was calculated as $CE = C_t/C_{th} \times 100\%$, where C_t is the total coulombs calculated by integrating the current over time ($C_t = \Sigma\, I\, \Delta t$, where Δt is the time interval of one HRT), and C_{th} is the theoretical amount of coulombs available based on the COD removed in the MFC over the same amount of time, calculated as $C_{th} = [F\, b\, (COD_{in} - COD_{out})\, Q\, \Delta t]/M$, where F is Faraday's constant, $b = 4$ is the number of electrons exchanged per mole of oxygen, COD_{in} and COD_{out} are the influent and effluent COD, Q is the flow rate, Δt is the time interval (HRT), and $M = 32$ is the molecular weight of oxygen (Logan et al. 2006).

Chemical oxygen demand (COD) and total suspended solids (TSS) were measured using standard methods (APHA, 1998). Total COD (tCOD) and soluble COD (sCOD) were measured using HACH system (method 5220, HACH Company, Loveland, CO). All samples for sCOD measurement were filtered through 0.45 μm pore diameter syringe filters (polyvinylidenedifluoride, PVDF, 25 mm size, Restek Corporation). Conductivity and pH were measured immediately after sampling using a probe (SevenMulti, Mettler-Toledo International Inc.). Biogas (200 μL samples) of the AFMBR headspace was sampled using gastight syringes

(250 μL; Hamilton Samplelock Syringe) and analyzed using two gas chromatographs (SRI Instruments) for H_2, N_2, CH_4, and CO_2, as described previously (Call et al. 2009). Gas was collected and measured directly using a 10 mL glass syringe (Air-Tite Products Co., Inc., VA, USA) inserted into the top of the AFMBR. Dissolved methane was also measured as described previously (Shin et al. 2011) by transferring a liquid sample from the AFMBR reactor into a serum bottle (6.5 mL, Wheaton, Millville, NJ, USA) without any air contact or headspace, and sealed with a blue rubber stopper. Some liquid (1.5 mL) was then replaced by N_2 gas from the bottle with a syringe. The serum bottle containing liquid sample was autoclaved to prevent biological activity. After establishing gas-liquid equilibrium by shaking the bottle for several hours at room temperature, the amount of dissolved methane was back-calculated from the measured methane amount in the headspace. All samples were collected and analyzed in triplicate.

5.3 Results and discussion

5.3.1 Performance of MFCs

The start-up time needed for the SEA MFCs was shorter than that required for the SPAs. The SEA MFCs produced a stable voltage of 0.59 ± 0.03 V (1000 Ω) after 3 days, while the SPAs produced 0.51 ± 0.04 V after 3 days, and required 10 d to achieve a stable voltage of 0.58 ± 0.01 V. There was no appreciable difference in start-up time between the upstream or downstream MFC within the individual flow paths (data not shown).

The power produced by the SEAs and SPAs changed over time. Based on the polarization data obtained after 1 month, the SEA-U MFC produced a maximum power of 0.31 mW (89 mW/m^2, normalized to the cathode projected surface area of 35 cm^2), which was comparable to that of SPA-U (0.33 mW) (Fig. 5-2a). Although the same current was produced with these two configurations, the SEA-U had better cathode performance but showed poorer anode performance than the SPA-U (Fig. 5-3b and c). The downstream MFCs produced slightly lower maximum power densities than the upstream ones, with 0.28 mW for SEA-D and 0.27 mW for SPA-D (Fig.

5-2a). The downstream MFCs generally had more positive anode potentials than the first MFCs (Fig. 5-3b), likely due to the reduced substrate concentrations.

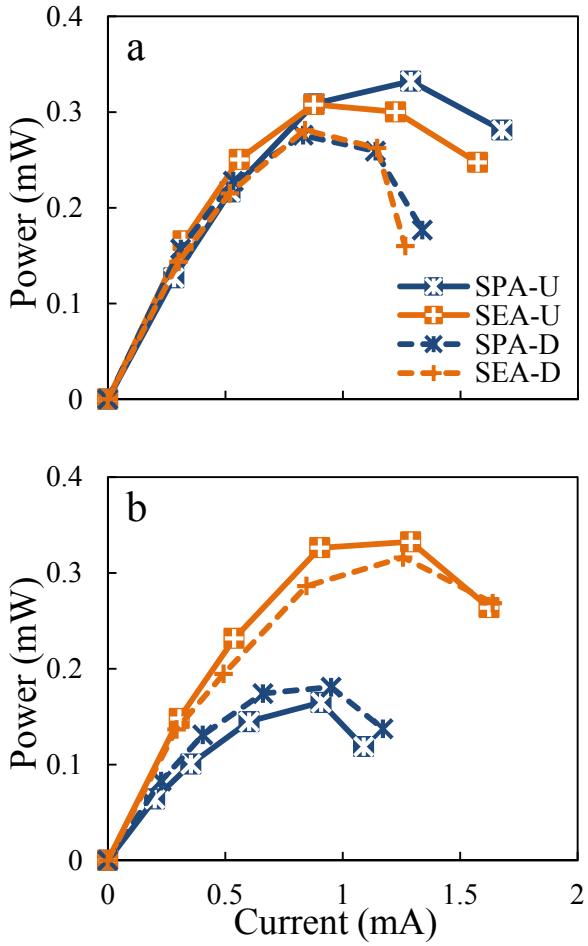

Figure 5-2 Power production of the SEA and SPA MFCs at different time after start-up, after (a) 1 month and (b) 5 months. (U = the first upstream MFC, and D = the second downstream MFC prior to the AFMBR).

After 5 months, the maximum power densities of the SEA MFCs were relatively unchanged (0.33 mW for SEA-U and 0.32 mW for SEA-D) (Fig. 5-2b), and the wastewater composition fed into the reactor was relatively unchanged based on the influent tCOD concentrations (210 ± 11 mg/L at 5 months, compared to 224 ± 17 mg/L at 1 month). However, the maximum power produced by SPA MFCs substantially decreased to 0.16 mW (SPA-U) and 0.18 mW (SPA-D) (Fig. 5-2b). The reason for these decreases was a large reduction in cathode potentials (Fig. 5-3f), which was likely due to biofouling (Zhang et al. 2014, Zhang et al. 2011b). While the cathodes

used for the SEA configuration contained a separator that covered the cathode, the SPA cathodes were directly exposed to the wastewater, and thus they were more prone to fouling (Fig. 5-3f).

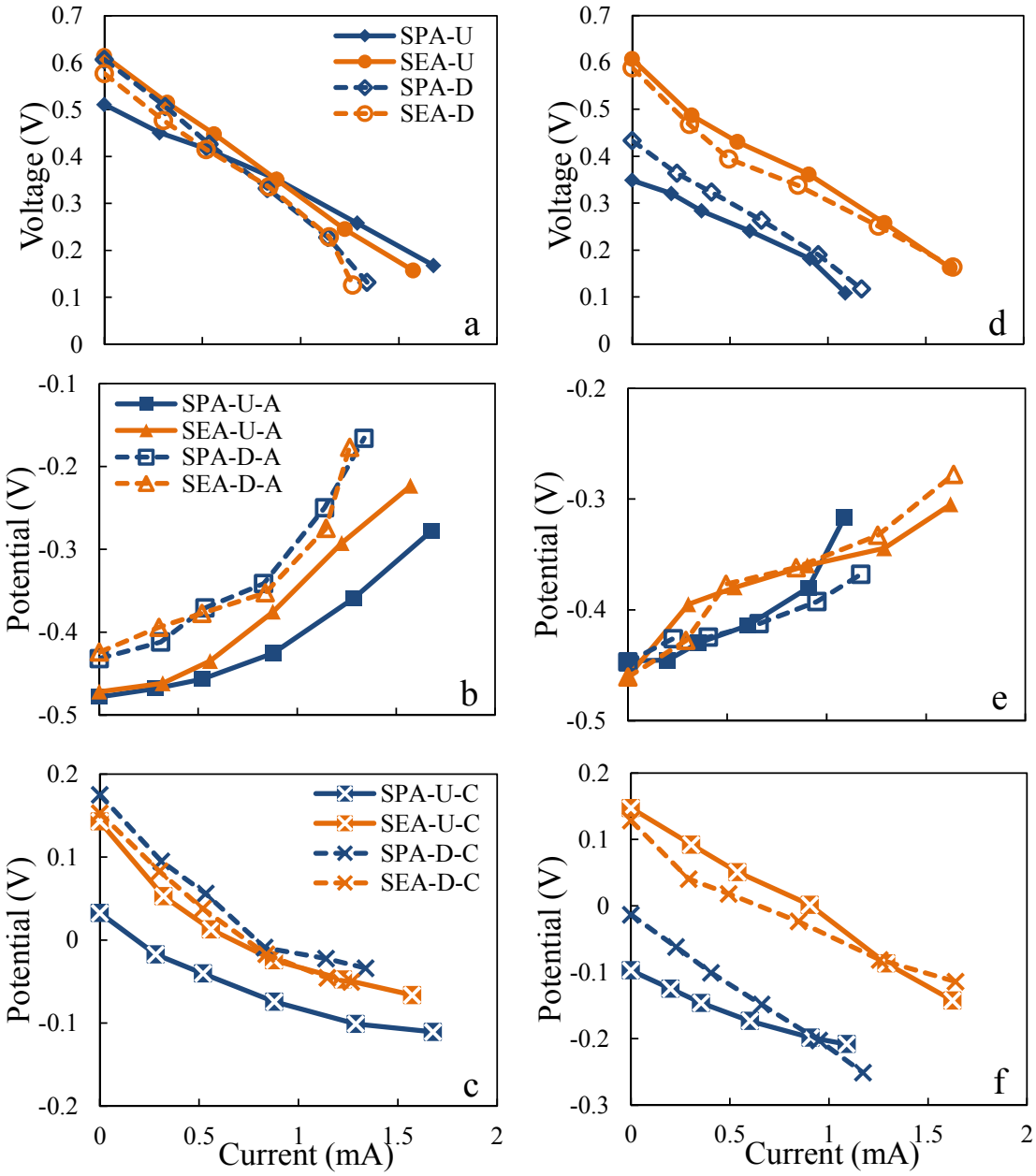

Figure 5-3 Voltage, anode potential and cathode potential of the SEA and SPA MFCs at different time after start-up: (a) voltage, (b) anode potential and (c) cathode potential at 1 month, and (d) voltage, (e) anode potential and (f) cathode potential at 5 month. The letters "A" in (b) indicated the anodes, and "C" in (c) the cathodes.

The maximum power density of 89 ± 6 mW/m^2 produced by the SEA MFC in these continuous flow tests was lower than the maximum power densities obtained in two other studies

with domestic wastewater when the MFC was operated in fed-batch mode [120 mW/m^2 (Ahn and Logan 2013) or 328 ± 11 mW/m^2 (Ahn et al. 2014)]. The lower power density here was likely due to a lower influent COD [217 ± 18 mg/L, compared to 275 ± 71 mg/L (Ahn and Logan 2013) and 303 ± 69 mg/L (Ahn et al. 2014)], and operation under continuous flow conditions, where the average substrate concentration was lower than that in the fed-batch reactors at the beginning of the cycle (Ahn and Logan 2012).

The different electrode configurations (SEA or SPA) did not appreciably affect the extent of COD removal. tCOD removal was 28 ± 7% for SEA-U, comparable to 34 ± 3% for SPA-U. The downstream MFCs had slightly lower tCOD removals than the upstream MFCs, with 16 ± 5% for SEA-D and 19 ± 5% for SPA-D, likely due to the lower substrate concentrations. Fed-batch tests with domestic wastewater have shown that COD removal in MFCs is first order with respect to concentration (unpublished data). Thus, the reduction in COD concentration would have reduced removal rates in the downstream reactors. sCOD removals showed the same trends as tCOD, with greater removals in the upstream reactors (27 ± 10% for SEA-U, 32 ± 5% for SPA-U) than the downstream ones (17 ± 5% for SEA-D, and 26 ± 7% for SPA-D). Note that these COD removals were based on the combination of all data at the different external resistances used in the polarization tests, as the effluent COD concentrations in these tests did not change significantly with the different external resistances. These COD removals were lower than those obtained in previous studies operated in fed-batch mode using the same domestic wastewater source (62 – 93%), due to the short HRT (4 h) in this study compared to much longer fed-batch cycle times (12 – 36 h) (Ahn et al. 2014, Ahn and Logan 2013). Increasing the HRT to 24 h increased COD removals to 67 ± 2%, which was about the same as that obtained in fed-batch mode (65 ± 1%; 500 Ω resistance, data not shown). However, a long HRT is not desirable for efficient wastewater treatment, and thus the shorter HRT was used here.

The CEs increased in proportion to the current (lower resistance), even though the COD removals remained relatively constant with different resistances. At the maximum power density

(0.31 ± 0.02 mW, 0.86 ± 0.02 mA), the overall CE of the SEA MFCs was 18% (13% for SEA-U and 28% for SEA-D). Over time, changes in the CEs paralleled those on maximum power densities. The SEA and SPA MFCs had comparable overall CEs at 1 month (range of 6 – 29%), but after 5 months the SEA MFCs remained relatively unchanged while those of the SPA MFCs decreased (range of 4 – 20%) with the decreased currents. CE values obtained here under continuous flow conditions were comparable to those previously reported for fed-batch conditions (2 – 31%) (Ahn et al. 2014). Overall, these results suggested that the SEA configuration was superior to the SPA design on the basis of fixed HRTs as over time it maintained higher power densities and CEs with the same level of wastewater treatment.

5.3.2 Wastewater treatment with the second stage AFMBR

The two-stage MFC-AFMBR system achieved excellent treatment levels in terms of COD and TSS removals. The AFMBR was first inoculated with anaerobic sludge and fed the effluent from MFCs for two weeks. After that, the membrane module was installed, and the MFC-AFMBR system was operated continuously for 50 days. tCOD further decreased from the influent concentration to the AFMBR of 107 ± 10 mg/L to 16 ± 3 mg/L in the effluent, providing an overall tCOD removal for the two stages of 92.5% (49.1% for the MFCs, and 43.4% for the AFMBR) (Fig. 5-4). The effluent sCOD concentration was identical to the tCOD, and therefore there was a lower sCOD removal of 86.2% (influent sCOD of 114 ± 10 mg/L) (Fig. 5-4). A larger percent of sCOD was removed by MFCs (50.3%) than by AFMBR (35.9%), while particulate COD removal was 47.9% for MFCs compared to 52.1% for the AFMBR. The effluent contained <1 mg/L of TSS due to filtration of the wastewater through the membrane, resulting in >99.6% TSS removal (Fig. 5-4). These COD and TSS removals are comparable to those obtained using a staged anaerobic fluidized membrane bioreactor (SAF-MBR) treating domestic wastewater (Yoo et al. 2012). There was little overall change in pH, as the influent pH to the MFCs of 7.6 ± 0.1 decreased to 7.1 ± 0.1 in the MFCs effluent, but it increased to 7.5 ± 0.2 following treatment in

the AFMBR. Also there were no large changes in conductivity, with 1473 ± 33 mS/cm for the MFCs influent, 1457 ± 15 mS/cm for the MFCs effluent, and 1420 ± 19 mS/cm for the AFMBR effluent.

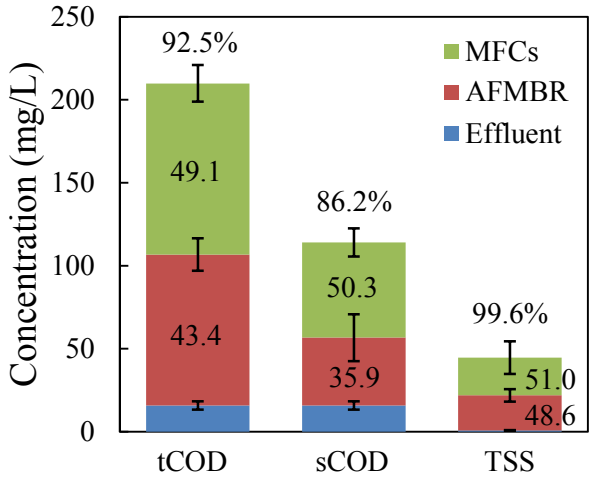

Figure 5-4 Influent and effluent concentrations, and removals of tCOD, sCOD and TSS for the two-stage MFC-AFMBR system. The values inside the figures were the percent of the influent concentration that was removed by the MFCs, AFMBR and the whole system.

The AFMBR was operated continuously for 50 days at a high membrane flux of 16 LMH, even without cleaning by backwashing or using chemicals. Most of the increase in the TMP, from 0.015 bar to 0.035 bar, occurred during the first 8 days of operation (Fig. 5-5). Thereafter, it slowly increased to 0.050 bar during the rest of the test (Fig. 5-5). Liquid (9 mL) was withdrawn from the AFMBR twice a week (0.16% of the total influent flow) to removal finer material and excess suspended solids from days 8 to 50, as suggested in a previous AFMBR study (Kim et al. 2011a). The membrane flux of 16 LMH here is higher than that previously reported for the AFMBR following an AFB (11 LMH), with a PVDF hollow-fiber membrane with the same pore size as the one here (0.1 μm) (Yoo et al. 2012). In that study, the TMP reached 0.25 bar in 3 days when the membrane flux was increased to 14 LMH (Yoo et al. 2012), which is much higher than the maximum TMP observed here. The stable operation of the flux through the AFMBR without appreciable membrane fouling was likely due to a combination of factors here that included the

scouring effect of the GAC particles on the membrane surface, intermittent filtration, and periodic removal of suspended solids.

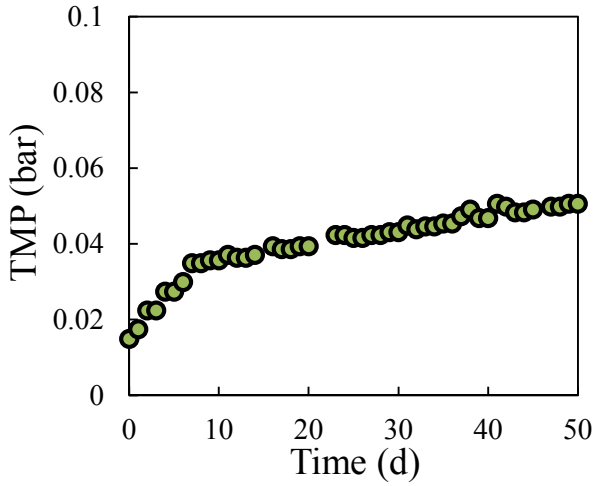

Figure 5-5 TMP for the AFMBR during the 50 days operation.

5.3.3 Energy balance

Energy usage for the two-stage MFC-AFMBR system was calculated as previously described (Kim et al. 2011a, Yoo et al. 2012). The energy requirements were calculated as 0.0107 kWh/m^3 for fluidizing the GAC particles, and 0.0014 kWh/m^3 for pumping permeate through the membranes, resulting in a total electrical energy requirement for the AFMBR of 0.0186 kWh/m^3 (Table 5-1). The electrical energy requirement for pumping liquid through the MFCs was negligible compared to that needed for the AFMBR (Table 5-1). The higher energy requirement for the AFMBR was primarily due to pumping needed for liquid recirculation to maintain the GAC fluidization. The energy needed for this is proportional to the total reactor flow rate and the hydraulic head loss of the system (Vennard and Street 1982). In an AFMBR reactor with a given configuration, the minimum recirculation flow rate and the hydraulic head loss are fixed, and thus the energy requirement for recirculation is inversely proportional to the permeate flow rate or the HRT (Ge et al. 2013). Therefore, the high permeate flux and low HRT achieved for the AFMBR in this study were favorable for reducing the energy requirement to 0.0186 kWh/m^3, compared

with higher energy requirements reported in previous studies (0.027 – 0.040 kWh/m^3) (Ge et al. 2013, Kim et al. 2011a, Yoo et al. 2012).

Table 5-1 Electrical energy requirements and production for the MFC-AFMBR system

Characteristic	**MFCs**	**AFMBR**	**System total**
Electrical Energy required			
Energy for hydraulic loss			
Reactor head loss, cm H_2O	0.5	2.5	
Reactor influent plus recirculation flow rate, mL/min	1.1	171.1	
Hydraulic energy requirement, kW [a]	0.001(10^{-6})	0.699(10^{-6})	
Required pumping energy, kWh/m^3 [b]	0.00001	0.0107	0.0107
Energy for permeate extraction			
Average TMP, cm H_2O		50.8	
Permeate flow rate, mL/min		1.1	
Permeate energy requirement, kW		0.090(10^{-6})	
Required pumping energy, kWh/m^3 [c]		0.0014	
Total pumping energy required for system, kWh/m^3	0.00001	0.0121	0.0121
Total electrical energy required for pumps, kWh/m^3	0.000015	0.0186	0.0186
Electrical Energy Produced			
MFC maximum power, mW [d]	1.28		
Electrical energy production, kWh/m^3	0.0197		0.0197
Electrical energy produced/required			1.06

[a] Energy requirement = 9.8QE, where Q (m^3/s) is flow rate and E (m-H_2O) is head loss (Kim et al. 2011a).
[b] Energy per unit of influent flow rate.
[c] Assume energy efficiency of 65% in conversion of electrical energy to pump energy (Kim et al. 2011a).
[d] Based on the maximum power produced by the SEA MFCs in series.

Electrical energy could be produced directly from the MFCs. Based on the maximum power that could be produced by the SEA configuration after 5 months of operation (0.33 mW for SEA-U and 0.32 mW for SEA-D, Fig. 5-2), the total power that could be produced by the four MFCs coupled to the AFMBR was 1.28 mW (four times 0.32 mW) (Table 5-1). If all of this electrical energy was recovered, the net electrical energy available for the system operation would be 0.0197 kWh/m^3. This would be enough to supply the 0.0186 kWh/m^3 required to operate the system, although in practice there would be energy losses that would affect overall energy recovery, but these energy losses are not well studied. Direct electricity production by MFCs is advantageous, compared to methanogenic reactors that require combustion of the methane to

produce power, as the conversion efficiency of methane to electricity is typically only 33% (Kim et al. 2011a).

The additional energy that could be recovered from the methane production in AFMBR was not included in this energy balance as it would have been difficult to recover. Total methane production in the AFMBR was 1.57 mL-CH_4/L-liquid treated at ambient temperature and pressure, with most of this present as dissolved methane (1.5 mL/L). The energy value of this amount of methane is 0.015 kWh/m^3 (methane combustion, assuming 800 kJ/mol), equivalent to electrical energy producing of 0.005 kWh/m^3 (33% energy recovery) which could theoretically add 27% more energy into the system. However, as most of this methane is dissolved and below its saturation concentration (28 mL/L for ambient conditions), it would have be difficult to recover. The amount of methane that theoretically could be produced in the AFMBR was 8.6 mL/L, assuming that 50% of the COD could be converted into methane (Wen et al. 1999), and the conversion rate was 0.16 mL-CH_4/mg-COD (obtained in batch test, Appendix C). It is not clear for now what processes occurred relative to COD removal as the methane production was only 18% of that possible by methanogenesis alone. More methane might be recovered in the future with improvements in the configuration and operation of the AFMBR.

5.4 Conclusions

The two-stage MFC-AFMBR system could be used to effectively treat domestic wastewater (primary clarifier effluent) at ambient temperatures, producing a high effluent quality with a near neutral energy requirement (or net positive energy production), with no membrane cleaning needed even after 50 d of operation. tCOD was reduced from 210 ± 11 mg/L to 16 ± 3 mg/L, resulting in 92.5% overall COD removal, with >99% removal of TSS to a final effluent concentration of <1 mg/L. The high permeate flux (16 LMH) and low HRT (1 h) here resulted in an overall low energy requirement for the AFMBR of only 0.0186 kWh/m^3. Thus, the energy produced by only the MFCs (0.0197 kWh/m^3) was theoretically sufficient to meet the energy

demands for the system operation. An additional benefit of the MFC-AFMBR system should be a low sludge production rate. Although sludge production was not measured here, previous studies have shown that the sludge production by anaerobic MFC and AFMBR processes are less than those of conventional aerobic processes such as activated sludge (Rabaey and Verstraete 2005, Yoo et al. 2012).

Chapter 6

Current generation in microbial electrolysis cells with addition of amorphous ferric hydroxide, Tween 80, or DNA

Abstract

Iron-oxide nanoparticles and the Tween 80 have previously been shown to improve power generation in microbial fuel cells (MFCs), presumably by improving electron transfer from the bacteria to the anode. We examined whether several chemicals would affect current production in single-chamber microbial electrolysis cells (MECs), where hydrogen gas is produced at the cathode, using mixed cultures and *Geobacter sulfurreducens*. Tween 80 did not increase the current. $Fe(OH)_3$ addition increased the maximum current density of both the mixed cultures (from 6.1 ± 0.9 A/m^2 to 8.8 ± 0.3 A/m^2) and pure cultures (from 4.8 ± 0.5 A/m^2 to 7.4 ± 1.1 A/m^2). Improved current production was sustained even after iron was no longer added to the medium. It was demonstrated that increased current was resulted from improved cathode performance. Analysis using electrochemical impedance spectroscopy (EIS) showed that the iron primarily reduced the diffusion resistance of the cathode, and scanning electron microscopy (SEM) images showed the formation of highly porous structures on the cathode. The addition of DNA also did not improve MEC or MFC performance. These results demonstrated that among these treatments only $Fe(OH)_3$ addition is a viable method for enhancing current densities in MECs, primarily by improving cathode performance.

6.1 Introduction

A bioelectrochemical system (BES) is a device in which organic matter is oxidized by microorganisms using the anode as an electron acceptor, with electrons transferred through an external circuit to the cathode for final reduction of various chemical species. In microbial fuel cells (MFCs), oxygen is usually reduced on the cathode, although other terminal electron

This chapter was published in the paper: Ren, L. J., Tokash, J. C., Regan, J. M., and Logan, B. E. (2012). Current generation in microbial electrolysis cells with addition of amorphous ferric hydroxide, Tween 80, or DNA. *International Journal of Hydrogen Energy*, 37(22), 16943-16950.

acceptors have been used (Logan 2008, Logan et al. 2006). In a microbial electrolysis cell (MEC), oxygen is omitted from the cathode chamber and hydrogen evolution occurs when a sufficient additional voltage is added (Call and Logan 2008, Logan 2008). In both types of BESs, improvements in system performance are needed to enable the commercialization of these processes for wastewater treatment and other applications such as biofuel production (Cheng et al. 2006b, Du et al. 2007, Rozendal et al. 2006).

Electron transfer rates from microorganisms on the anode, and to chemicals at the cathode, are critical for BES performance (Malvankar et al. 2012a, Wen et al. 2011). Several methods have been examined to improve performance, including adding materials such as carbon nanotubes and graphene to the electrode surfaces (Feng et al. 2011, Wang et al. 2011b, Xie et al. 2012). An alternative approach is the addition of chemicals that affect bacteria on the anode and improve current densities. For example, the power density of an air-cathode, single-chamber MFC was increased by 8.7 times following the addition of 80 mg/L of Tween 80, a non-ionic surfactant (Wen et al. 2011). The increase was presumed to be a result of increased permeability of microbial cell membranes, because this surfactant is known to change the cell membrane structure by forming trans-membrane channels. Conductive and semi-conductive iron-oxide nanoparticles as hematite, magnetite, or ferrihydrite have also been shown to increase current production of MFCs by over 30 times (Kato et al. 2010). It was believed that this increase resulted from the nanoparticles improving transfer of electrons from the microorganisms to the anode, but the analysis was insufficient to determine which electrode was responsible for the change in performance. In both cases, tests were conducted using MFCs, where oxygen transfer into the reactor can play a role in reactor performance and biological activity (Huang et al. 2012, Liu et al. 2004, Min and Logan 2004, Morris and Jin 2012).

Other factors are known to affect the stability and electrical conductivity of biofilms. For example, it has been shown that extracellular DNA (eDNA) is important in biofilm formation, and that removal of DNA (using DNase) affects the initial establishment of the biofilm

(Whitchurch et al. 2002). eDNA enhances the strength of both pure- and mixed-culture microbial biofilms by enhancing cell-to-cell interconnections (Allesen-Holm et al. 2006, Dominiak et al. 2011). There is also evidence that eDNA is electrically conductive, with electron transfer occurring due to charge transport along the DNA strands (Fink and Schonenberger 1999, Gorodetsky et al. 2008). In BESs, electrons are thought to be able to move through the biofilm by electron transfer between a series of redox proteins (electron superexchange) (Strycharz-Glaven et al. 2011), although others have indicated that it is due to a metallic-like conductivity of the biofilm (Malvankar et al. 2011). One criticism of the electron superexchange mechanism is insufficient proximity of cytochromes to enable electron transfer (Malvankar et al. 2012b). We therefore wondered if eDNA might be important for electron conductivity of exoelectrogenic biofilms, and whether it was needed for biofilm integrity and stable current generation. To date, there has been no examination of a possible role for eDNA in BESs.

In order to better understand the effects of different types of chemicals on the performance of BESs, we examined the effects of amorphous ferric hydroxide [$Fe(OH)_3$], Tween 80, and eDNA addition on current generation in MECs. By using MECs, we were able to avoid any additional effects of oxygen intrusion into the reactors on current generation. High current densities in BESs have been correlated to the presence of different *Geobacter* species (Logan and Regan 2006a, Lovley 2006b). Therefore, we tested both a pure culture of *Geobacter sulfurreducens* and mixed cultures (wastewater inoculum). The improved performance of the iron oxide-supplemented systems was further investigated using electrochemical impedance spectroscopy (EIS) and scanning electron microscopy (SEM).

6.2 Materials and methods

6.2.1 Reactor construction and operation

Single chambered mini-MECs were constructed as described previously (Call and Logan 2011b) using 5 mL clear glass serum bottles (Wheaton). The anode was a graphite plate with a

thickness of 0.32 cm and dimensions of 1.5 cm × 1 cm (Grade GM-10; GraphiteStore.com, Inc.). Stainless steel (SS) mesh (Type 304, Mesh size 60 × 60; McMaster-Carr) was cut to the same projected area, and used as the cathode. Additional tests to determine the effects of $Fe(OH)_3$ on hydrogen generation were conducted using larger single-chamber MECs made with 100 mL, wide-mouth bottles (PYREX® Media Bottles, Graduated, Corning®) sealed with butyl rubber stoppers. These larger reactors were used in order to produce more gas for analysis than that produced by mini MECs. The same anode and cathode materials were used, with electrode dimensions of 4.5 cm × 2 cm. A gas bag (250 mL) and gastight tubing were used to collect bio-gas through a syringe needle inserted through the stopper. Reactors used for *G. sulfurreducens* cultures were sparged with anaerobic gas (CO_2/N_2, [20/80]) and autoclaved. Reference electrodes (Ag/AgCl; BASi) were used in some experiments to record anode and cathode potentials by inserting the electrode (0.57-cm diameter) through a hole cut in the butyl stopper (0.79-cm diameter), with the tip placed between the anode and cathode. All electrode potential values were reported here versus Ag/AgCl [+200 mV versus standard hydrogen electrode (SHE)]. MECs were connected to a programmable power supply (model 3645A; Circuit 128 Specialists, Inc.) with a circuit containing a 10 Ω resistor connected in series for recording the voltage produced by each reactor. All tests were operated at an applied potential of E_{AP} = 0.7 V (Call et al. 2009, Rozendal et al. 2006).

Further tests on the effects of eDNA were examined in MFCs to obtain a more comprehensive examination of the effect of this chemical on current generation, as no data is reported of a possible role so far for eDNA in BESs. Single-chamber, air-cathode MFCs were constructed using cube-shaped blocks of Lexan with a single cylindrical chamber (14 mL, 7 cm^2 cross sectional area) as previously described (Liu and Logan 2004). The anode was a graphite plate treated with ammonia gas at 700 °C for 1 hour (Cheng and Logan 2007), connected to titanium wire, and then placed at one end of the cylindrical chamber. Two different anode sizes were used: 1 cm × 1 cm, and 0.7 cm × 1 cm. The air cathode (projected surface area of 7 cm^2)

was made of carbon cloth (30 wt.% wetproof, Fuelcellearth, #CC640WP30), and had a catalyst loading of 0.5 mg-Pt/cm^2 on the water side, and four PTFE diffusion layers on the air side (Cheng et al. 2006a). The electrode spacing was 2 cm from the front of the graphite plate anode to the surface of the cathode. The terminals of the MFCs were connected to resistor boxes using copper wires, with the voltage across the resistor recorded using a multimeter (model 2700; Keithley Instruments, Inc.). Reactors were operated in fed-batch mode, with medium replacement after current or voltage dropped below 0.15 mA or 0.05 V. All tests were conducted in duplicate reactors in a temperature controlled room (30 °C).

6.2.2 Microorganisms and medium

Cell suspensions of *G. sulfurreducens* were prepared from a stock culture as previously described (Call et al. 2009), in an acetic acid growth medium using fumarate (22.5 g/L) as the electron acceptor. MECs were inoculated with *G. sulfurreducens* in the late exponential growth phase using 2.5 mL of the culture and 2.5 mL of growth medium. The mixed culture inoculum for MECs and MFCs was effluent from MFCs previously inoculated by wastewater and then operated with acetate as the substrate.

Growth medium was made using a buffer (PBS-50 or BBS-30) and (per liter): 1.0 g CH_3COONa, 10 mL vitamins, and 10 mL minerals (Balch et al. 1979). PBS-50 contained (per liter): 0.31 g NH_4Cl, 2.45 g $NaH_2PO_4 \cdot H_2O$, 0.13 g KCl, 4.58 g Na_2HPO_4 (pH = 7.2 ± 0.2, conductivity γ = 7.8 ± 0.2 mS/cm). BBS-30 contained (per liter): 1.5 g NH_4Cl, 0.7 g $NaH_2PO_4 \cdot H_2O$, 0.1 g KCl, 2.5 g $NaHCO_3$ (pH = 7.3 ± 0.2, γ = 7.7 ± 0.2 mS/cm). The BBS-30 medium was sparged with CO_2/N_2 [20/80] before use. All growth media were prepared, autoclaved, and stored in 125 mL sealed serum bottles.

Amorphous $Fe(OH)_3$ was synthesized by adjusting the pH of a $FeCl_3 \cdot 6H_2O$ solution (0.4 M) to pH = 7.0 with 10 M NaOH (Lovley 2006a). Tween 80 (TWEEN® 80, P4780-100ML) and Salmon sperm DNA (DNA, sodium salt, D1626) were purchased from Sigma-Aldrich. $Fe(OH)_3$,

Tween 80, and DNA were prepared in DI water (10× stocks) and diluted into the medium. DNA was pre-adsorbed onto MFC anodes by dipping the ammonia-treated graphite plates into the DNA solution (120 mg/L) for 24 hours, to produce a final loading of 217 ± 1 mg-DNA/m^2 based on the change in absorbance of the DNA solution. $Fe(OH)_3$, Tween 80, and DNA were added after MEC reactors demonstrated stable performance based on comparable current production over at least three consecutive cycles.

6.2.3 Chemical and electrochemical analyses

MEC reactors were analyzed (200 μL) for headspace composition using gastight syringes (250 uL; Hamilton Samplelock Syringe) and two gas chromatographs (SRI Instruments) for H_2, O_2, N_2, and CO_2 as described previously (Call et al. 2009). Gas production was quantified using the nitrogen-addition method, by measuring the gas composition in a gas bag before and after the addition of 10 mL of N_2. Conductivity and pH were measured using a probe (SevenMulti, Mettler-ToledoInternational Inc.). SEM was used to examine the surface of the electrodes (Field Emission Scanning Electron Microscope, LEO 1530 FEG, at 5 kV).

A multimeter (model 2700; Keithley Instruments, Inc.) was used to record voltages at 20 minute intervals, with the current calculated using Ohm's law ($I = U/R$), where U is the measured voltage (V), and R the external resistance (Ω). Current density (j; A/m^2) and power density (W/m^2) were normalized to the cathode projected surface area (Hong et al. 2011). Polarization and power density curves were obtained using the single-cycle method by changing the external resistances from an open circuit to 10000, 5000, 2000, 1000, 700, 400, 300, 200, 100, 80, 50, and 20 Ω, with the resistance changed after a minimum of 30 min.

Half-cell cyclic voltammetry (CV) was conducted on both the cathode and the anode (working electrode), with a platinum flag (projected area of 1 cm^2) as the counter electrode, and an Ag/AgCl reference electrode located between the working and counter electrodes. Scan range in CV was chosen according to the working potential of the electrode, with –1.3 V to –0.7 V for

the cathodes and –0.6 V to –0.1 V for the anodes, at a scan rate of 1 mV/s for 4 cycles (third cycle shown in plots). This scan rate was slow enough to avoid Type M overshoot that can occur using higher scan rates (Velasquez-Orta et al. 2009). EIS was conducted on the reactors under half cell conditions, with either the cathode or anode as the working electrode, and the other electrode as the counter electrode. The polarized conditions were chosen to be close to MEC operating potentials, which were –1.1 V for the cathode and –0.4 V for the anode. The frequency range was 100 kHz to 10 mHz with a sinusoidal perturbation of 10 mV amplitude (Wen et al. 2011, Zhang et al. 2011b). EIS spectra were fitted to an equivalent circuit (EC) (Appendix D, Scheme D-1), based on the flooded-agglomerate model (Springer and Raistrick 1989, Zhang et al. 2011b), to extract the Ohmic, charge transfer, and diffusion resistances. A constant phase element (CPE) was used instead of a capacitor in order to adapt to nonhomogeneous conditions, such as electrode roughness and distributed reaction rates (He and Mansfeld 2009, Zhang et al. 2011a).

6.3 Results

6.3.1 Increased current density and hydrogen production rate following $Fe(OH)_3$ addition

The maximum current densities increased by almost 50% after addition of 10 mM $Fe(OH)_3$ for both the mixed cultures (from 6.1 ± 0.9 A/m^2 to 8.8 ± 0.3 A/m^2) and *G. sulfurreducens* (from 4.8 ± 0.5 A/m^2 to 7.4 ± 1.1 A/m^2) in the mini-MECs with the BBS-30 medium (Fig. 6-1). The change in current resulted from improved performance of the cathodes (more positive cathode potentials). For mixed culture, the cathode potential increased from –1.1 ± 0.07 V to –1.04 ± 0.06 V following iron addition, while for *G. sulfurreducens*, cathode potentials increased from –1.09 ± 0.04 V to –1.05 ± 0.05 V (Fig. D-1). There was no change in the cathode potentials of the controls, with –1.115 ± 0.005 for mixed culture and –1.101 ± 0.008 for *G. sulfurreducens*. There were small increases in the anode potentials of these reactors, likely as a result of larger overpotentials due to the increased current densities. Therefore, changes in anode potentials would not have accounted for the overall improved reactor performance. When the phosphate

buffer was used (PBS-50), however, there was no significant increase in current density following $Fe(OH)_3$ addition (Fig. 6-1).

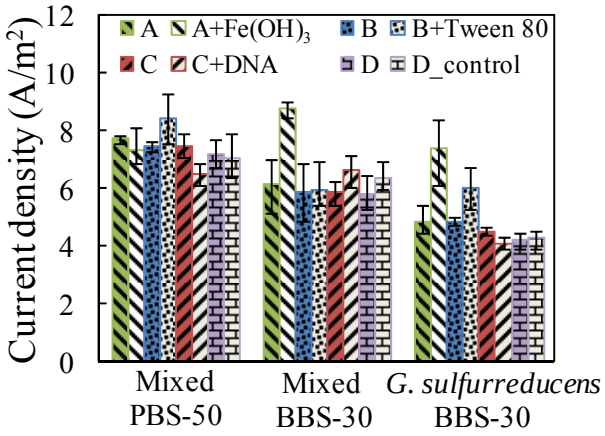

Figure 6-1 Maximum current density of mixed cultures and *G. sulfurreducens* in PBS-50 or BBS-30 medium before and after addition of $Fe(OH)_3$, Tween 80, or DNA. Reactors were run in duplicate for at least two cycles under each condition, and averaged data were reported here. The letters A through D indicate results for duplicate reactors in the presence and absence of the indicated chemicals: A with $Fe(OH)_3$, B with Tween 80, and C with DNA addition (D remained a control, with no chemical addition).

The addition of $Fe(OH)_3$ could result in Fe(III) reduction at the cathode, which might adversely affect hydrogen production. To examine whether $Fe(OH)_3$ addition affected hydrogen production, we conducted tests using larger MECs. Measurements were made during three phases: Phase I, during stable current production by *G. sulfurreducens* in BBS-30 medium; Phase II, with $Fe(OH)_3$ addition to the medium; and Phase III, with no further iron addition to the medium. Bio-gas composition (65.3 ± 1.7 % hydrogen, 18.2 ± 1.0 % carbon dioxide and 17.0 ± 1.4 % nitrogen) was the same during all three phases (Fig. 6-2). However, the hydrogen production rate increased from 23.2 ± 0.1 mL/d to 26.5 ± 0.1 mL/d following $Fe(OH)_3$ addition, and this rate remained high even after $Fe(OH)_3$ was no longer added (Fig. 6-2). The increased hydrogen production rate resulted from the cycle time decreasing from 5.9 ± 0.1 days (Phase I) to 5.4 ± 0.3 days (Phase II and III) due to a 15% increase in maximum current density following addition of $Fe(OH)_3$.

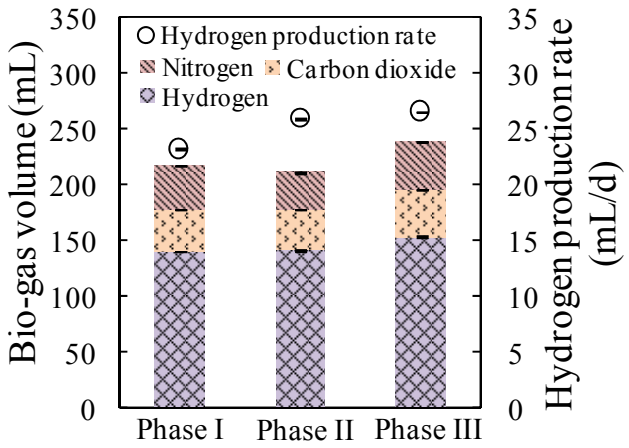

Figure 6-2 Bio-gas volumes and hydrogen production rates of larger MECs during the three phases of $Fe(OH)_3$ addition.

6.3.2 Electrochemical tests and SEM images

The electrodes of the mixed-culture MECs were separately analyzed using CV, with a platinum counter electrode. Following $Fe(OH)_3$ addition with BBS-30 medium, the overpotential of the anode increased slightly compared to the control (no addition) at voltages more negative than –0.35 V (Fig. D-2a). However, the performance of the cathode was clearly improved, with a substantial reduction in overpotential as demonstrated and an overall 43% increase in performance (based on the slopes in the CVs over a potential range of –1.1 V to –1.2 V) (Fig. D-2b).

Analysis of the components of the internal resistance using EIS at a cathode potential of –1.1 V showed that there was a large change in the cathode diffusion resistance following $Fe(OH)_3$ addition, resulting in an overall decrease in the internal resistance by 43% (Fig. 6-3). However, there was only a slight decrease in the anode resistance (12%) at an anode potential of –0.4 V. EIS results therefore provided good agreement with the CV and MEC tests that the $Fe(OH)_3$ addition primarily affected cathode, and not anode, performance.

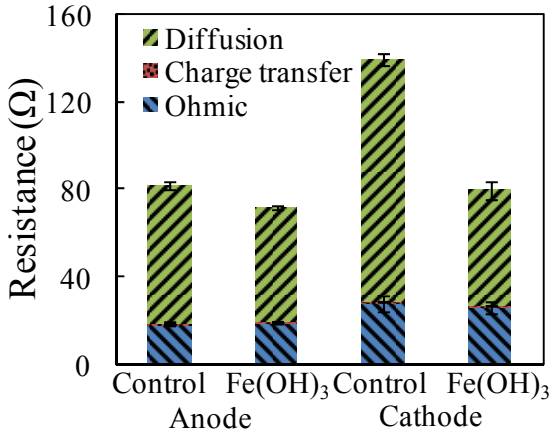

Figure 6-3 Electrode resistances of control reactors and those with $Fe(OH)_3$ addition. EIS plots and fits were shown in Fig. D-3.

The cathode turned black following $Fe(OH)_3$ addition, suggesting the production of magnetite, as opposed to brown which would indicate ferrous hydroxide $Fe(OH)_2$ or greyish yellow for wüstite (FeO). Analysis of the electrodes using SEM showed that addition of $Fe(OH)_3$ caused formation of a highly porous structure on the cathode surface, which would have increased the specific surface area of the electrode. In contrast, new stainless steel wire had a relatively smooth surface (Fig. 6-4a), while the control surface (no iron addition) had some, but much fewer particles with irregular shapes (Fig. 6-4b). The surface of the cathode after $Fe(OH)_3$ addition appeared to be very porous and had nearly spherical particles (~50 nm in diameter) stacked together (Fig. 6-4c). A biofilm of rod-shaped objects, as well as a more complex structure, was evident on the surfaces of the anodes from the MECs with and without $Fe(OH)_3$, with no obvious differences between these surfaces (Fig. 6-4e and f).

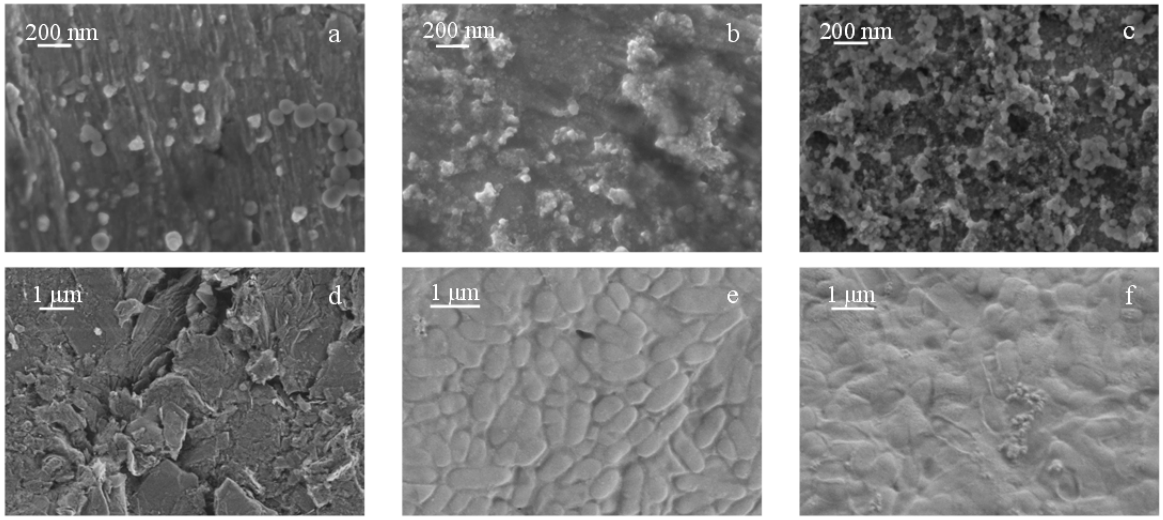

Figure 6-4 SEM images of anode and cathode electrode surfaces: (a) new cathode; (b) control cathode; (c) cathode after $Fe(OH)_3$ addition with BBS-30 medium; (d) new anode; (e) control anode; and (f) anode following $Fe(OH)_3$ addition into the BBS-30 medium.

6.3.3 Effect of buffer type on current density increase by $Fe(OH)_3$

Additional experiments were conducted to better understand the different effects of the phosphate and bicarbonate buffers. Six mini-MEC reactors were inoculated with mixed culture as above and PBS-50 medium, and operated for multiple cycles until stable performance was obtained. $Fe(OH)_3$ was then added to two MECs using the PBS-50 medium for five cycles, while two MECs reactors were maintained as controls (no iron addition, PBS-50 medium). Following this period, all four MECs were switched to BBS-30 [no $Fe(OH)_3$]. The two remaining MECs were first switched from PBS-50 to BBS-30 for four cycles, followed by BBS-30 with $Fe(OH)_3$ addition for four more cycles, and then these two reactors were switched back to PBS-50.

When the reactors were switched from PBS-50 to BBS-30, all six reactors showed a drop in current density (Fig. 6-5). The current density increase was small (<12%, or from 6.6 $\pm$ 0.1 A/m^2 to 7.4 $\pm$ 0.2 A/m^2) when $Fe(OH)_3$ was added with PBS-50 (Fig. 6-5a). However, the current density increased by almost 80% to 7.5 $\pm$ 0.1 A/m^2 following iron addition with BBS-30 (Fig. 6-5b). This showed that the improved current with $Fe(OH)_3$ addition required high concentrations of bicarbonate ions, and not phosphate ions. The change in current was not due to changes in

solution resistance as the two buffers had the same ionic conductivity. Once the improved current production in the BBS-30 was obtained, and $Fe(OH)_3$ was no longer added, higher current generation was maintained even in the PBS-50 medium (Fig. 6-5b).

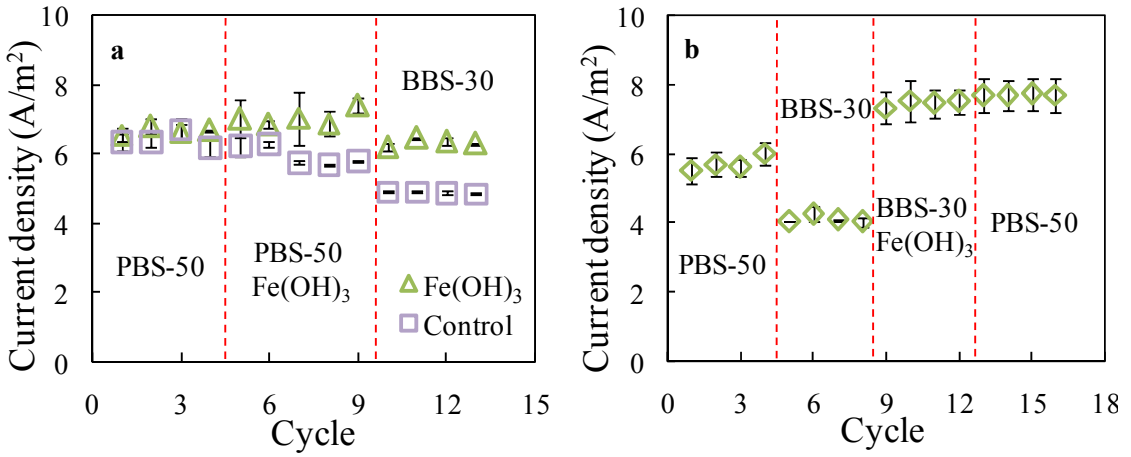

Figure 6-5 Current density using mixed cultures in PBS-50 and BBS-30 medium: (a) $Fe(OH)_3$ addition with PBS-50 medium; and (b) $Fe(OH)_3$ addition following a change from the PBS-50 medium to a BBS-30 medium.

6.3.4 Effects of Tween 80

There was no effect on current density when Tween 80 was added at a concentration of 5 mg/L to the MECs. Although the current density of the mixed culture in PBS-50 and *G. sulfurreducens* initially slightly increased (<20%) (Fig. 6-1), this increase was not sustained after two cycles even though the Tween 80 continued to be added to solution. Higher Tween 80 concentrations were examined based on those used in a previous MFC study (5, 20, and 80 mg/L) (Wen et al. 2011). There was no effect on current density with 5 mg/L or 20 mg/L (Fig. 6-6), and adding 80 mg/L decreased the current densities of both the mixed cultures (Fig. 6-6a) and *G. sulfurreducens* (Fig. 6-6b).

EIS tests performed during fed-batch cycles (Fig. 6-6) showed that the anode and cathode electrode resistances were unchanged with an addition of Tween 80 up to 20 mg/L (Fig. D-4a). When 80 mg/L of Tween was used, the anode and the cathode ohmic resistances each increased by 10 Ω. The anode diffusion resistance was about twice that of the control, and the cathode

diffusion resistance increased by 17% (Fig. D-4b). The ohmic resistance increased slightly due to a decrease in solution conductivity to 6.2 ± 0.3 mS/cm at 80 mg/L of Tween 80, compared to 7.5 ± 0.1 mS/cm at 5 mg/L and 7.3 ± 0.2 mS/cm at 20 mg/L. Solution pH decreased only slightly from 7.2 to 7.0 with Tween 80 concentrations up to 80 mg/L.

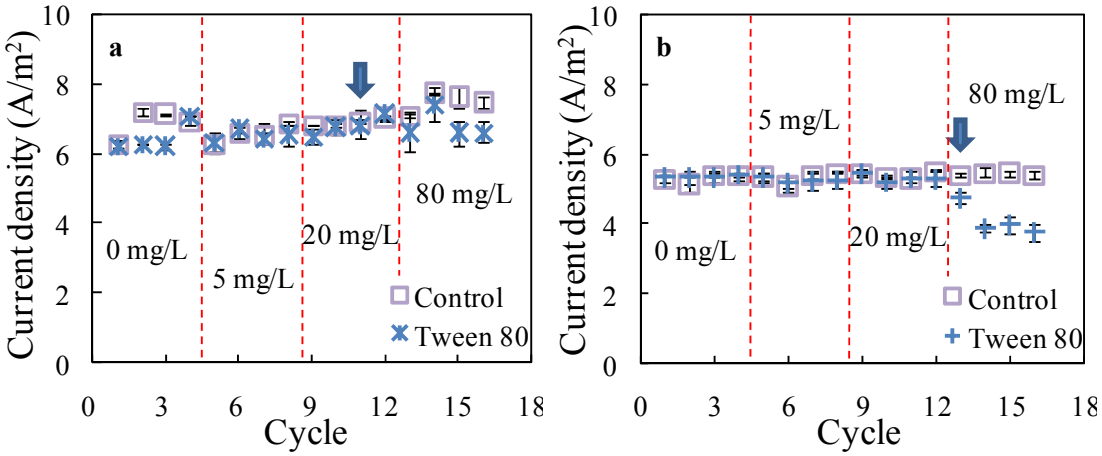

Figure 6-6 Current density of mixed culture and *G. sulfurreducens* in BBS-30 medium with increased Tween 80 concentrations: (a) mixed culture; and (b) *G. sulfurreducens*. Arrows indicate the cycles in which EIS was performed.

6.3.5 Effect of DNA in MECs and MFCs

When DNA was added into solution using the mini-MECs (10 mg/L), there was no significant change in current densities in any of the reactors (within ± SD of 0.45 A/m^2) (Fig. 6-1). Additional tests were conducted using MFCs, with the anode first modified by adsorption of DNA, but the maximum power density with DNA on the anode (0.58 W/m^2) was essentially the same as that of the control (0.60 W/m^2) (Fig. 6-7). The anode size was decreased to try to produce conditions where current generation was more limited by the anode than the cathode (so that improved current densities could be observed if produced). Decreasing the anode surface area from 1 cm^2 to 0.7 cm^2 decreased the maximum power density from 0.65 W/m^2 to 0.60 W/m^2, indicating a 32 % increase in power per anode area (from 4.55 W/m^2 to 6.00 W/m^2 when normalized by anode area) (Fig. 6-7). The reactors were then operated over four additional cycles at the resistance that produced the maximum power (250 Ω) (Fig. 6-7). However, the same results

were obtained under these constant-resistance conditions, with the average power density following DNA addition (0.58 ± 0.01 W/m^2) being about the same as that of the control (0.59 ± 0.01 W/m^2, no DNA addition) (Fig. D-5). These results confirmed that DNA addition did not improve current or power generation.

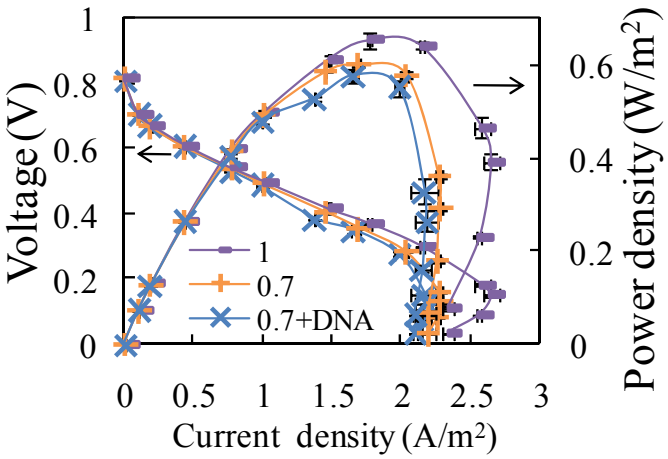

Figure 6-7 Power density and polarization curves of MFC with different sized anodes: 1 cm^2 anode (1), 0.7 cm^2 anode (0.7), and 0.7 cm^2 anode modified by DNA (0.7+DNA).

6.4 Discussion

6.4.1 Increased current density by $Fe(OH)_3$ addition in a bicarbonate medium

Addition of $Fe(OH)_3$ increased current production by almost 50% for both mixed and the pure cultures when using a bicarbonate medium (Fig. 6-1). The increased current density was due to improved cathode performance, likely from an increase in surface area due to the formation of highly porous structure on its surface (Fig. 6-4). Electrochemical analyses using CV and EIS showed that cathode performance was improved, resulting in a lower overpotential (Fig. D-2b) and more positive potentials (Fig. D-1). This reduction in overpotential was not due to a catalytic effect of the deposited material as the initial potential of the cathode following $Fe(OH)_3$ additions was similar to that of the control (ca. –0.7 V in CV tests) (Fig. D-2b) (Tokash and Logan 2011, Vrubel et al. 2012). The slopes in the CV scans were larger after $Fe(OH)_3$ addition than those of the controls (Fig. D-2b), consistent with improved performance through increased surface area (Chan and Eikerling 2011, Verbrugge and Liu 2005). While the specific chemical composition of

the porous material on the surface was not examined, it was likely magnetite for several reasons: the black color; it was electrically conductive (gold sputtering was not needed for SEM imaging); previous studies have shown electrochemical deposition of magnetite using a stainless steel electrode at similar potentials (Kothari et al. 2006); and bacteria are able to reduce $Fe(OH)_3$ to magnetite (Lovley and Phillips 1988), which may have contributed to a decrease in the coulombic efficiency by 3.6 % in the presence of $Fe(OH)_3$ in mixed culture mini-MECs (from 94.5 % to 91.1 %).

Once current density was increased through the addition of the $Fe(OH)_3$, this increase in current density and the corresponding hydrogen production rate were sustained in subsequent cycles even when the iron was no longer added to the bicarbonate medium (Fig. 6-2 and 6-5). If increased current density was due to chemical reduction of $Fe(OH)_3$, then the current density should have been reduced to the former level when the iron was omitted from the medium. Also, the increased current density was not due to any pH or conductivity change (Table D-1). Thus, it is clear from these results that the effect of the $Fe(OH)_3$ was to improve cathode performance through an increase in surface area, and that there were no secondary effects of chemical reactions in solution or impairment of the hydrogen evolution reaction at the cathode (Fig. 6-2).

The use of a phosphate buffer medium increased current slightly compared to a bicarbonate medium (same conductivity) (Fig. 6-1 and 6-5), but $Fe(OH)_3$ addition yielded little to no improvement in performance when it was added to a phosphate medium. At the neutral pH conditions used here, the main chemical species were HCO_3^- and NH_4^+ with the BBS-30 medium (pK_{A1} = 6.37 and pK_{A2} = 10.33 for H_2CO_3; pK_B = 9.26 for NH_3), and $H_2PO_4^-$ and HPO_4^{2-} in PBS-50 medium (pK_{A1} = 2.12, pK_{A2} = 7.21, and pK_{A3} = 12.32 for H_3PO_4) (Sawyer et al. 2003). Fe^{3+} and Fe^{2+} ions can complex with $H_2PO_4^-$ and HPO_4^{2-}ions, but not HCO_3^- or NH_4^+ (Stumm and Morgan 1996). This suggests that complexation or sorption of $H_2PO_4^-$ and HPO_4^{2-} species to the deposited iron prevented an increase in hydrogen evolution rate seen in the presence of the non-interacting bicarbonate and ammonium species (Fig. 6-5b). There could have been an adverse

effect of phosphate on the anode biofilm, as very high concentrations of phosphate buffer have been shown to reduce current generation by *G. sulfurreducens* (Call and Logan 2011b). However, electrochemical tests clearly showed the main impact of the $Fe(OH)_3$ addition was to the cathode.

6.4.2 Effect of DNA or Tween 80 on performance

The addition of DNA did not improve either MEC or MFC performance (Fig. 6-1 and 6-7). The enhanced effect of Tween 80 on power generation shown by others using MFCs (Wen et al. 2011) could not be verified here using MECs. Addition of Tween 80 at concentrations up to 20 mg/L had no effect here on current densities for either mixed cultures, in two different types of media, or for the pure culture (Fig. 6-1 and 6-6). EIS spectra also showed that there was no effect on the internal resistances at these Tween 80 concentrations compared to the controls (Fig. D-4a). However, an adverse effect on current production was observed at the highest concentration (80 mg/L) of Tween 80 (Fig. 6-6), and EIS tests showed that there were increased electrode internal resistances (primarily diffusion resistance), primarily associated with the anode (Fig. D-4b). Additional tests by others have also failed to show improved performance using Tween 80 in MFCs with glucose as the substrate (C. Werner, personal communication). These results conclusively demonstrate that Tween 80 cannot be used to increase power generation in MECs or MFCs.

6.5 Conclusions

Adding $Fe(OH)_3$ to MECs improved current densities with a bicarbonate buffer for both mixed cultures and *G. sulfurreducens*, while the addition of Tween 80 or DNA did not. The improved performance resulted from formation of a highly porous structure on the cathode, which reduced the cathode overpotential and increased maximum current densities by almost 50%. There was no adverse impact of $Fe(OH)_3$ addition on hydrogen production rates. An increase in current density following $Fe(OH)_3$ addition required the use of a bicarbonate medium, as no substantial enhancement in current was observed with a phosphate buffer. These results showed

that current densities can be improved by $Fe(OH)_3$ addition, primarily through an increase in the cathode surface area, and that this improved performance was sustained once cathode performance was improved even after iron is no longer added to the medium.

Chapter 7

Treatability studies on different refinery wastewater samples using high-throughput microbial electrolysis cells (MECs)

Abstract

High-throughput microbial electrolysis cells (MECs) were used to perform treatability studies on many different refinery wastewater samples all having appreciably different characteristics, which resulted in large differences in current generation. A de-oiled refinery wastewater sample from one site (DOW1) produced the best results, with 2.1 ± 0.2 A/m^2 (maximum current density), 79% chemical oxygen demand removal, and 82% headspace biological oxygen demand removal. These results were similar to those obtained using domestic wastewater. Two other de-oiled refinery wastewater samples also showed good performance, with a de-oiled oily sewer sample producing less current. A stabilization lagoon sample and a stripped sour wastewater sample failed to produce appreciable current. Electricity production, organics removal, and startup time were improved when the anode was first acclimated to domestic wastewater. These results show mini-MECs are an effective method for evaluating treatability of different wastewaters.

7.1 Introduction

Wastewater treatment currently consumes a significant amount of the electricity produced in the USA (McCarty et al. 2011). In order to offset the costs of wastewater treatment, alternative methods are being developed to capture energy or produce useful chemicals from wastewaters (Logan and Rabaey 2012). Microbial fuel cells (MFCs) have been shown to generate electricity using complex sources of organic matter while simultaneously treating the wastewater (Pant et al. 2010). Many types of wastewaters have been examined using MFCs, including municipal (Liu et al. 2004, Min and Logan 2004, You et al. 2006), food processing (Oh and Logan 2005), brewery (Feng et al. 2008), animal (Min et al. 2005), and paper recycling wastewaters (Huang and Logan

This chapter was published in the paper: Ren, L. J., Siegert, M., Ivanov, I., Pisciotta, J. M., and Logan, B. E. (2013). Treatability studies on different refinery wastewater samples using high-throughput microbial electrolysis cells (MECs). *Bioresource Technology*, 136, 322-328.

2008). However, fewer wastewater studies (Cusick et al. 2010, Wagner et al. 2009) have been conducted using microbial electrolysis cells (MECs), where hydrogen gas is produced instead of electrical power. The treatability of a wastewater in an MEC can be different from that obtained in an MFC due to leakage of oxygen through the MFC cathode. For example, the percent of electrons from the substrate captured as electrical current (coulombic efficiency) is typically much higher in an MEC than an MFC (Cusick et al. 2010). In order to more easily evaluate the treatability of wastewaters using MECs, rapid and inexpensive evaluation techniques are needed. Recently, a simple and inexpensive type of small MEC (mini-MEC) was described that showed promise as a method for high-throughput screening of wastewater samples, as these reactors required a small sample volume, they had a simple configuration, and many reactors could be powered using only a single power source (Call and Logan 2011b). However, they have not been extensively tested with different types of wastewaters.

The strength and treatability using aerobic processes of wastewaters are often evaluated using chemical oxygen demand (COD), biochemical oxygen demand (BOD), and a BOD/COD ratio (Alvares et al. 2001, Mantzavinos et al. 2001). A high BOD/COD ratio can lead to effective aerobic treatment in processes such as activated sludge. However, the utility of a BOD test or the BOD/COD ratio for predicting the biodegradability of different wastewaters in anaerobic bioelectrochemical systems (BESs), such as MFCs and MECs, has not been sufficiently evaluated. The BOD procedure tests biodegradability under aerobic conditions, and thus a high BOD/COD ratio might not guarantee effective treatment in BESs where the anode is the electron acceptor instead of oxygen. This suggests that the use of COD and BOD concentrations as indicators of successful treatment of wastewaters in BESs needs to be evaluated.

Refinery operations are quite complex and require large volumes of water, and the composition of refinery wastewaters can vary substantially among different sites (Benyahia et al. 2005). A typical refinery wastewater treatment process consists of primary mechanical and physicochemical methods, such as oil-water separation, followed by secondary biological

treatment (Yavuz et al. 2010). Activated sludge has been the most commonly employed biological treatment process (Shariati et al. 2011), with alternatives such as sequencing batch reactors (Lee et al. 2004) and membrane bioreactors (MBR) (Viero et al. 2008). All of these current wastewater treatment technologies are very energy intensive due to the requirement for aeration of the wastewater to provide dissolved oxygen for microorganisms. This energy utilization could be avoided by using MECs which are completely sealed off from air, where the anode is used as the electron acceptor with hydrogen gas produced at the cathode (Cusick et al. 2010). To our knowledge, no studies have yet examined the treatability of refinery wastewaters as the fuel for MECs.

In this study, we examined the treatability of six different refinery wastewater samples collected at various points in the existing treatment processes at several different facilities. Mini-MECs were used to allow analysis of large numbers of samples with sufficient replicates. These wastewater samples were evaluated alone or mixed with domestic wastewater to determine if treatability could be improved by providing microorganisms and nutrients. The effectiveness of MEC treatment was examined based on current generation over multiple fed-batch cycles. Additional tests were conducted to determine whether pre-conditioning of the electrodes with exoelectrogenic biofilms using domestic wastewater would enhance the treatability of the refinery wastewater. For these tests, refinery wastewater (RW) was treated in MECs initially acclimated using only domestic wastewater (DW) or the 50:50 RW+DW mixture.

7.2 Materials and methods

7.2.1 Wastewater samples

Refinery wastewater samples were collected from four refinery facilities, kept in ice coolers and shipped to the Pennsylvania State University within 2 days. Upon arrival, all samples were stored at 4 °C. Six samples were collected and tested: de-oiled wastewaters (the final combination of the processing wastewaters and prior to biological treatment) from three different facilities

designated as DOW1, DOW2, DOW3; a de-oiled oily sewer (DOSW) at a fourth facility prior to biological treatment; treated refinery wastewater sent to a lagoon that contained high concentrations of algae (LGW, same facility as DOW2); and stripped sour water (SSW, same facility as DOW3). The CODs ranged from 150 to 1400 mg/L. Some wastewaters were sampled more than once from the same spot to more fully evaluate the effects of wastewater variability from a specific source. These additional samples were identified with a second (Roman) number, as DOW1(II), DOW2(II), DOW3(II), and DOSW(II). These abbreviations were summarized in Table E-1 (Appendix E).

Domestic wastewater was obtained from the primary clarifier effluent at the Pennsylvania State University wastewater treatment plant (University Park, PA, USA) immediately before tests (<1 hr). This wastewater typically has a COD in the range of 300 – 450 mg/L (Hays et al. 2011).

7.2.2. Reactor construction and experiment configuration

Single chambered mini-MECs were constructed as described previously (Call and Logan 2011b) using 5 mL clear glass serum bottles (Wheaton, Millville, NJ, USA). Anodes were graphite plates, 1.5 cm length × 1 cm width, and 0.32 cm thick (Grade GM-10; GraphiteStore.com, Inc.). Stainless steel mesh (Type 304, Mesh size 50 × 50; McMaster-Carr) was cut to the same projected area and used as the cathode. Reactors were sparged with anaerobic gas (CO_2/N_2, [20/80]) and autoclaved prior to inoculation. MECs were connected to a programmable power supply (model 3645A; Circuit 128 Specialists, Inc.) with a circuit containing a 10 Ω resistor (in series) that was used to calculate the current from the measured voltage drop across the resistor. All MECs were operated at an applied voltage of 0.7 V (Call et al. 2009, Rozendal et al. 2006). Reactors were operated in fed-batch mode, with substrate replacement, followed by anaerobic gas sparging, after the current decreased to <0.02 mA.

Reactors were fed different combinations of refinery wastewater (RW) and domestic wastewater (DW) in order to determine the effect of the inoculum and wastewater on treatment

efficiency. For every wastewater sample, four different combinations were tested: refinery wastewater sample alone; a 50:50 (vol:vol) mixture with domestic wastewater (50:50 RW+DW mixture) to provide microorganisms or nutrients; an open circuit control with the 50:50 RW+DW mixture; and domestic wastewater as a positive control on current generation. DW was used as a positive control because it was well known for current production in BESs (Hays et al. 2011). All tests were conducted using triplicate reactors at a fixed temperature (30 °C).

Following these experiments, additional tests were conducted using the DOW1(II), DOW2(II), DOW3(II) and DOSW(II) samples. MECs originally fed DW and the 50:50 RW+DW mixture were all fed only full strength RW (referred as cross-feeding) to determine whether pre-acclimation of the anode with a rich microbial inoculum would enhance the treatability. For each test the open circuit reactors, initially fed the 50:50 RW+DW mixture, were also fed RW and operated as open circuit control for organics removal in the absence of current generation. These cross-feeding tests were conducted using duplicate reactors at a fixed temperature (30 °C) (the third reactor was sacrificed for future molecular biology studies).

7.2.3. Measurements and chemical analyses

A multimeter (model 2700; Keithley Instruments, Inc.) was used to record voltages measured across the resistor at 20 minute intervals. Current was calculated using Ohm's law ($I = U/R$; A), where U (V) was the measured voltage, and R (Ω) the external resistance of 10 Ω. Total coulombs recovered was calculated by integrating the current over time ($C_t = \Sigma\, I \cdot \Delta t$; C), where Δt was the time interval of 20 minutes. Current density (j; A/m^2) was normalized to the cathode projected surface area of 1.5 cm^2.

Chemical oxygen demand (COD) and soluble COD (sCOD) were measured using standard methods (method 5220, HACH COD system, HACH Company, Loveland, CO) (APHA 1998). All samples for sCOD measurement were filtered through 0.45 μm pore diameter syringe filters (polyvinylidenedifluoride, PVDF, 25 mm size, Restek Corporation). Biological oxygen demand

(BOD) was determined using a three-day, non-dilution headspace BOD (HBOD) test at 20 °C (Logan and Patnaik 1997). This test has been shown to be easier and faster to conduct than a traditional five-day BOD test, and it provides essentially the same information in three days instead of five days (Hays et al. 2011, Min et al. 2004), and it does not require sample dilution (Min et al. 2004). The HBOD of a refinery wastewater was measured without external seed, and also estimated using the 50:50 mixture of the refinery and domestic wastewater samples, indicated by asterisk ($HBOD^*$), by subtracting one half of the HBOD obtained in tests using only DW, from the 50:50 RW+DW mixture. The advantage of this method was that the DW serves as a rich microbial seed for the oxygen demand test. COD, sCOD, and HBOD analyses were performed at the beginning and end of batch cycles after the MEC reactors demonstrated stable performance (based on comparable current production over at least three consecutive cycles). Conductivity and pH were measured using a probe (SevenMulti, Mettler-Toledo International Inc.).

7.3 Results and discussion

7.3.1 COD, HBOD and other wastewater characteristics

The six refinery wastewater samples varied appreciably in terms of organic strength and biodegradability as they were collected at different locations in the refinery wastewater treatment processes (before or after secondary biological treatment, before or after primary oil separation) and from different facilities. CODs ranged from a low of 136 ± 7 mg/L (LGW) to a high of 1309 ± 4 mg/L [DOW3(II)], with most samples in the range of ca. 400 to 1000 mg/L (Fig. 7-1). The pH of almost all of the RW samples was neutral or slightly alkaline (7.2 to 8.9), indicating that they were in a range suitable for bioelectrochemical treatment (He et al. 2008) (Table E-2). The only exception was SSW sample which had a pH of 10.5. The conductivities ranged from 1.3 to 6.4 mS/cm, with the higher conductivities known to be more favorable for higher current densities as this reduces the MEC internal resistance.

The HBODs ranged from nearly zero for the SSW sample, to 390 ± 10 mg/L for the DOW3 sample (Fig. 7-1). The COD/HBOD ratio was calculated to evaluate its use as a predictor of the relative biodegradability of the refinery wastewater samples. COD/HBOD ratios varied over a large range (2.3 to 4310) compared to 1.85 for the DW (Fig. E-1). The estimated biodegradability of the different RW samples when adding a rich microbial inoculum, calculated as the HBOD*, indicated in most cases that more of the organic matter in the RWs was degraded aerobically when the samples were combined with DW. The only exception was the DOW1 and DOW1(II) samples, which had HBOD* values of 151 ± 8 mg/L and 312 ± 16 mg/L, same with the HBODs of 142 ± 5 mg/L and 293 ± 10 mg/L (Fig. 7-1). The COD/HBOD* ratios ranged from ca. 2 to 4, except for the DOW3 sample (COD/HBOD* = 1.6). These ratios based on the 50:50 mixture tests were lower and more consistent than the COD/HBOD ratios due to the higher and more consistent biochemical oxygen demands (Fig. 7-1).

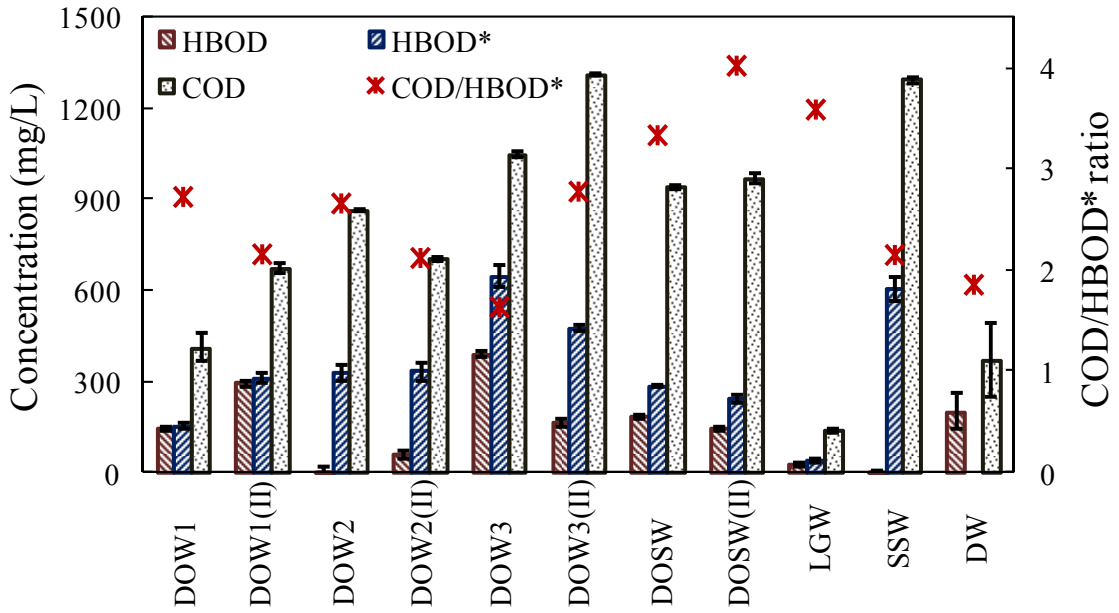

Figure 7-1 COD, HBOD, HBOD*, and the ratio of COD/HBOD* for the different refinery wastewater samples, with domestic wastewater (DW) as a positive control. The reported COD and HBOD values for the DW samples were averages for the whole test period (four months).

A comparison of the HBOD and HBOD* results suggested that the HBODs of some of the wastewater samples [DOW2, DOW2(II), and SSW] were underestimated due to an insufficient initial microbial inoculum in the RW samples (Fig. 7-1). The high pH of 10.5 also might be a cause for the low HBOD measured for SSW. An HBOD* that was larger than the HBOD could also indicate that just diluting the RW samples increased aerobic biodegradability, perhaps due to toxicity of chemicals in the samples to the microorganisms. It might also be that addition of the DW improved degradation of organic matter in the RWs due to nutrients in the DW. Taking this into account, the ratios of COD/HBOD [2.3 to 8.1, excluding DOW2, DOW2(II), and SSW] and COD/HBOD* indicated that the COD in the RW samples was biodegradable, but relatively less biodegradable than typical DW (with a COD/HBOD ration of 1.85) in an oxygen-based degradation test.

7.3.2 Current production in MEC tests

The wastewater samples demonstrated very different current profiles over each fed-batch cycle. Part of the results for the SSW and DOW1 samples were shown as two examples of different current profiles (Fig. 7-2a and b). No electricity was generated by the SSW sample (Fig. 7-2a), but when it was combined with the DW (50:50) the current rapidly increased to a peak of about 0.1 mA, and then the current slowly decreased over several days. The total area of the current profile (total coulombs recovered) was about two thirds of that obtained using only DW, indicating little biodegradability of the COD in the SSW sample under the anaerobic condition in MECs (Fig. 7-2d). A broad peak indicated sustained biodegradation of the organics in the sample. The peak height in the SSW sample mixed with DW suggested that the complex organic matter was slowly degraded over time, as the maximum peak height was lower than that possible in these types of mini MECs (for example 0.24 mA produced by the DW) (Fig. 7-2a). In other tests, such as those using the DOW1 sample, there was a much higher peak (nearly 0.3 mA) at the start of the cycle, with a rapid decrease and then little current during the rest of the cycle (Fig. 7-2b).

The rapid decrease in the DOW1 current profile suggested this sample contained both relatively biodegradable matter that was degraded very quickly (high peak heights), and recalcitrant components (current not sustained over time).

A comparison of the maximum current produced (peak heights) and total recovery of substrate as electrical current (Coulombs) by these different types of samples indicates that the three de-oiled final combined RW samples (DOW1, DOW2, and DOW3) showed the best results in terms of bio-electrochemical performance (Fig. 7-2c and d). The original DOW1 sample produced a high maximum current density of 1.7 ± 0.1 A/m^2 (DOW1), with the highest current [2.1 ± 0.2 A/m^2, DOW1(II)] obtained in the second test. This current density was even higher than that obtained with DW (1.5 ± 0.4 A/m^2), indicating that COD in the DOW1 samples were better substrates for electricity generation in MECs than DW. The DOW3 sample produced a high maximum current density of 1.5 ± 0.4 A/m^2, but a resampling at this site produced much less current [0.8 ± 0.2 A/m^2, DOW3(II)]. For the LGW and SSW, there was very little current production.

The maximum current densities of the 50:50 RW+DW mixtures followed similar trends as that obtained with the full strength RW tests, with the highest values obtained for the three de-oiled samples [1.79 ± 0.01 A/m^2 on average for DOW1, 1.8 ± 0.1 A/m^2 for DOW2, 2.4 ± 0.1 A/m^2 for DOW3, and 1.4 ± 0.2 A/m^2 for DOW3(II)], followed by the DOSW (averaging 1.1 ± 0.1 A/m^2), and LGW and SSW (0.5 ± 0.1 A/m^2 for both) (Fig. 7-2c). The 50:50 RW+DW mixtures had higher maximum current densities than the full strength RWs in all tests except for those with the DOW1 sample (Fig. 7-2c), indicating that combining with DW enhanced current production.

The total coulombs recovered for the three de-oiled final combined RW samples, DOW1 (17 ± 2 C), DOW1(II) (29 C ± 8 C), DOW2 and DOW2(II) (23 ± 1 C on average), and DOW3 (34 ± 9 C) were the largest among all the samples except for DOW3(II) (8 ± 1 C) (Fig. 7-2d). In comparison, the DW samples alone produced 16 ± 5 C. The DOSW produced 7 ± 1 C, followed by LGW (1.0 ± 0.1C) and SSW (0.05 ± 0.02 C). The recovery of coulombs from the 50:50

RW+DW mixtures was not larger than that obtained from the full strength wastewaters (after accounting for relative amounts of the wastewaters in the samples). This result in terms of total coulombs was therefore different from the comparison of the diluted and full strength wastewaters on the basis of maximum current.

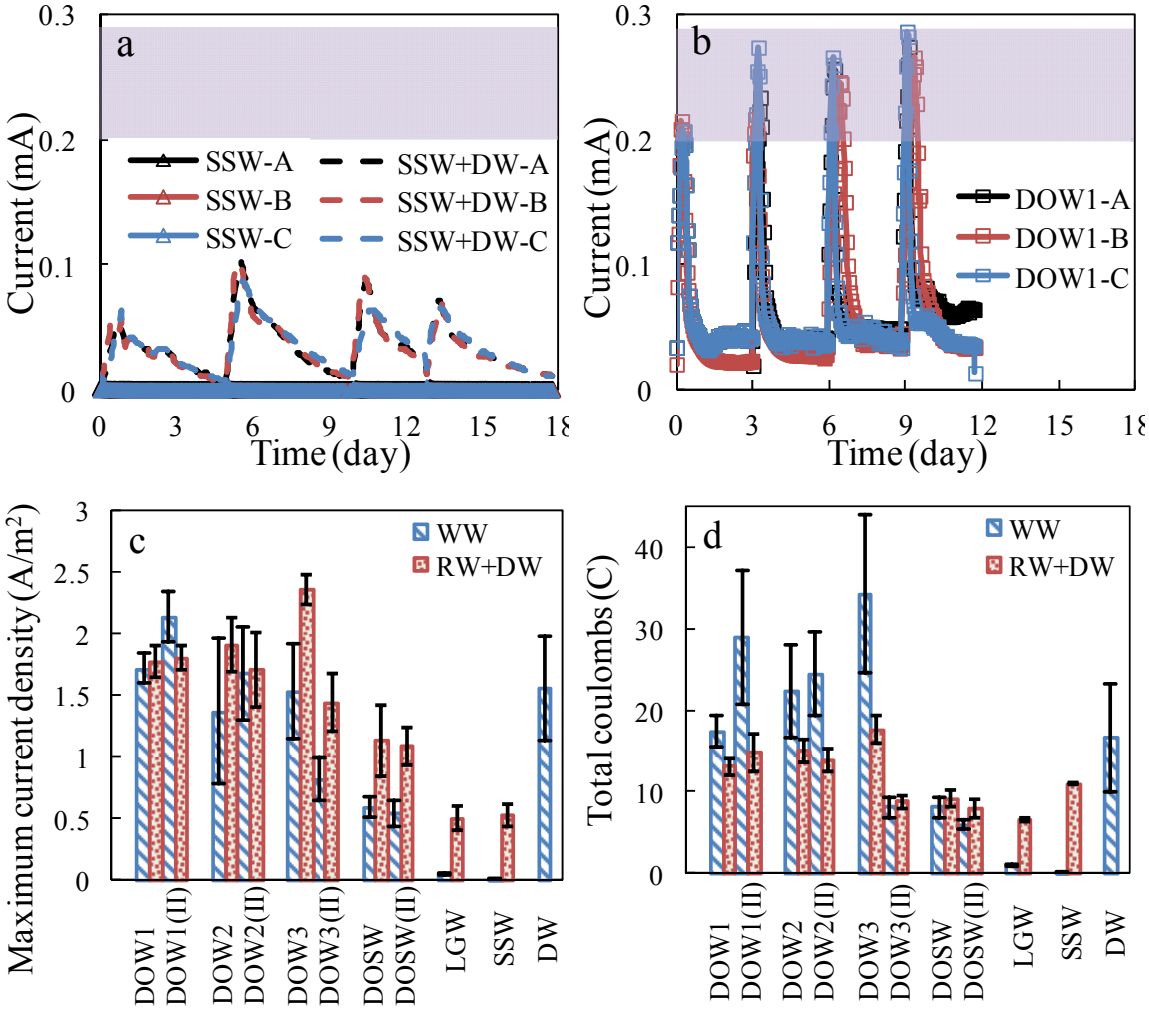

Figure 7-2 Current production of the refinery and domestic wastewaters: (a) example of SSW showing poor current generation over the duration of a cycle; (b) example of DOW1 showing good current generation over the duration of a cycle; (c) maximum current densities; and (d) total coulombs. The shaded areas in (a) and (b) indicate the range in the maximum current produced by domestic wastewater (DW) samples. Full strength refinery wastewaters and domestic wastewater is indicated by blue stripes (WW), while the 50:50 wastewater mix is indicated by red dots (RW+DW) in (c) and (d).

7.3.3 Enhanced treatment due to current generation

The bio-electrochemical treatment of the refinery wastewaters clearly improved treatment, as the COD and HBOD removals in the MECs with current generation were all larger than the open circuit controls (based on comparison of the 50:50 RW+DW mixtures with treatment and with open circuits; Fig. 7-3). Current production increased the COD removals by 40 – 300% for the different RW samples, with an overall removal in the range of 50 – 80% for all wastewaters except the SSW (23%). The increase in HBOD removal was smaller, but it still increased by 30 – 200% compared to open circuit controls, with total HBOD removals in the range of 70 – 90%, but a lower overall removal again measured for the SSW (55%) (Fig. 7-3).

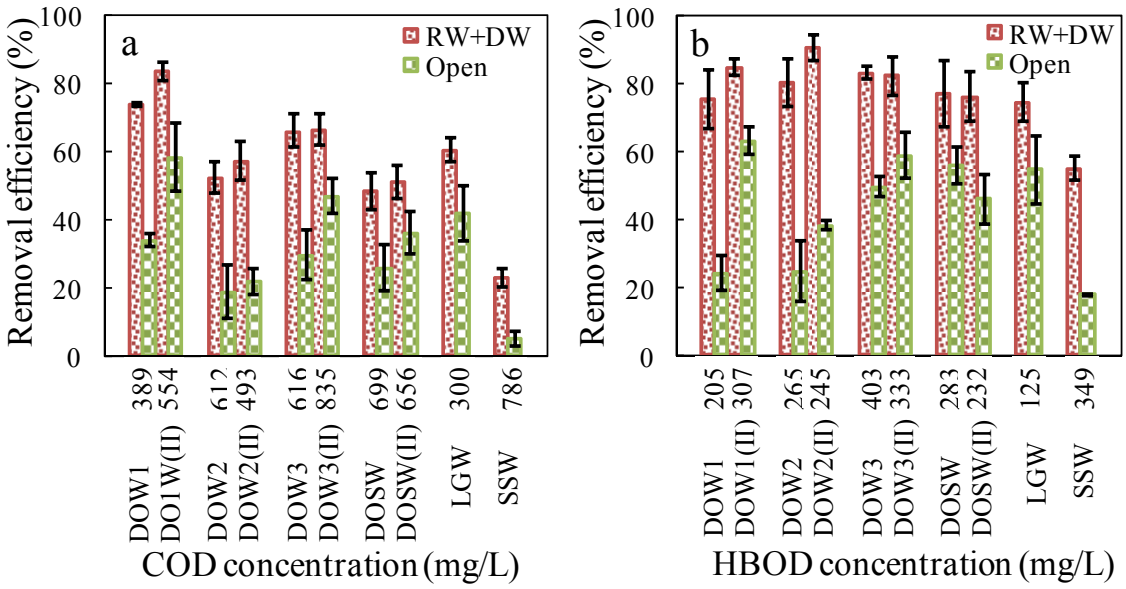

Figure 7-3 COD and HBOD removal efficiency of the 50:50 refinery wastewater + domestic wastewater mixture (RW+DW) compared with the open circuit 50:50 mixture (Open): (a) COD removal efficiency; (b) HBOD removal efficiency.

A comparison of the COD and HBOD removal efficiencies for both the full strength RW tests and the mixtures (50:50 RW+DW) also indicated that the de-oiled final combined RW samples (DOW1, DOW2, and DOW3) had the highest organic removals among these different types of samples, with >50% COD removal and >60% HBOD removal (Fig. E-2). The HBOD removal (0 – 20%) of the full strength DOW2 samples was an exception due to the low starting

HBOD measured lack of bacteria inoculum. As a positive control, 73% COD removal and 93% HBOD removals was achieved using DW (Fig. E-2). The DOSW samples followed with 34 – 51% COD removal and 50 – 77% HBOD removal, while the LGW sample showed COD removals of 5% (full strength) and 60% (50:50 mixture) with 67 – 74% HBOD removal. There was no organic matter removal for SSW if it was not combined with DW. The organic removals for the 50:50 RW+DW mixtures were higher than for the full strength refinery samples (Fig. E-2). This was presumably owed to the high biodegradability of the DW. Another reason might be that more of the organic matter in RWs was degraded after combining with DW, as indicated by the higher HBOD* values measured using the 50:50 mixture (Fig. 7-1).

All of these comparisons of the different refinery wastewater samples in terms of current production and treatment efficiency demonstrated that the three de-oiled final combined wastewater samples (DOW1, DOW2, DOW3) were good fuels for MECs. As these samples were from wastewaters treated using conventional biological treatment processes, there was sufficient biodegradable organic matter and conductivity (2 – 3 mS/cm, compared to 1.3 ± 0.3 mS/cm of DW) for good performance of the MECs. The DOW1 samples produced comparable results to those that obtained with DW, with maximum current density of 2.1 ± 0.2 A/m^2, 79% COD removal, and 82% HBOD removal. The success of treatment and current generation with these samples suggests that MECs (or likely also MFCs) could be used as a single biological treatment step, or also as a pre-treatment step prior to biological aerobic treatment for polishing.

Although the DOSW sample was also de-oiled, it did not show good performance in the MEC tests. One possible reason could have been concentrations of toxic compounds that were not sufficiently removed by the oil/water separation step. While these chemicals may have been present in the other DOW samples, dilution with other wastewater streams may have lowered them prior to final treatment. It was not possible to conduct a detailed chemical analysis here. The LGW sample also produced little current in MECs, but this was likely due to the low concentration of biodegradable organic compounds (a BOD value of 23 ± 5 mg/L) as a result of

prior treatment in the upstream bioreactor. Despite a high HBOD* of 600 ± 40 mg/L, the SSW sample also showed little current production in the tested MECs. The reason for this was likely the high pH as samples were not adjusted for pH.

7.3.4 Relationship between biochemical oxygen demands and MEC performance

Several different approaches were used to evaluate treatability of the wastewater samples in terms of oxygen demand tests (HBOD, HBOD*, and COD), and the effectiveness of bio-electrochemical treatment (maximum current or total coulombs). The best linear relationship was found between HBOD removal and total coulombs (Fig. 7-4a), with an $R^2 = 0.91$ and a slope of 0.1 ($p<0.01$, Analysis of Variance), but only if data from DOW2, DOW2(II), and SSW were not included in this analysis. The DOW2 and SSW data were not used on the basis of HBOD measurements being much less than those of the 50:50 mixture, indicating that the HBOD values were not accurately determined due to insufficient microbial seeds in the samples. These wastewater samples were omitted from the analysis even though it could be seen that the SSW result did show good agreement with the regression line produced by analysis of the other samples (Fig. E-4a).

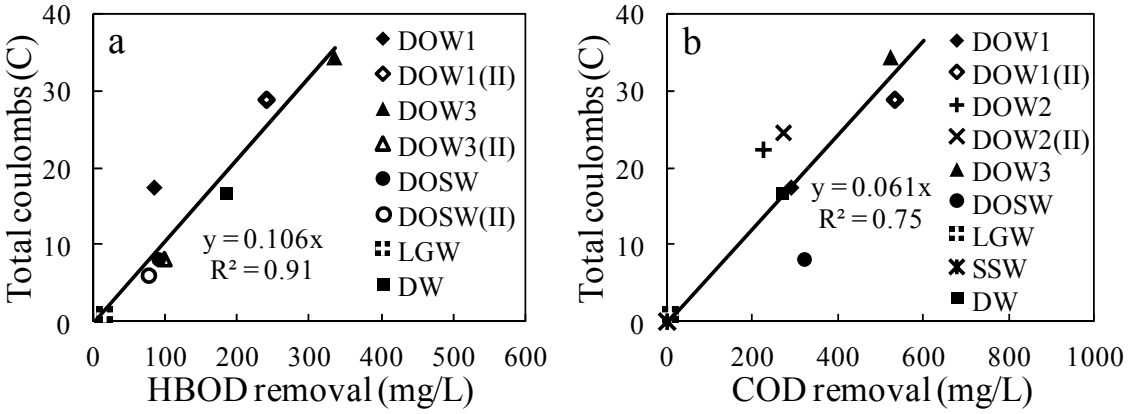

Figure 7-4 Correlation between electricity production and oxygen demand. The DOW2 and SSW were omitted in plot (a); and the DOW3(II) and DOSW(II) were omitted in (b).

The relationship between the total coulombs and COD removal was significant (slope of 0.06, with $p<0.01$; $R^2 = 0.75$), but the correlation was not as good as that found between

coulombs and HBOD removal with or without the inclusion of the DOW3(II) and DOSW(II) data (Fig. 7-4b). DOW3(II) and DOSW(II) data were not used in the analysis due to the low sCOD (less than 50% of total COD, Fig. E-3b).

Correlations between the starting HBOD, HBOD*, and COD were less significant, with R^2 values of 0.85 for HBOD, 0.51 for HBOD*, and 0.42 for COD versus total coulombs recovered in MECs (Fig. E-4). Although the correlations obtained using the starting BOD (with or without the DW addition) were better than those obtained using the starting COD, none of these were judged to be a sufficient predictor of MEC performance.

7.3.5 Effect of pre-acclimation to domestic wastewater on refinery wastewater treatment

The cross-feeding tests showed that in almost all cases the MECs pre-acclimated to the DW or the 50:50 RW+DW mixture had better current generation than those acclimated only to full strength RW. The only exception was the DOW1(II) sample. When full strength RW was fed to the MEC reactors acclimated with different combinations of RW and DW, the maximum current densities of the MECs pre-acclimated to the DW were about the same as reactors pre-acclimated to the 50:50 RW+DW mixture, but they were much higher (1 – 2 fold) than those acclimated only to RW (Fig. 7-5a). For the DOW1(II) sample, the pre-acclimated reactor (both to DW and the 50:50 mixture) produced maximum current densities similar to those obtained only to RW. In contrast to differences in current densities with the different acclimation procedures, for MECs fed the same RW sample, the total recovered coulombs showed no differences among the reactors acclimated to RW, 50:50 RW+DW, and DW (Fig. 7-5b).

In terms of organic removal, reactors always fed the DW produced the same COD and HBOD* removal efficiencies as those always tested using the 50:50 mixture. This was also observed for most RW samples [DOW1(II), DOW3(II), and DOSW(II)]. Pre-acclimation of the MECs to the DW or the 50:50 RW+DW mixture increased the COD and HBOD* removals by two times, compared with those obtained fed only DOW2(II) wastewater (Fig. 7-6). These

findings suggested that acclimating MECs to DW prior to testing any other wastewaters might be a useful method in general for conducting MEC treatability tests.

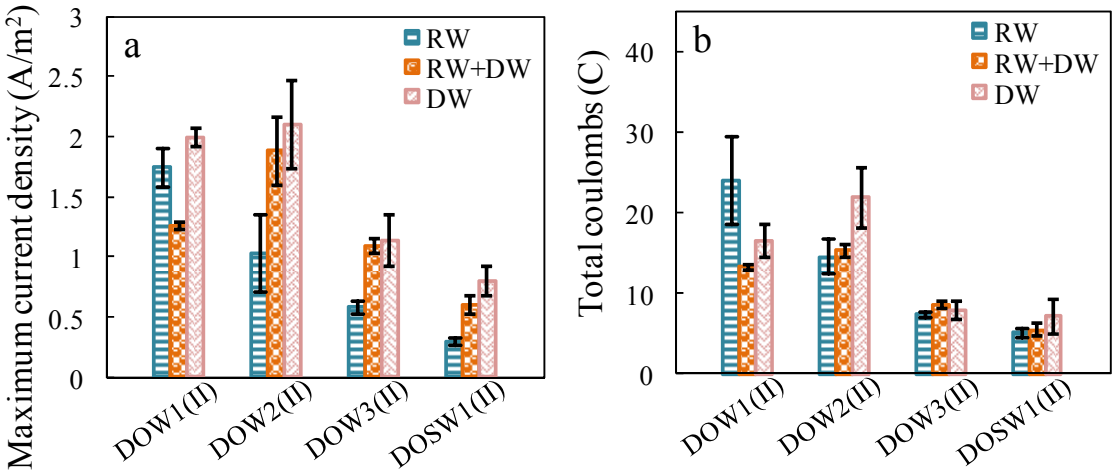

Figure 7-5 Maximum current density and total coulombs produced by the refinery wastewater samples during cross-feeding tests: (a) maximum current density; (b) total coulombs. MEC reactors acclimated to only refinery wastewater was indicated by "RW", to the 50:50 refinery wastewater + domestic wastewater mixture by "RW+DW", and to only domestic wastewater by "DW".

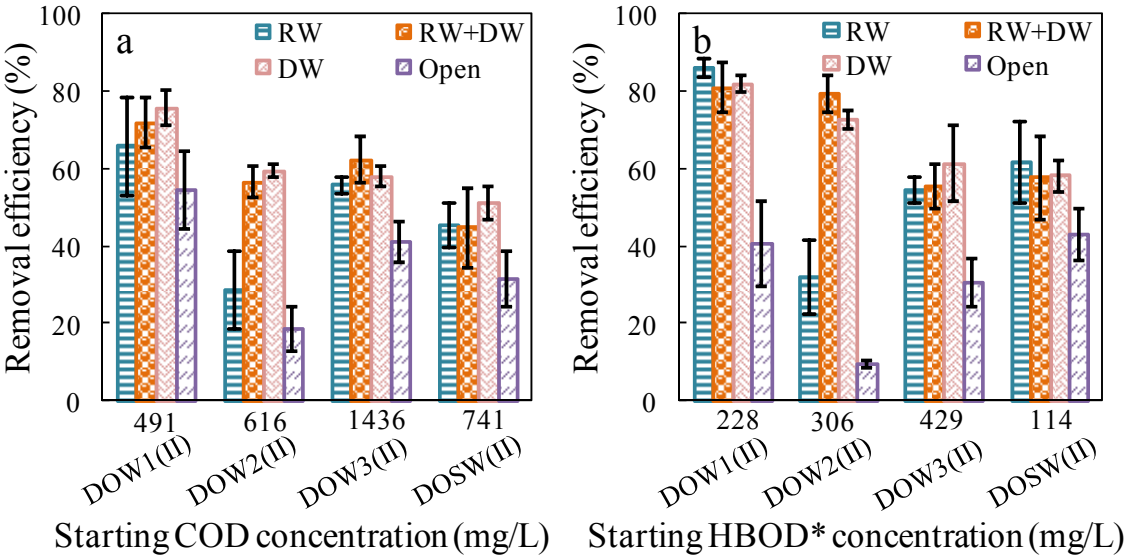

Figure 7-6 COD and HBOD* removal efficiency of the refinery wastewater samples during cross-feeding tests: (a) COD removal efficiency; (b) HBOD* removal efficiency. MEC reactors acclimated to only refinery wastewater was indicated by "RW", to the 50:50 refinery wastewater + domestic wastewater mixture by "RW+DW", and to only domestic wastewater by "DW". The open circuit 50:50 mixture was also fed full strength refinery wastewater and kept open circuit (Open).

Pre-acclimating the MECs to DW or the 50:50 RW+DW mixture had another advantage of saving time needed for reactor starting up. While MEC reactors fed the DW or the 50:50 mixture took only one week to produce stable performance, reactors fed RW usually needed longer time. Depending on the samples, the start-up time of the MECs tested with only RW varied from one week (DOW1) to as long as one and a half months (DOW2; 1.5 weeks for DOSW, and one month for DOW3). Therefore, pre-acclimation of the anodes with DW improved performance of MECs with respect to electricity production and organics removal, and also ensured a more rapid start-up of the reactors for stable current generation.

7.4 Conclusions

The different refinery wastewater samples varied in terms of current production and treatability in MEC tests. All three de-oiled wastewater samples from combined sources showed good performance, with one sample producing results comparable to those obtained with DW. Other samples produced low current densities due to high initial pH or a low BOD. The most successful approach for starting up MECs was pre-acclimation with domestic wastewater, as this improved electricity production, treatability, and reactor start-up. These results demonstrated the feasibility of using MECs as a treatment or pre-treatment (before secondary biological treatment) of some types of refinery wastewaters.

Chapter 8

Future work

In this dissertation, I showed that substrate concentration differences caused the slightly lower power production in the multi-electrode MFCs with a parallel electrical connection, and the increased substrate consumption by exoelectrogens resulted in the increased CEs and COD removals at higher current. I developed a two-stage MFC-AFMBR system as an energy-efficient wastewater treatment process with high effluent quality. I also investigated the feasibility of using mini-MECs as an effective high-throughput evaluation method for various objectives. These studies mostly focused on a specific operational aspect of MFCs, or demonstrated the feasibility of a new process. Thus, more research is needed to obtain a more comprehensive understanding of these systems. Systematic evaluations are needed as listed below.

1. A systematic impedance test of the internal resistance is suggested for the multi-electrode MFCs with individual circuits and parallel connection, when there are large substrate concentration changes under continuous flow conditions. These data will enable the modeling of such multi-electrode systems, to address more issues toward system scale-up.
2. Further optimization of the performance of the individual and combined MFC and AFMBR reactors is needed, such as adjusting the HRTs and operating at lower temperatures. Following these optimization studies, it should be possible to better evaluate the economics of this system compared to traditional treatment systems. The produced methane should be captured for use or destroyed to avoid its release into the air as it is a potent greenhouse gas.
3. Treatability of different wastewater sources should be tested side-by-side using mini-MECs, and larger MECs and MFCs. A better evaluation on the credibility and reliability of the screening results obtained in mini-MECs can be achieved by

comparing the current production and treatment efficiencies of the wastewater samples in these different systems.

References

Aelterman, P., Rabaey, K., Pham, H. T., Boon, N., and Verstraete, W. (2006). Continuous electricity generation at high voltages and currents using stacked microbial fuel cells. *Environ. Sci. Technol.*, 40(10), 3388-3394.

Ahn, Y., Hatzell, M. C., Zhang, F., and Logan, B. E. (2014). Different electrode configurations to optimize performance of multi-electrode microbial fuel cells for generating power or treating domestic wastewater. *J. Power Sources*, 249, 440-445.

Ahn, Y., and Logan, B. E. (2010). Effectiveness of domestic wastewater treatment using microbial fuel cells at ambient and mesophilic temperatures. *Bioresour. Technol.*, 101(2), 469-475.

Ahn, Y., and Logan, B. E. (2012). A multi-electrode continuous flow microbial fuel cell with separator electrode assembly design. *Appl. Microbiol. Biotechnol.*, 93(5), 2241-2248.

Ahn, Y., and Logan, B. E. (2013). Domestic wastewater treatment using multi-electrode continuous flow MFCs with a separator electrode assembly design. *Appl. Microbiol. Biotechnol.*, 97(1), 409-416.

Allen, R. M., and Bennetto, H. P. (1993). Microbial fuel-cells - Electricity production from carbohydrates. *Appl. Biochem. Biotechnol.*, 39, 27-40.

Allesen-Holm, M., Barken, K. B., Yang, L., Klausen, M., Webb, J. S., Kjelleberg, S., Molin, S., Givskov, M., and Tolker-Nielsen, T. (2006). A characterization of DNA release in *Pseudomonas aeruginosa* cultures and biofilms. *Mol. Microbiol.*, 59(4), 1114-1128.

Alvares, A. B. C., Diaper, C., and Parsons, S. A. (2001). Partial oxidation by ozone to remove recalcitrance from wastewaters - A review. *Environ. Technol.*, 22(4), 409-427.

Andersen, S. J., Pikaar, I., Freguia, S., Lovell, B. C., Rabaey, K., and Rozendal, R. A. (2013). Dynamically adaptive control system for bioanodes in serially stacked bioelectrochemical systems. *Environ. Sci. Technol.*, 47(10), 5488-5494.

Angenent, L. T., and Wrenn, B. A. (2008). Optimizing mixed-culture bioprocessing to convert wastes into bioenergy. *Bioenergy*, J. D. Wall, C. S. Harwood, and A. Demain, eds., ASM Press, Herndon, VA, USA, 179-194.

APHA (1998). Standard Methods for the Examination of Water and Wastewater. L. S. Clesceri, A. E. Greenberg, and A. D. Eaton, eds., American Public Health Association, American Water Works Association, Water Environment Federation, Washington DC.

Appels, L., Lauwers, J., Degreve, J., Helsen, L., Lievens, B., Willems, K., Van Impe, J., and Dewil, R. (2011). Anaerobic digestion in global bio-energy production: Potential and research challenges. *Renew. Sust. Energy Rev.*, 15(9), 4295-4301.

Balch, W. E., Fox, G. E., Magrum, L. J., Woese, C. R., and Wolfe, R. S. (1979). Methanogens - Re-evaluation of a unique biological group. *Microbiol. Rev.*, 43(2), 260-296.

Balkema, A. J., Preisig, H. A., Otterpohl, R., and Lambert, F. J. D. (2002). Indicators for the sustainability assessment of wastewater treatment systems. *Urban Water*, 4(2), 153-161.

Bard, A. J., and Faulkner, L. R. (2001). *Electrochemical Methods: Fundamentals and Applications*, John Wiley & Sons New York.

Benyahia, F., Abdulkarim, M., Zekri, A., Chaalal, O., and Hasanain, H. (2005). Bioremediation of crude oil contaminated soils - A black art or an engineering challenge? *Process Saf. Environ.*, 83(B4), 364-370.

Biffinger, J., Ribbens, M., Ringeisen, B., Pietron, J., Finkel, S., and Nealson, K. (2009). Characterization of electrochemically active bacteria utilizing a high-throughput voltage-based screening assay. *Biotechnol. Bioeng.*, 102(2), 436-444.

Bouallagui, H., Touhami, Y., Cheikh, R. B., and Hamdi, M. (2005). Bioreactor performance in anaerobic digestion of fruit and vegetable wastes. *Process Biochem.*, 40(3-4), 989-995.

Brentner, L. B., Peccia, J., and Zimmerman, J. B. (2010). Challenges in developing biohydrogen as a sustainable energy source: Implications for a research agenda. *Environ. Sci. Technol.*, 44(7), 2243-2254.

Buffiere, P., Mirquez, L. D., Steyer, J. P., Bernet, N., and Delgenes, J. P. (2008). Anaerobic digestion of solid wastes needs research to face an increasing industrial success. *Int. J. Chem. Reactor Eng.*, 6(1).

Call, D. F., and Logan, B. E. (2008). Hydrogen production in a single chamber microbial electrolysis cell lacking a membrane. *Environ. Sci. Technol.*, 42(9), 3401-3406.

Call, D. F., and Logan, B. E. (2011a). Lactate oxidation coupled to iron or electrode reduction by *Geobacter sulfurreducens* PCA. *Appl. Environ. Microbiol.*, 77(24), 8791-8794.

Call, D. F., and Logan, B. E. (2011b). A method for high throughput bioelectrochemical research based on small scale microbial electrolysis cells. *Biosens. Bioelectron.*, 26(11), 4526-4531.

Call, D. F., Wagner, R. C., and Logan, B. E. (2009). Hydrogen production by *Geobacter* species and a mixed consortium in a microbial electrolysis cell. *Appl. Environ. Microbiol.*, 75(24), 7579-7587.

CAMBRIAN (2013a). Cambrian Innovation Inc. Cambrian's EcoVolt Bioelectric Wastewater Treatment System Now Commercially Available. <http://cambrianinnovation.com/ecovolt-now-commercially-available/>.

CAMBRIAN (2013b). Cambrian Innovation Inc. EcoVolt Bioelectric Wastewater Treatment. <http://cambrianinnovation.com/wp-content/uploads/2012/11/EcoVolt-brochure-updated3.pdf>.

CAMBRIAN (2013c). Cambrian Innovation Inc. EcoVolt, The World's First Bioelectric Treatment Process. <http://cambrianinnovation.com/solutions/ecovolt/>.

Chan, K., and Eikerling, M. (2011). A pore-scale model of oxygen reduction in ionomer-free catalyst layers of PEFCs. *J. Electrochem. Soc.*, 158(1), B18-B28.

Chen, C. C., Lin, C. Y., and Lin, M. C. (2002). Acid-base enrichment enhances anaerobic hydrogen production process. *Appl. Microbiol. Biotechnol.*, 58(2), 224-228.

Chen, C. Y., Yang, M. H., Yeh, K. L., Liu, C. H., and Chang, J. (2008). Biohydrogen production using sequential two-stage dark and photo fermentation processes. *Int. J. Hydrogen Energy*, 33(18), 4755-4762.

Chen, Y. P., Zhao, Y., Qiu, K. Q., Chu, J., Lu, R., Sun, M., Liu, X. W., Sheng, G. P., Yu, H. Q., Chen, J., Li, W. J., Liu, G., Tian, Y. C., and Xiong, Y. (2011). An innovative miniature microbial fuel cell fabricated using photolithography. *Biosens. Bioelectron.*, 26(6), 2841-2846.

Chen, Z., Huang, Y. C., Liang, J. H., Zhao, F., and Zhu, Y. G. (2012). A novel sediment microbial fuel cell with a biocathode in the rice rhizosphere. *Bioresour. Technol.*, 108, 55-59.

Cheng, S. A., Liu, H., and Logan, B. E. (2006a). Increased performance of single-chamber microbial fuel cells using an improved cathode structure. *Electrochem. Commun.*, 8(3), 489-494.

Cheng, S. A., Liu, H., and Logan, B. E. (2006b). Increased power generation in a continuous flow MFC with advective flow through the porous anode and reduced electrode spacing. *Environ. Sci. Technol.*, 40(7), 2426-2432.

Cheng, S. A., and Logan, B. E. (2007). Ammonia treatment of carbon cloth anodes to enhance power generation of microbial fuel cells. *Electrochem. Commun.*, 9(3), 492-496.

Cheng, S. A., and Logan, B. E. (2011). Increasing power generation for scaling up single-chamber air cathode microbial fuel cells. *Bioresour. Technol.*, 102(6), 4468-4473.

Cheng, S. A., Xing, D. F., Call, D. F., and Logan, B. E. (2009). Direct biological conversion of electrical current into methane by electromethanogenesis. *Environ. Sci. Technol.*, 43(10), 3953-3958.

Ching, L. (2010). Eliminating 'Yuck': A simple exposition of media and social change in water reuse policies. *Int. J. Water Resour. D.*, 26(1), 111-124.

Chong, M. L., Sabaratnam, V., Shirai, Y., and Hassan, M. A. (2009). Biohydrogen production from biomass and industrial wastes by dark fermentation. *Int. J. Hydrogen Energy*, 34(8), 3277-3287.

Chung, G., Lansey, K., Blowers, P., Brooks, P., Ela, W., Stewart, S., and Wilson, P. (2008). A general water supply planning model: Evaluation of decentralized treatment. *Environ. Modell. Softw.*, 23(7), 893-905.

Cooper, N. (2009). Collaboration advances microbial fuel cell commercialization. <http://advance.uconn.edu/2009/090504/09050409.htm>.

Cornel, P., and Schaum, C. (2009). Phosphorus recovery from wastewater: Needs, technologies and costs. *Water Sci. Technol.*, 59(6), 1069-1076.

Cusick, R. D., Bryan, B., Parker, D. S., Merrill, M. D., Mehanna, M., Kiely, P. D., Liu, G., and Logan, B. E. (2011). Performance of a pilot-scale continuous flow microbial electrolysis cell fed winery wastewater. *Appl. Microbiol. Biotechnol.*, 89(6), 2053-2063.

Cusick, R. D., Kiely, P. D., and Logan, B. E. (2010). A monetary comparison of energy recovered from microbial fuel cells and microbial electrolysis cells fed winery or domestic wastewaters. *Int. J. Hydrogen Energy*, 35(17), 8855-8861.

Cusick, R. D., and Logan, B. E. (2012). Phosphate recovery as struvite within a single chamber microbial electrolysis cell. *Bioresour. Technol.*, 107, 110-115.

Das, D., and Veziroglu, T. N. (2008). Advances in biological hydrogen production processes. *Int. J. Hydrogen Energy*, 33(21), 6046-6057.

Dekker, A., Ter Heijne, A., Saakes, M., Hamelers, H. V. M., and Buisman, C. J. N. (2009). Analysis and improvement of a scaled-up and stacked microbial fuel cell. *Environ. Sci. Technol.*, 43(23), 9038-9042.

Demirer, G. N., and Chen, S. (2005). Two-phase anaerobic digestion of unscreened dairy manure. *Process Biochem.*, 40(11), 3542-3549.

Dewan, A., Beyenal, H., and Lewandowski, Z. (2008). Scaling up microbial fuel cells. *Environ. Sci. Technol.*, 42(20), 7643-7648.

Ditzig, J., Liu, H., and Logan, B. E. (2007). Production of hydrogen from domestic wastewater using a bioelectrochemically assisted microbial reactor (BEAMR). *Int. J. Hydrogen Energy*, 32(13), 2296-2304.

Dominiak, D. M., Nielsen, J. L., and Nielsen, P. H. (2011). Extracellular DNA is abundant and important for microcolony strength in mixed microbial biofilms. *Environ. Microbiol.*, 13(3), 710-721.

Du, P. W., and Eisenberg, R. (2012). Catalysts made of earth-abundant elements (Co, Ni, Fe) for water splitting: Recent progress and future challenges. *Energy Environ. Sci.*, 5(3), 6012-6021.

Du, Z. W., Li, H. R., and Gu, T. Y. (2007). A state of the art review on microbial fuel cells: A promising technology for wastewater treatment and bioenergy. *Biotechnol. Adv.*, 25(5), 464-482.

EIA (2013). International Energy Outlook 2013 (IEO2013).

ElMekawy, A., Hegab, H. M., Dominguez-Benetton, X., and Pant, D. (2013). Internal resistance of microfluidic microbial fuel cell: Challenges and potential opportunities. *Bioresour. Technol.*, 142, 672-682.

Eom, H., Chung, K., Kim, I., and Han, J. I. (2011). Development of a hybrid microbial fuel cell (MFC) and fuel cell (FC) system for improved cathodic efficiency and sustainability: The M2FC reactor. *Chemosphere*, 85(4), 672-676.

EPA (2012). Climate Change Indicators in the United States.

Erable, B., Etcheverry, L., and Bergel, A. (2011). From microbial fuel cell (MFC) to microbial electrochemical snorkel (MES): Maximizing chemical oxygen demand (COD) removal from wastewater. *Biofouling*, 27(3), 319-326.

Etnier, C., and Guterstam, B. (1991). *Proc., Int. Conf. Ecological engineering for wastewater treatment*, Stensund, Bokskogen, Sweden.

Fan, Y. Z., Hu, H. Q., and Liu, H. (2007). Enhanced coulombic efficiency and power density of air-cathode microbial fuel cells with an improved cell configuration. *J. Power Sources*, 171(2), 348-354.

Fedorovich, V., Varfolomeev, S. D., Sizov, A., and Goryanin, I. (2009). Multi-electrode microbial fuel cell with horizontal liquid flow. *Water Sci. Technol.*, 60(2), 347-355.

Feng, L. Y., Chen, Y. G., and Chen, L. (2011). Easy-to-operate and low-temperature synthesis of gram-scale nitrogen-doped graphene and its application as cathode catalyst in microbial fuel cells. *ACS Nano*, 5(12), 9611-9618.

Feng, Y. J., Wang, X., Logan, B. E., and Lee, H. (2008). Brewery wastewater treatment using air-cathode microbial fuel cells. *Appl. Microbiol. Biotechnol.*, 78(5), 873-880.

Feng, Y. J., Yang, Q., Wang, X., and Logan, B. E. (2010). Treatment of carbon fiber brush anodes for improving power generation in air-cathode microbial fuel cells. *J. Power Sources*, 195(7), 1841-1844.

Fink, H. W., and Schonenberger, C. (1999). Electrical conduction through DNA molecules. *Nature*, 398(6726), 407-410.

Foley, J., de Haas, D., Hartley, K., and Lant, P. (2010). Comprehensive life cycle inventories of alternative wastewater treatment systems. *Water Res.*, 44(5), 1654-1666.

Freguia, S., Rabaey, K., Yuan, Z. G., and Keller, J. (2007). Electron and carbon balances in microbial fuel cells reveal temporary bacterial storage behavior during electricity generation. *Environ. Sci. Technol.*, 41(8), 2915-2921.

Galvez, A., Greenman, J., and Ieropoulos, I. (2009). Landfill leachate treatment with microbial fuel cells: Scale-up through plurality. *Bioresour. Technol.*, 100(21), 5085-5091.

Gardner, G. (1997). Recycling organic waste: From urban pollutant to farm resource. *Worldwatch Institute*, paper 135, 58 p.

Ge, Z., Ping, Q., and He, Z. (2013). Hollow-fiber membrane bioelectrochemical reactor for domestic wastewater treatment. *J. Chem. Technol. Biotechnol.*, 88(8), 1584-1590.

Goodstein, D., and Intriligator, M. (2012). *Climate Change and the Energy Problem: Physical Science and Economics Perspective*, World Scientific Publishing Co., Inc., Hackensack, NJ 07601, USA

Gorodetsky, A. A., Buzzeo, M. C., and Barton, J. K. (2008). DNA-mediated electrochemistry. *Bioconjugate Chem.*, 19(12), 2285-2296.

Guest, J. S., Skerlos, S. J., Barnard, J. L., Beck, M. B., Daigger, G. T., Hilger, H., Jackson, S. J., Karvazy, K., Kelly, L., Macpherson, L., Mihelcic, J. R., Pramanik, A., Raskin, L., Van Loosdrecht, M. C. M., Yeh, D., and Love, N. G. (2009). A new planning and design paradigm to

achieve sustainable resource recovery from wastewater. *Environ. Sci. Technol.*, 43(16), 6126-6130.

Haddadi, S., Elbeshbishy, E., and Lee, H. S. (2013). Implication of diffusion and significance of anodic pH in nitrogen-recovering microbial electrochemical cells. *Bioresour. Technol.*, 142, 562-569.

Han, A., Hou, H. J., Li, L., Kim, H. S., and de Figueiredo, P. (2013). Microfabricated devices in microbial bioenergy sciences. *Trends Biotechnol.*, 31(4), 225-232.

Harnisch, F., and Schroder, U. (2010). From MFC to MXC: Chemical and biological cathodes and their potential for microbial bioelectrochemical systems. *Chem. Soc. Rev.*, 39(11), 4433-4448.

Hatzell, M. C., Kim, Y., and Logan, B. E. (2013). Powering microbial electrolysis cells by capacitor circuits charged using microbial fuel cell. *J. Power Sources*, 229, 198-202.

Hays, S., Zhang, F., and Logan, B. E. (2011). Performance of two different types of anodes in membrane electrode assembly microbial fuel cells for power generation from domestic wastewater. *J. Power Sources*, 196(20), 8293-8300.

He, Z. (2013). Microbial fuel cells: Now let us talk about energy. *Environ. Sci. Technol.*, 47(1), 332-333.

He, Z., Huang, Y. L., Manohar, A. K., and Mansfeld, F. (2008). Effect of electrolyte pH on the rate of the anodic and cathodic reactions in an air-cathode microbial fuel cell. *Bioelectrochemistry*, 74(1), 78-82.

He, Z., and Mansfeld, F. (2009). Exploring the use of electrochemical impedance spectroscopy (EIS) in microbial fuel cell studies. *Energy Environ. Sci.*, 2(2), 215-219.

He, Z., Minteer, S. D., and Angenent, L. T. (2005). Electricity generation from artificial wastewater using an upflow microbial fuel cell. *Environ. Sci. Technol.*, 39(14), 5262-5267.

Heidrich, E. S., Dolfing, J., Scott, K., Edwards, S. R., Jones, C., and Curtis, T. P. (2013). Production of hydrogen from domestic wastewater in a pilot-scale microbial electrolysis cell. *Appl. Microbiol. Biotechnol.*, 97(15), 6979-6989.

Hong, Y. Y., Call, D. F., Werner, C. M., and Logan, B. E. (2011). Adaptation to high current using low external resistances eliminates power overshoot in microbial fuel cells. *Biosens. Bioelectron.*, 28(1), 71-76.

Hou, H. J., Li, L., Ceylan, C. U., Haynes, A., Cope, J., Wilkinson, H. H., Erbay, C., de Figueiredo, P., and Han, A. (2012). A microfluidic microbial fuel cell array that supports long-term multiplexed analyses of electricigens. *Lab Chip*, 12(20), 4151-4159.

Hou, H. J., Li, L., Cho, Y., de Figueiredo, P., and Han, A. (2009). Microfabricated microbial fuel cell arrays reveal electrochemically active microbes. *PloS One*, 4(8).

Hou, H. J., Li, L., de Figueiredo, P., and Han, A. (2011). Air-cathode microbial fuel cell array: A device for identifying and characterizing electrochemically active microbes. *Biosens. Bioelectron.*, 26(5), 2680-2684.

Howe, K. J., Hand, D. W., Crittenden, J. C., Trussell, R. R., and Tchobanoglous, G. (2012). *Principles of Water Treatment, third ed.*, John Wiley&Sons, Inc., Hoboken, NJ.

Huang, L. P., Chai, X. L., Quan, X., Logan, B. E., and Chen, G. (2012). Reductive dechlorination and mineralization of pentachlorophenol in biocathode microbial fuel cells. *Bioresour. Technol.*, 111, 167-174.

Huang, L. P., and Logan, B. E. (2008). Electricity generation and treatment of paper recycling wastewater using a microbial fuel cell. *Appl. Microbiol. Biotechnol.*, 80(2), 349-355.

Ichihashi, O., and Hirooka, K. (2012). Removal and recovery of phosphorus as struvite from swine wastewater using microbial fuel cell. *Bioresour. Technol.*, 114, 303-307.

IEA (2012). Key World Energy Statistics. The international energy agency.

Ieropoulos, I., Greenman, J., and Melhuish, C. (2008). Microbial fuel cells based on carbon veil electrodes: Stack configuration and scalability. *Int. J. Energy Res.*, 32(13), 1228-1240.

Ieropoulos, I., Greenman, J., and Melhuish, C. (2010). Improved energy output levels from small-scale microbial fuel cells. *Bioelectrochemistry*, 78(1), 44-50.

Ieropoulos, I. A., Greenman, J., and Melhuish, C. (2013). Miniature microbial fuel cells and stacks for urine utilisation. *Int. J. Hydrogen Energy*, 38(1), 492-496.

Inoue, K., Qian, X. L., Morgado, L., Kim, B. C., Mester, T., Izallalen, M., Salgueiro, C. A., and Lovley, D. R. (2010). Purification and characterization of OmcZ, an outer-surface, octaheme c-type cytochrome essential for optimal current production by *Geobacter sulfurreducens*. *Appl. Environ. Microbiol.*, 76(12), 3999-4007.

Jenssen, P. D., and Skjelhaugen, O. J. (1994). Local ecological solutions for wastewater and organic waste treatment - A total concept for optimum reclamation and recycling. *Proc., Seventh International Symposium on Individual and Small Community Sewage systems*, Atlanta, ASAE., 379-387.

Jenssen, P. D., Vråle, L., and Lindholm, O. (2007). Sustainable wastewater treatment. *Proc., International conference on natural resources and environmental management and environmetal safety and health*, Kuching, Malaysia.

Jiang, D. Q., and Li, B. K. (2009). Novel electrode materials to enhance the bacterial adhesion and increase the power generation in microbial fuel cells (MFCs). *Water Sci. Technol.*, 59(3), 557-563.

Jin, B., van Leeuwen, H. J., Patel, B., and Yu, Q. (1998). Utilisation of starch processing wastewater for production of microbial biomass protein and fungal alpha-amylase by *Aspergillus oryzae*. *Bioresour. Technol.*, 66(3), 201-206.

Juang, C. P., Whang, L. M., and Cheng, H. H. (2011). Evaluation of bioenergy recovery processes treating organic residues from ethanol fermentation process. *Bioresour. Technol.*, 102(9), 5394-5399.

Jung, S., and Regan, J. M. (2011). Influence of external resistance on electrogenesis, methanogenesis, and anode prokaryotic communities in microbial fuel cells. *Appl. Environ. Microbiol.*, 77(2), 564-571.

Kato, S., Nakamura, R., Kai, F., Watanabe, K., and Hashimoto, K. (2010). Respiratory interactions of soil bacteria with (semi)conductive iron-oxide minerals. *Environ. Microbiol.*, 12(12), 3114-3123.

Katuri, K. P., Kavanagh, P., Rengaraj, S., and Leech, D. (2010). *Geobacter sulfurreducens* biofilms developed under different growth conditions on glassy carbon electrodes: Insights using cyclic voltammetry. *Chem. Commun.*, 46(26), 4758-4760.

Kim, B. H., Park, D. H., Shin, P. K., Chang, I. S., and Kim, H. J. (1999a). Mediator-less biofuel cell. *U.S. Patent 5976719*.

Kim, D., An, J., Kim, B., Jang, J. K., Kim, B. H., and Chang, I. S. (2012a). Scaling-up microbial fuel cells: Configuration and potential drop phenomenon at series connection of unit cells in shared anolyte. *ChemSusChem*, 5(6), 1086-1091.

Kim, H. J., Hyun, M. S., Chang, I. S., and Kim, B. H. (1999b). A microbial fuel cell type lactate biosensor using a metal-reducing bacterium, *Shewanella putrefaciens*. *J. Microbiol. Biotechnol.*, 9(3), 365-367.

Kim, J., Kim, K., Lee, R., McCarty, P. L., and Bae, J. (2012b). Physical aspects of GAC fluidization on membrane fouling in anaerobic fluidized membrane bioreactor. *IWA World Water Congress* Busan, Korea.

Kim, J., Kim, K., Ye, H., Lee, E., Shin, C., McCarty, P. L., and Bae, J. (2011a). Anaerobic fluidized bed membrane bioreactor for wastewater treatment. *Environ. Sci. Technol.*, 45(2), 576-581.

Kim, J. R., Cheng, S. A., Oh, S. E., and Logan, B. E. (2007). Power generation using different cation, anion, and ultrafiltration membranes in microbial fuel cells. *Environ. Sci. Technol.*, 41(3), 1004-1009.

Kim, Y., Hatzell, M. C., Hutchinson, A. J., and Logan, B. E. (2011b). Capturing power at higher voltages from arrays of microbial fuel cells without voltage reversal. *Energy Environ. Sci.*, 4(11), 4662-4667.

Kothari, H. M., Kulp, E. A., Limmer, S. J., Poizot, P., Bohannan, E. W., and Switzer, J. A. (2006). Electrochemical deposition and characterization of Fe_3O_4 films produced by the reduction of Fe(III)-triethanolamine. *J. Mater. Sci.*, 21(1), 293-301.

Kuntke, P., Smiech, K. M., Bruning, H., Zeeman, G., Saakes, M., Sleutels, T., Hamelers, H. V. M., and Buisrnan, C. J. N. (2012). Ammonium recovery and energy production from urine by a microbial fuel cell. *Water Res.*, 46(8), 2627-2636.

Lalaurette, E., Thammannagowda, S., Mohagheghi, A., Maness, P. C., and Logan, B. E. (2009). Hydrogen production from cellulose in a two-stage process combining fermentation and electrohydrogenesis. *Int. J. Hydrogen Energy*, 34(15), 6201-6210.

Lanas, V., Ahn, Y., and Logan, B. E. (2014). Effects of carbon brush anode size and loading on microbial fuel cell performance in batch and continuous mode. *J. Power Sources*, 247, 228-234.

Lanas, V., and Logan, B. E. (2013). Evaluation of multi-brush anode systems in microbial fuel cells. *Bioresour. Technol.*, 148, 379-385.

Lazarova, V., Choo, K. H., and Cornel, P. (2012). Meeting the challenges of the water-energy nexus: The role of reuse and wastewater treatment. *Water21*, April(14.2), 12-17.

Ledezma, P., Greenman, J., and Ieropoulos, I. (2012). Maximising electricity production by controlling the biofilm specific growth rate in microbial fuel cells. *Bioresour. Technol.*, 118, 615-618.

Ledezma, P., Greenman, J., and Ieropoulos, I. (2013). MFC-cascade stacks maximise COD reduction and avoid voltage reversal under adverse conditions. *Bioresour. Technol.*, 134, 158-165.

Lee, H. S., Vermaas, W. F. J., and Rittmann, B. E. (2010). Biological hydrogen production: Prospects and challenges. *Trends Biotechnol.*, 28(5), 262-271.

Lee, L. Y., Hu, J. Y., Ong, S. L., Ng, W. J., Ren, J. H., and Wong, S. H. (2004). Two-stage SBR for treatment of oil refinery wastewater. *Water Sci. Technol.*, 50(10), 243-249.

Lewis, K. (1966). Symposium on bioelectrochemistry of microorganisms. 4. Biochemical fuel cells. *Bacteriol. Rev.*, 30(1), 101-113.

Lewis, N. S., and Nocera, D. G. (2006). Powering the planet: Chemical challenges in solar energy utilization. *Proc. Natl. Acad. Sci. U.S.A.*, 103(43), 15729-15735.

Li, W. W., and Yu, H. Q. (2011). From wastewater to bioenergy and biochemicals via two-stage bioconversion processes: A future paradigm. *Biotechnol. Adv.*, 29(6), 972-982.

Li, Z. L., Yao, L., Kong, L. C., and Liu, H. (2008). Electricity generation using a baffled microbial fuel cell convenient for stacking. *Bioresour. Technol.*, 99(6), 1650-1655.

Li, Z. Q., Zhang, Y., LeDuc, P. R., and Gregory, K. B. (2011). Microbial electricity generation via microfluidic flow control. *Biotechnol. Bioeng.*, 108(9), 2061-2069.

Lindtner, S., Schaar, H., and Kroiss, H. (2008). Benchmarking of large municipal wastewater treatment plants treating over 100,000 PE in Austria. *Water Sci. Technol.*, 57(10), 1487-1493.

Liu, H., Cheng, S., Huang, L. P., and Logan, B. E. (2008). Scale-up of membrane-free single-chamber microbial fuel cells. *J. Power Sources*, 179(1), 274-279.

Liu, H., Cheng, S. A., and Logan, B. E. (2005). Production of electricity from acetate or butyrate using a single-chamber microbial fuel cell. *Environ. Sci. Technol.*, 39(2), 658-662.

Liu, H., and Logan, B. E. (2004). Electricity generation using an air-cathode single chamber microbial fuel cell in the presence and absence of a proton exchange membrane. *Environ. Sci. Technol.*, 38(14), 4040-4046.

Liu, H., Ramnarayanan, R., and Logan, B. E. (2004). Production of electricity during wastewater treatment using a single chamber microbial fuel cell. *Environ. Sci. Technol.*, 38(7), 2281-2285.

Liu, J. D., Liu, L. F., Gao, B., and Yang, F. L. (2013). Integration of bio-electrochemical cell in membrane bioreactor for membrane cathode fouling reduction through electricity generation. *J. Membr. Sci.*, 430, 196-202.

Liu, Z. D., Liu, J., Zhang, S. P., and Su, Z. G. (2009). Study of operational performance and electrical response on mediator-less microbial fuel cells fed with carbon- and protein-rich substrates. *Biochem. Eng. J.*, 45(3), 185-191.

Logan, B. E. (2004). Extracting hydrogen electricity from renewable resources. *Environ. Sci. Technol.*, 38(9), 160A-167A.

Logan, B. E. (2008). *Microbial Fuel Cells*, Wiley-Interscience, Hoboken, NJ.

Logan, B. E. (2009). Exoelectrogenic bacteria that power microbial fuel cells. *Nat. Rev. Microbiol.*, 7(5), 375-381.

Logan, B. E. (2010). Scaling up microbial fuel cells and other bioelectrochemical systems. *Appl. Microbiol. Biotechnol.*, 85(6), 1665-1671.

Logan, B. E. (2012). Essential data and techniques for conducting microbial fuel cell and other types of bioelectrochemical system experiments. *ChemSusChem*, 5(6), 988-994.

Logan, B. E., Call, D., Cheng, S., Hamelers, H. V. M., Sleutels, T., Jeremiasse, A. W., and Rozendal, R. A. (2008). Microbial electrolysis cells for high yield hydrogen gas production from organic matter. *Environ. Sci. Technol.*, 42(23), 8630-8640.

Logan, B. E., Hamelers, B., Rozendal, R. A., Schrorder, U., Keller, J., Freguia, S., Aelterman, P., Verstraete, W., and Rabaey, K. (2006). Microbial fuel cells: Methodology and technology. *Environ. Sci. Technol.*, 40(17), 5181-5192.

Logan, B. E., and Patnaik, R. (1997). A gas chromatographic-based headspace biochemical oxygen demand test. *Water Environ. Res.*, 69(2), 206-214.

Logan, B. E., and Rabaey, K. (2012). Conversion of wastes into bioelectricity and chemicals by using microbial electrochemical technologies. *Science*, 337(6095), 686-690.

Logan, B. E., and Regan, J. M. (2006a). Electricity-producing bacterial communities in microbial fuel cells. *Trends Biotechnol.*, 14(12), 512-518.

Logan, B. E., and Regan, J. M. (2006b). Microbial fuel cells - Challenges and applications. *Environ. Sci. Technol.*, 40(17), 5172-5180.

Long, S., and Cudney, E. (2012). Integration of energy and environmental systems in wastewater treatment plants. *Int. J. Energy Environ.*, 3(4), 521-530.

Lovley, D. R. (2006a). Dissimilatory Fe(III)- and Mn(IV)-Reducing Prokaryotes. *The Prokaryotes*, M. Dworkin, S. Falkow, E. Rosenberg, K. H. Schleifer, and E. Stackebrandt, eds., Springer New York, 635-658.

Lovley, D. R. (2006b). Microbial fuel cells: Novel microbial physiologies and engineering approaches. *Curr. Opin. Biotechnol.*, 17(3), 327-332.

Lovley, D. R., and Phillips, E. J. P. (1988). Novel mode of microbial energy metabolism: Organic carbon oxidation coupled to dissimilatory reduction of iron or manganese. *Appl. Environ. Microbiol.*, 54(6), 1472-1480.

Lu, N., Zhou, S. G., Zhuang, L., Zhang, J. T., and Ni, J. R. (2009). Electricity generation from starch processing wastewater using microbial fuel cell technology. *Biochem. Eng. J.*, 43(3), 246-251.

Müller, K., Geng, J., and Arlt, W. (2013). Reversible vs. irreversible conversion of hydrogen: How to store energy efficiently? *Energy Technol.*, 1(1), 42-47.

Malvankar, N. S., Tuominen, M. T., and Lovley, D. R. (2012a). Biofilm conductivity is a decisive variable for high-current-density *Geobacter sulfurreducens* microbial fuel cells. *Energy Environ. Sci.*, 5(2), 5790-5797.

Malvankar, N. S., Tuominen, M. T., and Lovley, D. R. (2012b). Comment on "On electrical conductivity of microbial nanowires and biofilms" by S. M. Strycharz-Glaven, R. M. Snider, A. Guiseppi-Elie and L. M. Tender, Energy Environ. Sci., 2011, 4, 4366. *Energy Environ. Sci.*, 5(3), 6247-6249.

Malvankar, N. S., Vargas, M., Nevin, K. P., Franks, A. E., Leang, C., Kim, B. C., Inoue, K., Mester, T., Covalla, S. F., Johnson, J. P., Rotello, V. M., Tuominen, M. T., and Lovley, D. R. (2011). Tunable metallic-like conductivity in microbial nanowire networks. *Nat. Nanotechnol.*, 6(9), 573-579.

Mantzavinos, D., Burrows, D. M. P., Willey, R., Lo Biundo, G., Zhang, S. F., Livingston, A. G., and Metcalfe, I. S. (2001). Chemical treatment of an anionic surfactant wastewater: Electrospray-MS studies of intermediates and effect on aerobic biodegradability. *Water Res.*, 35(14), 3337-3344.

McCarty, P. L., Bae, J., and Kim, J. (2011). Domestic wastewater treatment as a net energy producer - Can this be achieved? *Environ. Sci. Technol.*, 45(17), 7100-7106.

Mehanna, M., Kiely, P. D., Call, D. F., and Logan, B. E. (2010). Microbial electrodialysis cell for simultaneous water desalination and hydrogen gas production. *Environ. Sci. Technol.*, 44(24), 9578-9583.

Metz, B., Davidson, O. R., Bosch, P. R., Dave, R., and Meyer, L. A. (2007). *Climate Change 2007: Mitigation of Climate Change*, Cambridge University Press, Cambridge, United Kingdom and New York, NY, USA.

Min, B., Kim, J. R., Oh, S. E., Regan, J. M., and Logan, B. E. (2005). Electricity generation from swine wastewater using microbial fuel cells. *Water Res.*, 39(20), 4961-4968.

Min, B., and Logan, B. E. (2004). Continuous electricity generation from domestic wastewater and organic substrates in a flat plate microbial fuel cell. *Environ. Sci. Technol.*, 38(21), 5809-5814.

Min, B. K., Kohler, D., and Logan, B. E. (2004). A simplified headspace biochemical oxygen demand test protocol based on oxygen measurements using a fiber optic probe. *Water Environ. Res.*, 76(1), 29-36.

Morris, J. M., and Jin, S. (2012). Enhanced biodegradation of hydrocarbon-contaminated sediments using microbial fuel cells. *J. Hazard. Mater.*, 213–214(0), 474-477.

Muga, H. E., and Mihelcic, J. R. (2008). Sustainability of wastewater treatment technologies. *J. Environ. Manage.*, 88(3), 437-447.

Mukherjee, S., Su, S. C., Panmanee, W., Irvin, R. T., Hassett, D. J., and Choi, S. (2013). A microliter-scale microbial fuel cell array for bacterial electrogenic screening. *Sensor. Actuat. A-Phys.*, 201, 532-537.

Murali, V., Ong, S. A., Ho, L. N., Wong, Y. S., and Hamidin, N. (2013). Comprehensive review and compilation of treatment for azo dyes using microbial fuel cells. *Water Environ. Res.*, 85(3), 270-277.

Nam, J. Y., Cusick, R. D., Kim, Y., and Logan, B. E. (2012). Hydrogen generation in microbial reverse-electrodialysis electrolysis cells using a heat-regenerated salt solution. *Environ. Sci. Technol.*, 46(9), 5240-5246.

O'Hayre, R., Fabian, T., Lee, S. J., and Prinz, F. B. (2003). Lateral ionic conduction in planar array fuel cells. *J. Electrochem. Soc.*, 150(4), A430-A438.

O'Riordan, J., Lucey, W. P., Barraclough, C. L., and Corps., C. G. (2008). Resources from waste: An integrated approach to managing municipal water and waste systems. *Ind. Biotechnol.*, 4(3), 238-245.

Oh, S. E., and Logan, B. E. (2005). Hydrogen and electricity production from a food processing wastewater using fermentation and microbial fuel cell technologies. *Water Res.*, 39(19), 4673-4682.

Oh, S. E., and Logan, B. E. (2006). Proton exchange membrane and electrode surface areas as factors that affect power generation in microbial fuel cells. *Appl. Microbiol. Biotechnol.*, 70(2), 162-169.

Oh, S. E., and Logan, B. E. (2007). Voltage reversal during microbial fuel cell stack operation. *J. Power Sources*, 167(1), 11-17.

Oh, S. T., Kim, J. R., Premier, G. C., Lee, T. H., Kim, C., and Sloan, W. T. (2010). Sustainable wastewater treatment: How might microbial fuel cells contribute. *Biotechnol. Adv.*, 28(6), 871-881.

Palme, U., Lundin, M., Tillman, A. M., and Molander, S. (2005). Sustainable development indicators for wastewater systems - Researchers and indicator users in a co-operative case study. *Resour. Conserv. Recy.*, 43(3), 293-311.

Pant, D., Singh, A., Van Bogaert, G., Olsen, S. I., Nigam, P. S., Diels, L., and Vanbroekhoven, K. (2012). Bioelectrochemical systems (BES) for sustainable energy production and product recovery from organic wastes and industrial wastewaters. *RSC Adv.*, 2(4), 1248-1263.

Pant, D., Van Bogaert, G., Diels, L., and Vanbroekhoven, K. (2010). A review of the substrates used in microbial fuel cells (MFCs) for sustainable energy production. *Bioresour. Technol.*, 101(6), 1533-1543.

Pavan, P., Battistoni, P., Cecchi, F., and Mata-Alvarez, J. (2000). Two-phase anaerobic digestion of source sorted OFMSW (organic fraction of municipal solid waste): Performance and kinetic study. *Water Sci. Technol.*, 41(3), 111-118.

Pham, T. H., Aelterman, P., and Verstraete, W. (2009). Bioanode performance in bioelectrochemical systems: Recent improvements and prospects. *Trends Biotechnol.*, 27(3), 168-178.

Pham, T. H., Rabaey, K., Aelterman, P., Clauwaert, P., De Schamphelaire, L., Boon, N., and Verstraete, W. (2006). Microbial fuel cells in relation to conventional anaerobic digestion technology. *Eng. Life Sci.*, 6(3), 285-292.

Pinto, R. P., Tartakovsky, B., Perrier, M., and Srinivasan, B. (2010). Optimizing treatment performance of microbial fuel cells by reactor staging. *Ind. Eng. Chem. Res.*, 49(19), 9222-9229.

Potter, M. C. (1911). Electrical effects accompanying the decomposition of organic compounds. *Proc. R. Soc. Lond., B, Biol. Sci.*, 84(571), 260-276.

Rabaey, K., and Verstraete, W. (2005). Microbial fuel cells: Novel biotechnology for energy generation. *Trends Biotechnol.*, 23(6), 291-298.

Rader, G. K., and Logan, B. E. (2010). Multi-electrode continuous flow microbial electrolysis cell for biogas production from acetate. *Int. J. Hydrogen Energy*, 35(17), 8848-8854.

Reddy, P. V. L., Kim, K. H., and Song, H. (2013). Emerging green chemical technologies for the conversion of CH_4 to value added products. *Renew. Sust. Energy Rev.*, 24, 578-585.

Ren, N. Q., Guo, W. Q., Liu, B. F., Cao, G. L., and Ding, J. (2011). Biological hydrogen production by dark fermentation: Challenges and prospects towards scaled-up production. *Curr. Opin. Biotechnol.*, 22(3), 365-370.

Richter, H., McCarthy, K., Nevin, K. P., Johnson, J. P., Rotello, V. M., and Lovley, D. R. (2008). Electricity generation by *Geobacter sulfurreducens* attached to gold electrodes. *Langmuir*, 24(8), 4376-4379.

Rozendal, R. A., Hamelers, H. V. M., Euverink, G. J. W., Metz, S. J., and Buisman, C. J. N. (2006). Principle and perspectives of hydrogen production through biocatalyzed electrolysis. *Int. J. Hydrogen Energy*, 31(12), 1632-1640.

Sajana, T. K., Ghangrekar, M. M., and Mitra, A. (2013). Application of sediment microbial fuel cell for in situ reclamation of aquaculture pond water quality. *Aquac. Eng.*, 57, 101-107.

Sawyer, C. N., McCarty, P. L., and Parkin, G. F. (2003). *Chemistry for Environmental Engineering and Science*, McGraw-Hill, New York.

Schnurer, A., Zellner, G., and Svensson, B. H. (1999). Mesophilic syntrophic acetate oxidation during methane formation in biogas reactors. *FEMS Microbiol. Ecol.*, 29(3), 249-261.

Selembo, P. A., Merrill, M. D., and Logan, B. E. (2009). The use of stainless steel and nickel alloys as low-cost cathodes in microbial electrolysis cells. *J. Power Sources*, 190(2), 271-278.

Shariati, S. R. P., Bonakdarpour, B., Zare, N., and Ashtiani, F. Z. (2011). The effect of hydraulic retention time on the performance and fouling characteristics of membrane sequencing batch reactors used for the treatment of synthetic petroleum refinery wastewater. *Bioresour. Technol.*, 102(17), 7692-7699.

Shimoyama, T., Komukai, S., Yamazawa, A., Ueno, Y., Logan, B. E., and Watanabe, K. (2008). Electricity generation from model organic wastewater in a cassette-electrode microbial fuel cell. *Appl. Microbiol. Biotechnol.*, 80(2), 325-330.

Shin, C., Lee, E., McCarty, P. L., and Bae, J. (2011). Effects of influent DO/COD ratio on the performance of an anaerobic fluidized bed reactor fed low-strength synthetic wastewater. *Bioresour. Technol.*, 102(21), 9860-9865.

Sleutels, T., Ter Heijne, A., Buisman, C. J. N., and Hamelers, H. V. M. (2012). Bioelectrochemical systems: An outlook for practical applications. *ChemSusChem*, 5(6), 1012-1019.

Song, J., Liu, L. F., Yang, F. L., Ren, N. Q., and Crittenden, J. (2013). Enhanced electricity generation by triclosan and iron anodes in the three-chambered membrane bio-chemical reactor (TC-MBCR). *Bioresour. Technol.*, 147, 409-415.

Springer, T. E., and Raistrick, I. D. (1989). Electrical-impedance of a pore wall for the flooded-agglomerate model of porous gas-diffusion electrodes. *J. Electrochem. Soc.*, 136(6), 1594-1603.

Stafford, D. A., Wheatley, B. I., and Hughes, D. E. (1980). Anaerobic Digestion. Elsevier Science.

Sterling, M. C., Lacey, R. E., Engler, C. R., and Ricke, S. C. (2001). Effects of ammonia nitrogen on H_2 and CH_4 production during anaerobic digestion of dairy cattle manure. *Bioresour. Technol.*, 77(1), 9-18.

Strycharz-Glaven, S. M., Snider, R. M., Guiseppi-Elie, A., and Tender, L. M. (2011). On the electrical conductivity of microbial nanowires and biofilms. *Energy Environ. Sci.*, 4(11), 4366-4379.

Stumm, W., and Morgan, J. J. (1996). *Aquatic Chemistry: Chemical Equilibria and Rates in Natural Waters*, John Wiley & Sons, Inc., New York.

Su, X. Y., Tian, Y., Sun, Z. C., Lu, Y. B., and Li, Z. P. (2013). Performance of a combined system of microbial fuel cell and membrane bioreactor: Wastewater treatment, sludge reduction, energy recovery and membrane fouling. *Biosens. Bioelectron.*, 49, 92-98.

Sun, M., Sheng, G. P., Mu, Z. X., Liu, X. W., Chen, Y. Z., Wang, H. L., and Yu, H. Q. (2009). Manipulating the hydrogen production from acetate in a microbial electrolysis cell-microbial fuel cell-coupled system. *J. Power Sources*, 191(2), 338-343.

Sun, M., Sheng, G. P., Zhang, L., Xia, C. R., Mu, Z. X., Liu, X. W., Wang, H. L., Yu, H. Q., Qi, R., Yu, T., and Yang, M. (2008). An MEC-MFC-coupled system for biohydrogen production from acetate. *Environ. Sci. Technol.*, 42(21), 8095-8100.

Tao, Y., Chen, Y., Wu, Y., He, Y., and Zhou, Z. (2007). High hydrogen yield from a two-step process of dark- and photo-fermentation of sucrose. *Int. J. Hydrogen Energy*, 32(2), 200-206.

Tartakovsky, B., Manuel, M. F., Wang, H., and Guiot, S. R. (2009). High rate membrane-less microbial electrolysis cell for continuous hydrogen production. *Int. J. Hydrogen Energy*, 34(2), 672-677.

Tenca, A., Cusick, R. D., Schieuano, A., Oberti, R., and Logan, B. E. (2013). Evaluation of low cost cathode materials for treatment of industrial and food processing wastewater using microbial electrolysis cells. *Int. J. Hydrogen Energy*, 38(4), 1859-1865.

Tender, L. M., Gray, S. A., Groveman, E., Lowy, D. A., Kauffman, P., Melhado, J., Tyce, R. C., Flynn, D., Petrecca, R., and Dobarro, J. (2008). The first demonstration of a microbial fuel cell as a viable power supply: Powering a meteorological buoy. *J. Power Sources*, 179(2), 571-575.

Ter Heijne, A., Liu, F., van Rijnsoever, L. S., Saakes, M., Hamelers, H. V. M., and Buisman, C. J. N. (2011). Performance of a scaled-up microbial fuel cell with iron reduction as the cathode reaction. *J. Power Sources*, 196(18), 7572-7577.

Tian, Y., Ji, C., Wang, K., and Le-Clech, P. (2014). Assessment of an anaerobic membrane bio-electrochemical reactor (AnMBER) for wastewater treatment and energy recovery. *J. Membr. Sci.*, 450, 242-248.

Tokash, J. C., and Logan, B. E. (2011). Electrochemical evaluation of molybdenum disulfide as a catalyst for hydrogen evolution in microbial electrolysis cells. *Int. J. Hydrogen Energy*, 36(16), 9439-9445.

Tsai, H. Y., Wu, C. C., Lee, C. Y., and Shih, E. P. (2009). Microbial fuel cell performance of multiwall carbon nanotubes on carbon cloth as electrodes. *J. Power Sources*, 194(1), 199-205.

Velasquez-Orta, S. B., Curtis, T. P., and Logan, B. E. (2009). Energy from algae using microbial fuel cells. *Biotechnol. Bioeng.*, 103(6), 1068-1076.

Vennard, J. K., and Street, R. L. (1982). *Elementary Fluid Mechanics*, John Wiley & Sons, New York.

Verbrugge, M. W., and Liu, P. (2005). Microstructural analysis and mathematical modeling of electric double-layer supercapacitors. *J. Electrochem. Soc.*, 152(5), D79-D87.

Verstraete, W., and Vlaeminck, S. E. (2011). ZeroWasteWater: Short-cycling of wastewater resources for sustainable cities of the future. *Int. J. Sus. Dev. World*, 18(3), 253-264.

Viero, A. F., de Melo, T. M., Torres, A. P. R., Ferreira, N. R., Sant'Anna, G. L., Borges, C. P., and Santiago, V. M. J. (2008). The effects of long-term feeding of high organic loading in a submerged membrane bioreactor treating oil refinery wastewater. *J. Membr. Sci.*, 319(1-2), 223-230.

Vijayaraghavan, K., Ahmad, D., and Lesa, R. (2006). Electrolytic treatment of beer brewery wastewater. *Ind. Eng. Chem. Res.*, 45(20), 6854-6859.

Vrubel, H., Merki, D., and Hu, X. (2012). Hydrogen evolution catalyzed by MoS_3 and MoS_2 particles. *Energy Environ. Sci.*, 5(3), 6136-6144.

Wagner, R. C., Call, D. I., and Logan, B. E. (2010). Optimal set anode potentials vary in bioelectrochemical systems. *Environ. Sci. Technol.*, 44(16), 6036-6041.

Wagner, R. C., Regan, J. M., Oh, S. E., Zuo, Y., and Logan, B. E. (2009). Hydrogen and methane production from swine wastewater using microbial electrolysis cells. *Water Res.*, 43(5), 1480-1488.

Wang, A. J., Liu, W. Z., Cheng, S. A., Xing, D. F., Zhou, J. H., and Logan, B. E. (2009). Source of methane and methods to control its formation in single chamber microbial electrolysis cells. *Int. J. Hydrogen Energy*, 34(9), 3653-3658.

Wang, A. J., Sun, D., Cao, G. L., Wang, H. Y., Ren, N. Q., Wu, W. M., and Logan, B. E. (2011a). Integrated hydrogen production process from cellulose by combining dark fermentation, microbial fuel cells, and a microbial electrolysis cell. *Bioresour. Technol.*, 102(5), 4137-4143.

Wang, B., and Han, J. I. (2009). A single chamber stackable microbial fuel cell with air cathode. *Biotechnol. Lett.*, 31(3), 387-393.

Wang, H. M., Wu, Z. C., Plaseied, A., Jenkins, P., Simpson, L., Engtrakul, C., and Ren, Z. Y. (2011b). Carbon nanotube modified air-cathodes for electricity production in microbial fuel cells. *J. Power Sources*, 196(18), 7465-7469.

Wang, H. Y., Bernarda, A., Huang, C. Y., Lee, D. J., and Chang, J. S. (2011c). Micro-sized microbial fuel cell: A mini-review. *Bioresour. Technol.*, 102(1), 235-243.

Wang, K. P., Liu, Y. W., and Chen, S. L. (2011d). Improved microbial electrocatalysis with neutral red immobilized electrode. *J. Power Sources*, 196(1), 164-168.

Wang, X., Feng, Y. J., Liu, J., Lee, H., Li, C., Li, N., and Ren, N. Q. (2010). Sequestration of CO_2 discharged from anode by algal cathode in microbial carbon capture cells (MCCs). *Biosens. Bioelectron.*, 25(12), 2639-2643.

Wang, X., Liu, J. X., Ren, N. Q., Yu, H. Q., Lee, D. J., and Guo, X. S. (2012). Assessment of multiple sustainability demands for wastewater treatment alternatives: A refined evaluation scheme and case study. *Environ. Sci. Technol.*, 46(10), 5542-5549.

Wang, Y. K., Sheng, G. P., Shi, B. J., Li, W. W., and Yu, H. Q. (2013). A novel electrochemical membrane bioreactor as a potential net energy producer for sustainable wastewater treatment. *Sci. Rep.*, 3(1864), 1-6.

Ward, A. J., Hobbs, P. J., Holliman, P. J., and Jones, D. L. (2008). Optimisation of the anaerobic digestion of agricultural resources. *Bioresour. Technol.*, 99(17), 7928-7940.

WDRs (2010). World Development Report 2010: Development and Climate Change.

WEF Bioenergy from wastewater treatment.

Wei, J. C., Liang, P., and Huang, X. (2011). Recent progress in electrodes for microbial fuel cells. *Bioresour. Technol.*, 102(20), 9335-9344.

Wen, C., Huang, X., and Qian, Y. (1999). Domestic wastewater treatment using an anaerobic bioreactor coupled with membrane filtration. *Process Biochem.*, 35(3-4), 335-340.

Wen, Q., Kong, F. Y., Ma, F., Ren, Y. M., and Pan, Z. (2011). Improved performance of air-cathode microbial fuel cell through additional Tween 80. *J. Power Sources*, 196(3), 899-904.

Wett, B., Buchauer, K., and Fimml, C. (2007). Energy self-sufficiency as a feasible concept for wastewater treatment systems. *Proc., IWA Leading Edge Technology Conference*, Singapore.

Whitchurch, C. B., Tolker-Nielsen, T., Ragas, P. C., and Mattick, J. S. (2002). Extracellular DNA required for bacterial biofilm formation. *Science*, 295(5559), 1487-1487.

Winfield, J., Ieropoulos, I., Greenman, J., and Dennis, J. (2011). Investigating the effects of fluidic connection between microbial fuel cells. *Bioprocess Biosyst. Eng.*, 34(4), 477-484.

Xia, X., Tokash, J. C., Zhang, F., Liang, P., Huang, X., and Logan, B. E. (2013). Oxygen-reducing biocathodes operating with passive oxygen transfer in microbial fuel cells. *Environ. Sci. Technol.*, 47(4), 2085-2091.

Xie, S., Liang, P., Chen, Y., Xia, X., and Huang, X. (2011). Simultaneous carbon and nitrogen removal using an oxic/anoxic-biocathode microbial fuel cells coupled system. *Bioresour. Technol.*, 102(1), 348-354.

Xie, X., Yu, G., Liu, N., Bao, Z., Criddle, C. S., and Cui, Y. (2012). Graphene-sponges as high-performance low-cost anodes for microbial fuel cells. *Energy Environ. Sci.*, 5(5), 6862-6866.

Yan, H. J., and Regan, J. M. (2013). Enhanced nitrogen removal in single-chamber microbial fuel cells with increased gas diffusion areas. *Biotechnol. Bioeng.*, 110(3), 785-791.

Yang, F., Ren, L. J., Pu, Y. P., and Logan, B. E. (2013). Electricity generation from fermented primary sludge using single-chamber air-cathode microbial fuel cells. *Bioresour. Technol.*, 128, 784-787.

Yang, X. Y., Tian, G., Jiang, N., and Su, B. L. (2012). Immobilization technology: A sustainable solution for biofuel cell design. *Energy Environ. Sci.*, 5(2), 5540-5563.

Yavuz, Y., Koparal, A. S., and Ogutveren, U. B. (2010). Treatment of petroleum refinery wastewater by electrochemical methods. *Desalination*, 258(1-3), 201-205.

Ye, D., Yang, Y., Li, J., Zhu, X., Liao, Q., Deng, B., and Chen, R. (2013). Performance of a microfluidic microbial fuel cell based on graphite electrodes. *Int. J. Hydrogen Energy*, 38(35), 15710-15715.

Yoo, R., Kim, J., McCarty, P. L., and Bae, J. (2012). Anaerobic treatment of municipal wastewater with a staged anaerobic fluidized membrane bioreactor (SAF-MBR) system. *Bioresour. Technol.*, 120, 133-139.

You, S. J., Zhao, Q. L., Jiang, J. Q., and Zhang, J. N. (2006). Treatment of domestic wastewater with simultaneous electricity generation in microbial fuel cell under continuous operation. *Chem. Biochem. Eng. Q.*, 20(4), 407-412.

Zhang, B., Zhang, L. L., Zhang, S. C., Shi, H. Z., and Cai, W. M. (2005). The influence of pH on hydrolysis and acidogenesis of kitchen wastes in two-phase anaerobic digestion. *Environ. Technol.*, 26(3), 329-339.

Zhang, F., Ahn, Y., and Logan, B. E. (2014). Treating refinery wastewaters in microbial fuel cells using separator electrode assembly or spaced electrode configurations. *Bioresour. Technol.*, 152, 46-52.

Zhang, F., Cheng, S. A., Pant, D., Van Bogaert, G., and Logan, B. E. (2009). Power generation using an activated carbon and metal mesh cathode in a microbial fuel cell. *Electrochem. Commun.*, 11(11), 2177-2179.

Zhang, F., Ge, Z., Grimaud, J., Hurst, J., and He, Z. (2013a). Improving electricity production in tubular microbial fuel cells through optimizing the anolyte flow with spiral spacers. *Bioresour. Technol.*, 134, 251-256.

Zhang, F., Ge, Z., Grimaud, J., Hurst, J., and He, Z. (2013b). In situ investigation of tubular microbial fuel cells deployed in an aeration tank at a municipal wastewater treatment plant. *Bioresour. Technol.*, 136, 316-321.

Zhang, F., Ge, Z., Grimaud, J., Hurst, J., and He, Z. (2013c). Long-term performance of liter-scale microbial fuel cells treating primary effluent installed in a municipal wastewater treatment facility. *Environ. Sci. Technol.*, 47(9), 4941-4948.

Zhang, F., Merrill, M. D., Tokash, J. C., Saito, T., Cheng, S., Hickner, M. A., and Logan, B. E. (2011a). Mesh optimization for microbial fuel cell cathodes constructed around stainless steel mesh current collectors. *J. Power Sources*, 196(3), 1097-1102.

Zhang, F., Pant, D., and Logan, B. E. (2011b). Long-term performance of activated carbon air cathodes with different diffusion layer porosities in microbial fuel cells. *Biosens. Bioelectron.*, 30(1), 49-55.

Zhang, L., Li, J., Zhu, X., Ye, D. D., and Liao, Q. (2013d). Anodic current distribution in a liter-scale microbial fuel cell with electrode arrays. *Chem. Engin. J.*, 223, 623-631.

Zhang, X. Y., Cheng, S. A., Huang, X., and Logan, B. E. (2010). The use of nylon and glass fiber filter separators with different pore sizes in air-cathode single-chamber microbial fuel cells. *Energy Environ. Sci.*, 3(5), 659-664.

Zhang, X. Y., Cheng, S. A., Liang, P., Huang, X., and Logan, B. E. (2011c). Scalable air cathode microbial fuel cells using glass fiber separators, plastic mesh supporters, and graphite fiber brush anodes. *Bioresour. Technol.*, 102(1), 372-375.

Zhao, H. Z., Zhang, Y., Zhao, B., Chang, Y. Y., and Li, Z. S. (2012). Electrochemical reduction of carbon dioxide in an MFC-MEC system with a layer-by-layer self-assembly carbon nanotube/cobalt phthalocyanine modified electrode. *Environ. Sci. Technol.*, 46(9), 5198-5204.

Zhou, M. H., He, H. H., Jin, T., and Wang, H. Y. (2012). Power generation enhancement in novel microbial carbon capture cells with immobilized *Chlorella vulgaris*. *J. Power Sources*, 214, 216-219.

Zhou, M. H., Wang, H. Y., Hassett, D. J., and Gu, T. Y. (2013). Recent advances in microbial fuel cells (MFCs) and microbial electrolysis cells (MECs) for wastewater treatment, bioenergy and bioproducts. *J. Chem.Technol. Biot.*, 88(4), 508-518.

Zhu, F., Wang, W. C., Zhang, X. Y., and Tao, G. H. (2011). Electricity generation in a membrane-less microbial fuel cell with down-flow feeding onto the cathode. *Bioresour. Technol.*, 102(15), 7324-7328.

Zhu, G. C., Onodera, T., Tandukar, M., and Pavlostathis, S. G. (2013a). Simultaneous carbon removal, denitrification and power generation in a membrane-less microbial fuel cell. *Bioresour. Technol.*, 146, 1-6.

Zhu, X., Zhang, L., Li, J., Liao, Q., and Ye, D.-d. (2013b). Performance of liter-scale microbial fuel cells with electrode arrays: Effect of array pattern. *Int. J. Hydrogen Energy*, 38(35), 15716-15722.

Zhu, X. P., Yates, M. D., and Logan, B. E. (2012). Set potential regulation reveals additional oxidation peaks of *Geobacter sulfurreducens* anodic biofilms. *Electrochem. Commun.*, 22, 116-119.

Zhuang, L., Zheng, Y., Zhou, S. G., Yuan, Y., Yuan, H. R., and Chen, Y. (2012). Scalable microbial fuel cell (MFC) stack for continuous real wastewater treatment. *Bioresour. Technol.*, 106, 82-88.

Zhuang, L., and Zhou, S. G. (2009). Substrate cross-conduction effect on the performance of serially connected microbial fuel cell stack. *Electrochem. Commun.*, 11(5), 937-940.

Appendix A

Supporting information for Chapter 3

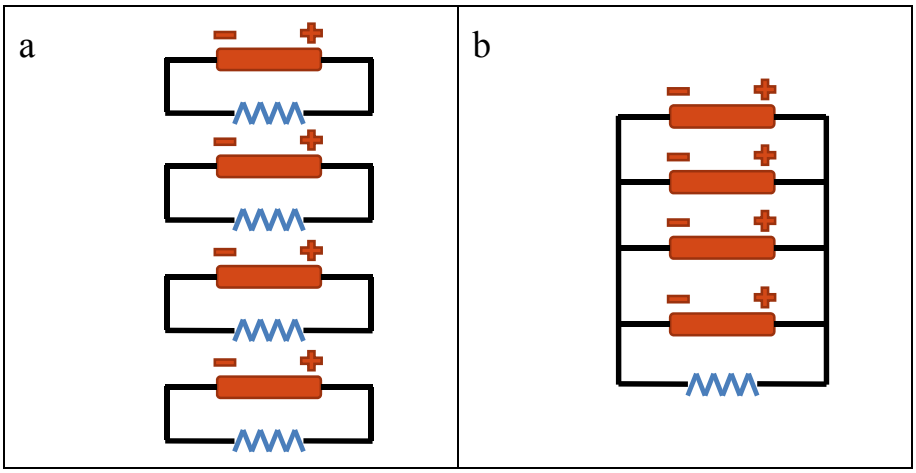

Scheme A-1 Equivalent electrical circuits for the electrode connections: (a) individual connection and (b) combined connection. The red boxes indicated the MFC reactors with the positive sign "+" for cathodes and negative sign "–" for anodes.

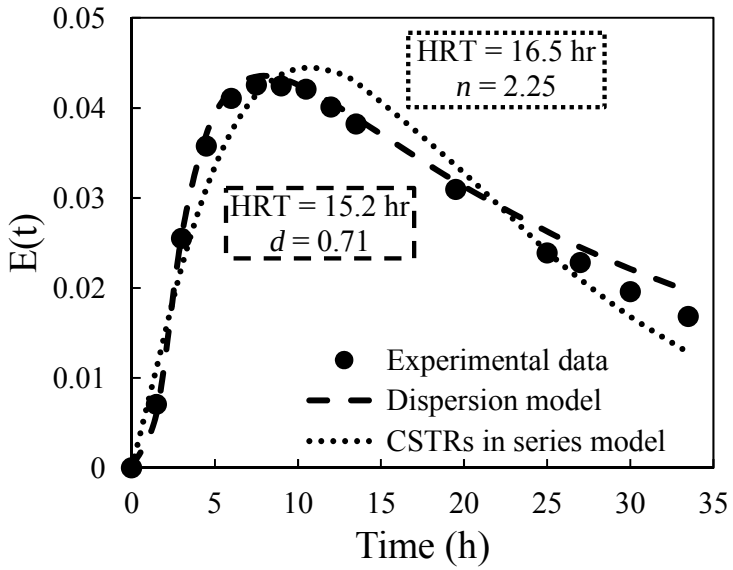

Figure A-1 Experimental data and modeling results of the tracer test, where HRT is the hydraulic retention time, *d* is the dispersion number, and *n* is the number of CSTRs in series.

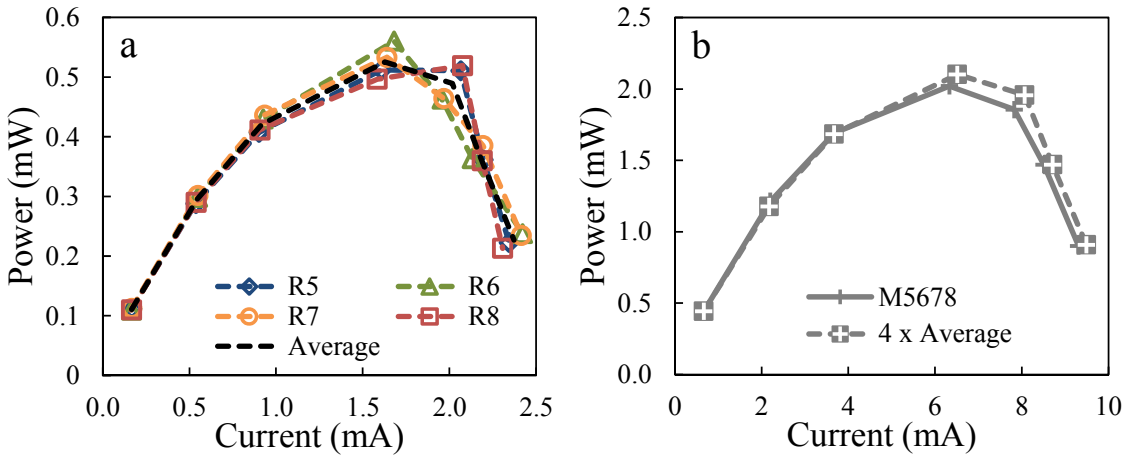

Figure A-2 Power production of the MFC reactors in fed-batch mode. (a) Individual connection showing the identical performance of the four MFC reactors (R5 to R8). (b) Combined connection where the summed power of the four individual reactors (4 × Average) compared to that of the combined reactor (M5678).

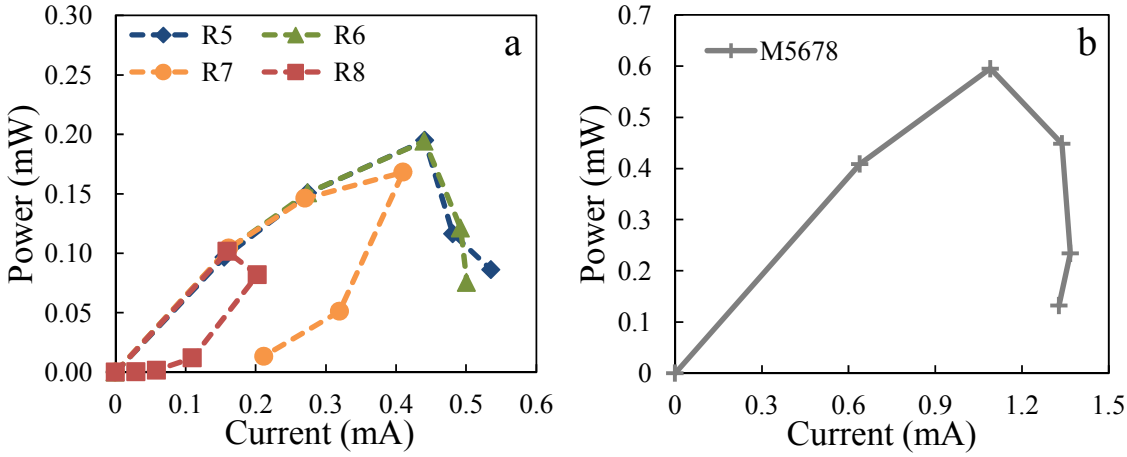

Figure A-3 Power production of the MFC reactors operated in continuous flow with the flow from R5 to R8. (a) Individual connection showing the different performance of the four MFC reactors (R5 to R8). (b) Combined connection (M5678).

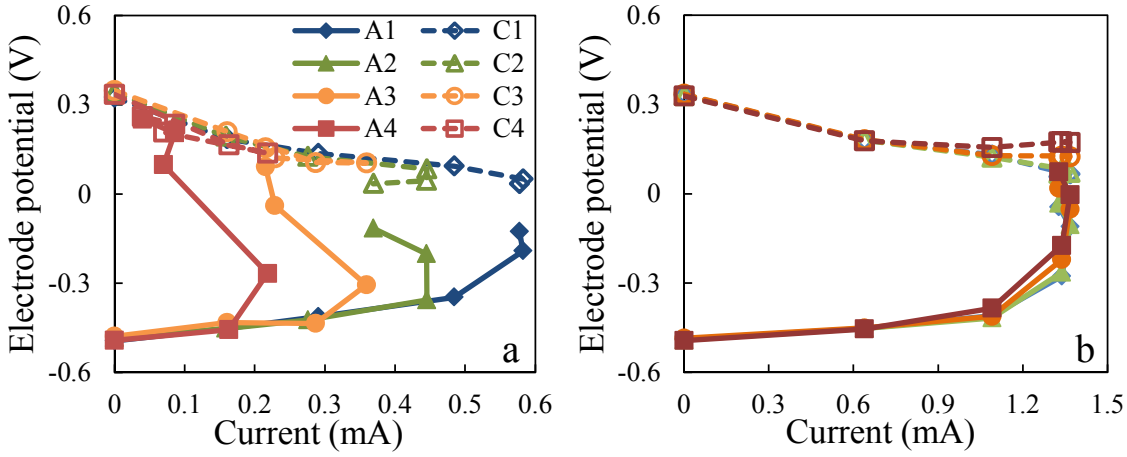

Figure A-4 Polarization curves of the MFC reactors operated in continuous flow with the flow from R1 to R4. (a) Individual connection showing the different performance of the four MFC reactors (R1 to R4). (b) Combined connection showing the potential of the individual electrodes (M1234). Letter "A" indicated the anodes and "C" the cathodes.

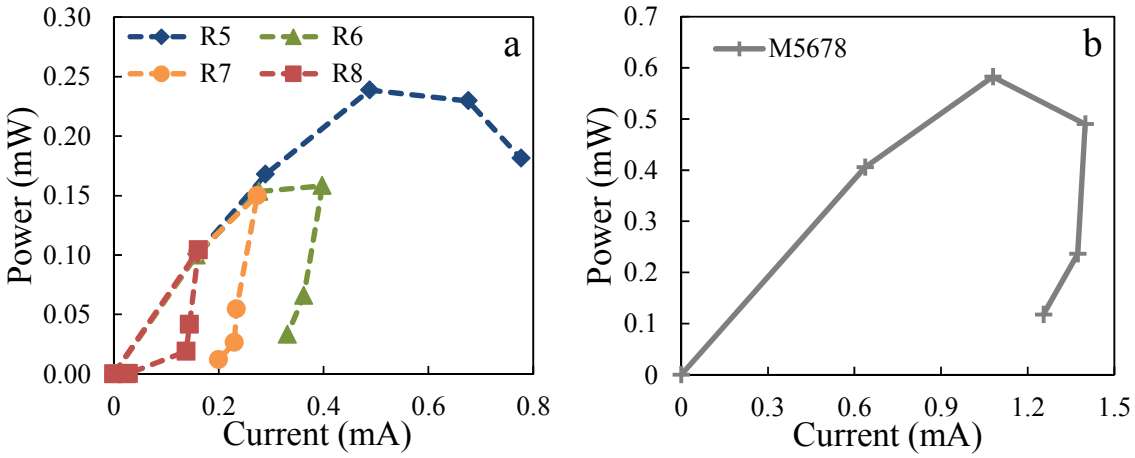

Figure A-5 Power production of the MFC reactors hydraulically connected using needles in continuous flow with the flow from R5 to R8. (a) Individual connection showing the different performance of the four MFC reactors (R5 to R8). (b) Combined connection (M5678).

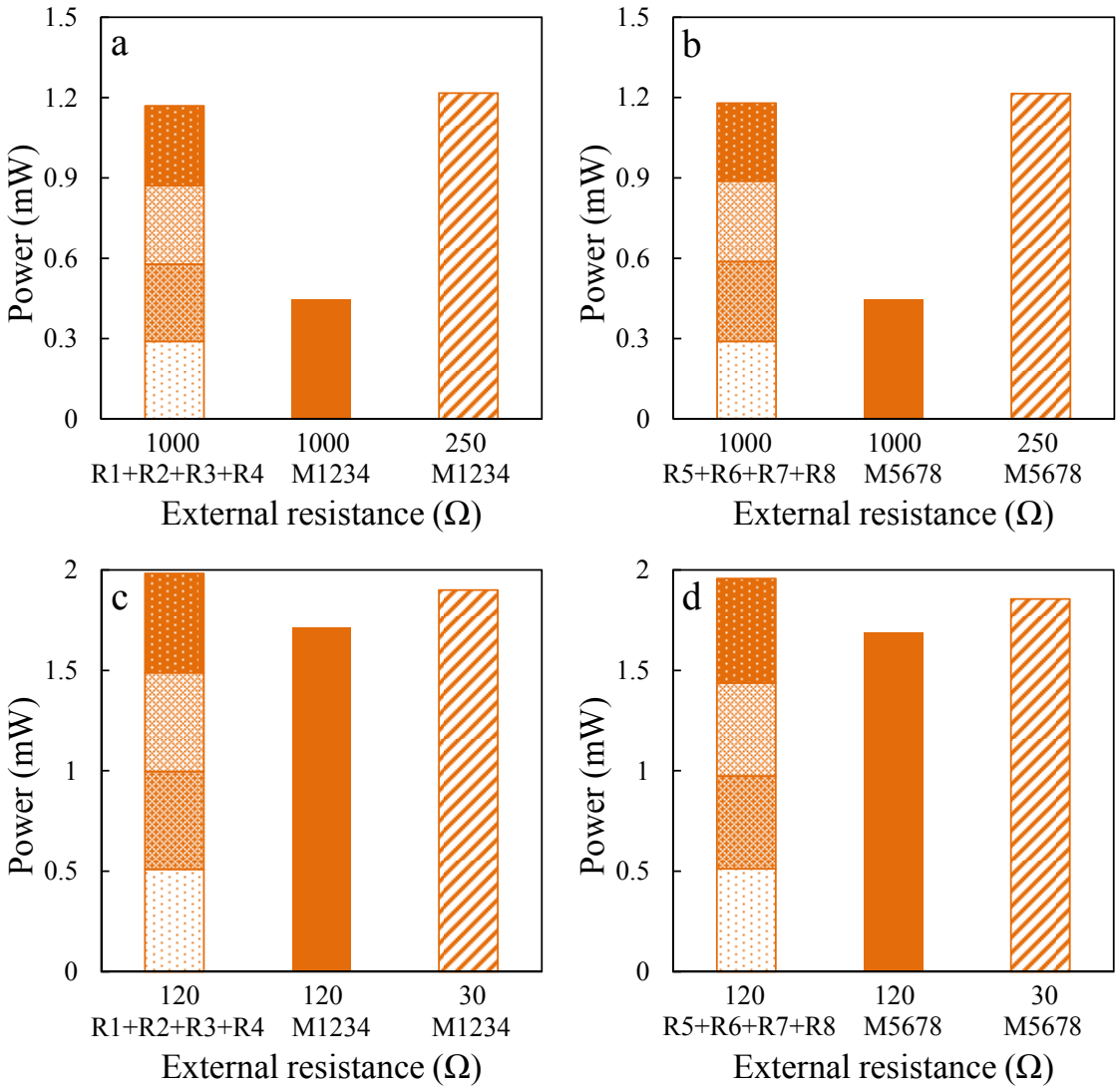

Figure A-6 Power output of the MFC reactors at individual connection (R1 to R8) and combined connection (M1234 and M5678) under different external resistances in fed-batch operation.

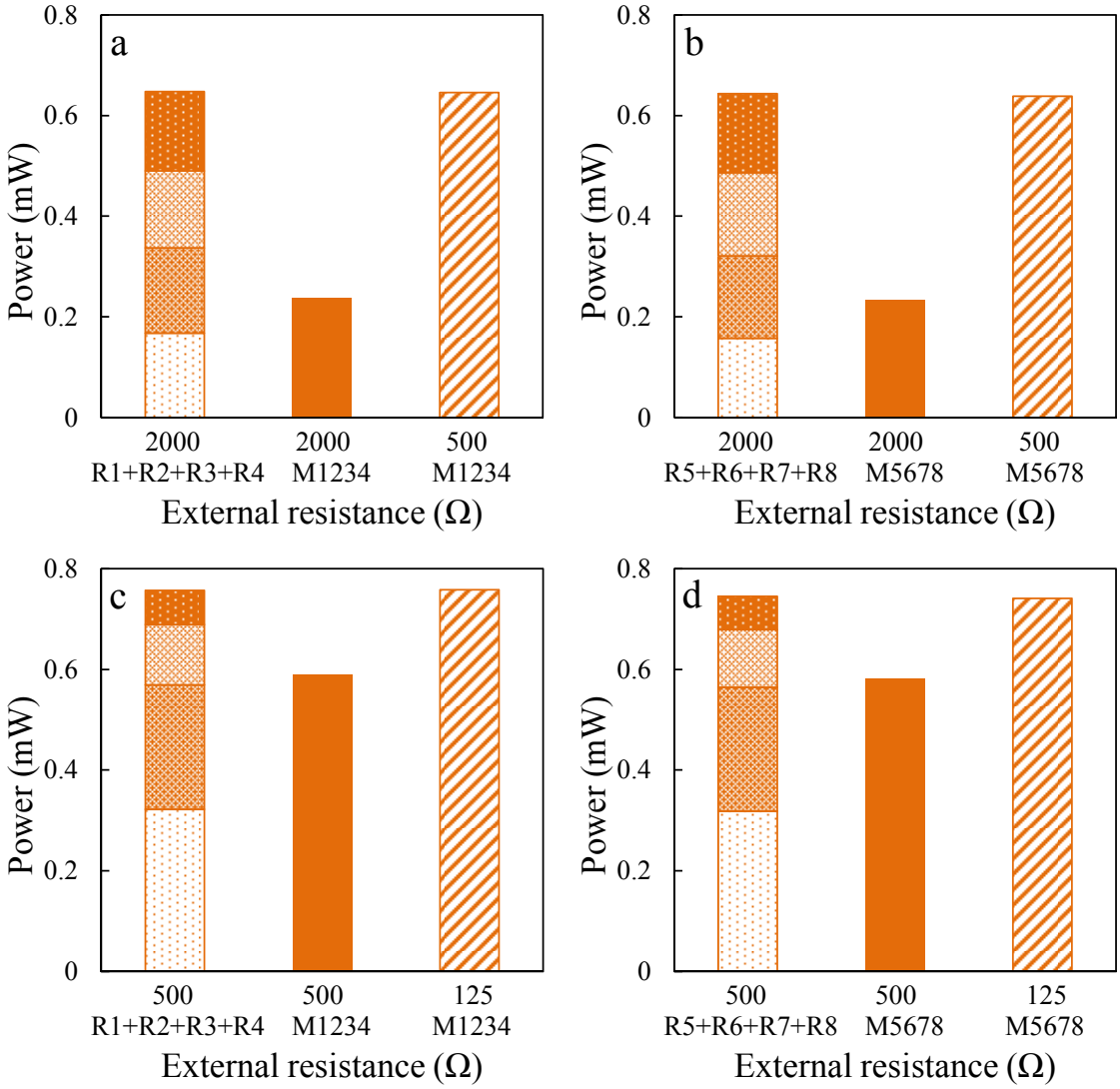

Figure A-7 Power output of the MFC reactors at individual connection (R1 to R8) and combined connection (M1234 and M5678) under different external resistances in continuous flow.

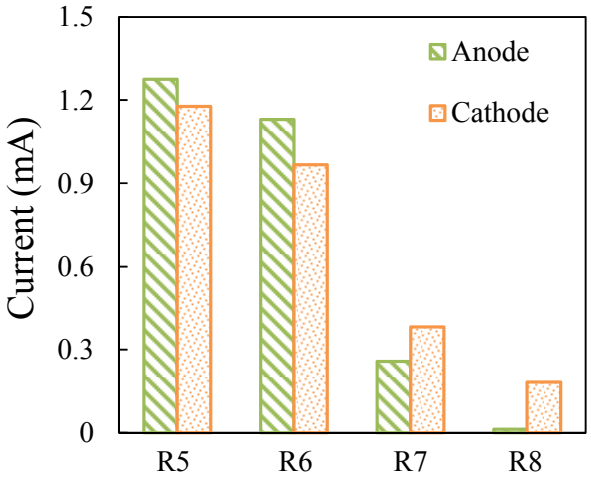

Figure A-8 Current output of the anodes and cathodes at combined connection (M5678, 125 Ω external resistance) in continuous flow.

Appendix B

Supporting information for Chapter 4

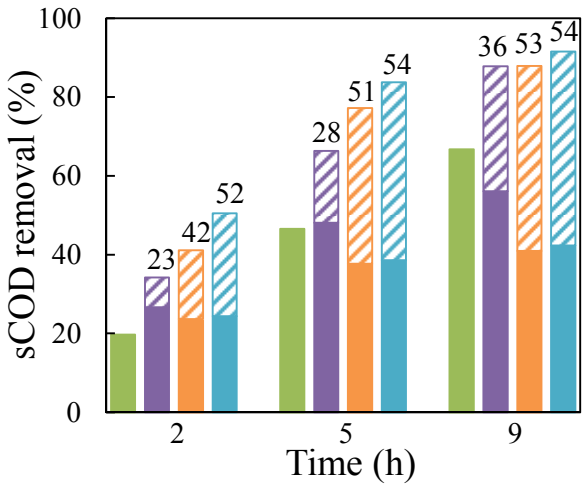

Figure B-1 sCOD removals (fraction of initial substrate concentration) and CEs over time in fed-batch cycles at different external resistances [open circuit (green), 1000 Ω (purple), 300 Ω (orange), and 100 Ω (blue)]. The shaded areas are the amount of sCOD accounted for by current, and the filled areas are that lost to oxygen leakage. The numbers above the stacked columns are the CE values.

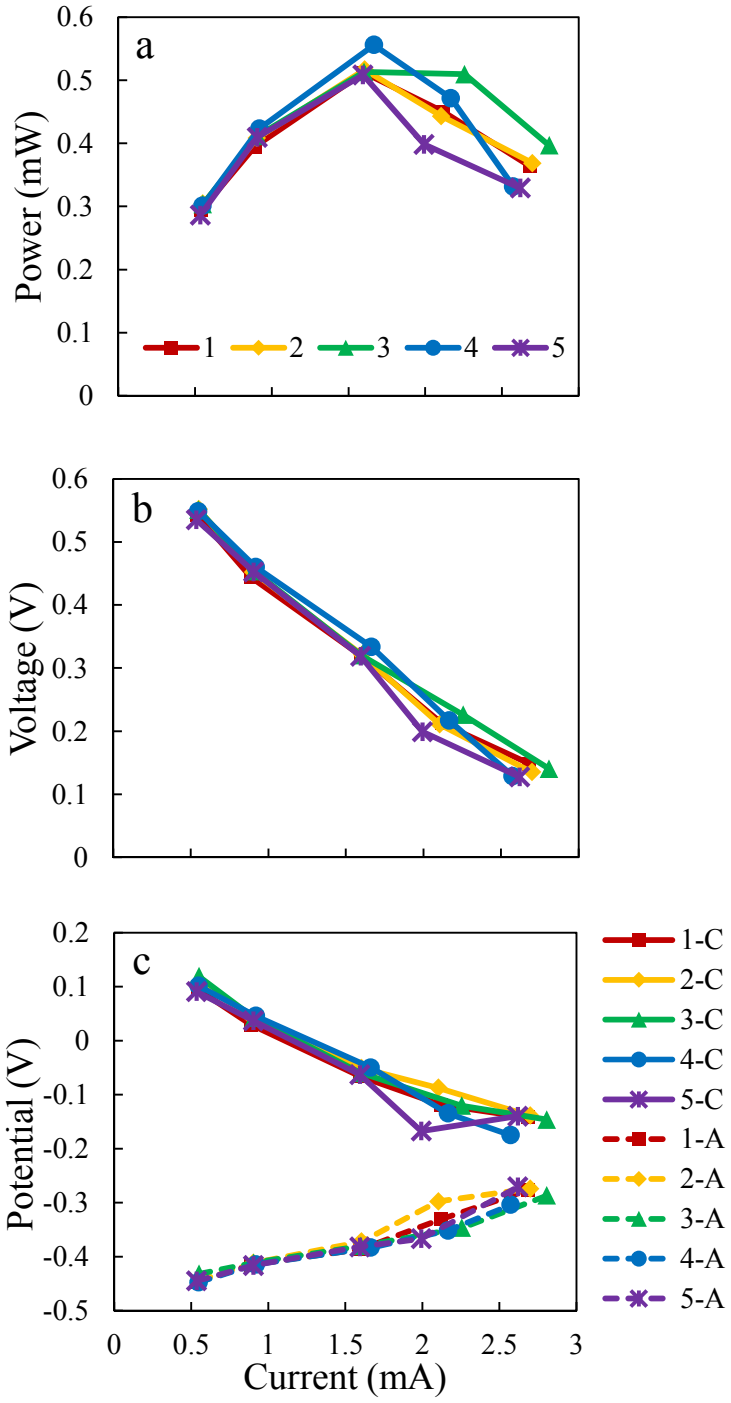

Figure B-2 Power, voltage and electrode potentials of the MFCs at different current: (a) power, (b) voltage, and (c) electrode potentials. The five duplicates were indicated by numbers "1" to "5", and in (c) the letter "C" indicated the cathodes and "A" indicated the anodes.

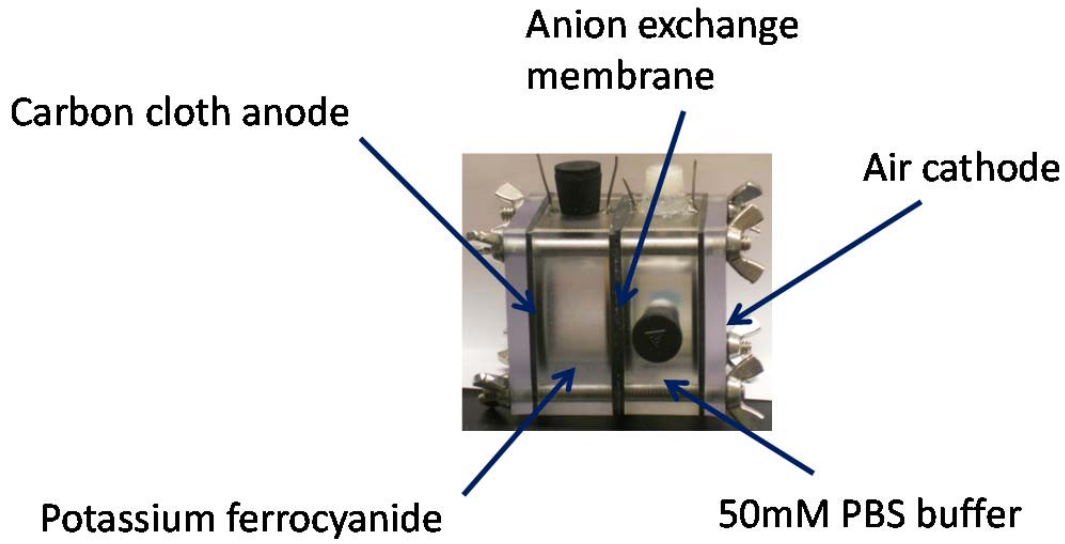

Figure B-3 Set-up of the abiotic reactor for the measurement of oxygen mass transfer coefficient of air-cathode.

B.1 Oxygen transfer calculation

In order to better understand substrate consumption by aerobic heterotrophs at open circuit compared to that with current production, we calculated the amount of oxygen that could be transferred into the bulk solution under these two different conditions based on the oxygen mass transfer coefficients measured in abiotic reactors.

With an open circuit, the oxygen mass transfer coefficient is $\boldsymbol{k} = 2.5 \times 10^{-3}$ cm/s, and assuming that the saturated oxygen concentration is $DO_s = 7.7$ mg/L and the oxygen concentration in the bulk solution is $DO = 1$ mg/L, we can get the oxygen flux as

$$J = \boldsymbol{k} \times (DO_s - DO)$$
$$= 2.5 \times 10^{-3} \text{ (cm/s)} \times (7.7 - 1) \text{ (mg/L)} = 2.5 \times 10^{-3} \text{ (cm/s)} \times 6.7 \text{ (mg/1000 cm}^3\text{)}$$
$$= 1.675 \times 10^{-5} \text{ (mg/s-cm}^2\text{)}$$

We know the cathode cross sectional area is $A = 7$ cm^2, and thus the total mass of oxygen that could be transferred into the bulk solution in $t = 9$ h is

$$m = J \times A \times t$$
$$= 1.675 \times 10^{-5} \text{ (mg/s-cm}^2\text{)} \times 7 \text{ (cm}^2\text{)} \times 9 \times 3600 \text{ (s)}$$
$$= 3.80 \text{ (mg)}$$

COD equivalent = 3.80 (mg) / 14 (mL) = 3.80 (mg) / 14×10^{-3} (L) = 271.4 (mg/L)

We know the influent COD concentration is averaged of 394.7 mg/L, and thus the percent of COD lost to oxygen leakage is therefore

271.4 (mg/L) / 394.7 (mg/L) = 68.7%

This is consistent with that measured in the open circuit tests, as we calculated that 67% of the substrate in the biotic MFCs was removed in 9 h. Thus, it is reasonable to assume that all of the substrate that removed was lost to heterotrophs using oxygen.

Similarly, we can calculate the COD lost to oxygen leakage at high current density, using the oxygen mass transfer coefficient measured when the current was 4.3 A/m^2, where $\boldsymbol{k} = 2.2 \times 10^{-3}$ cm/s, as

COD equivalent = 3.34 (mg) / 14 (mL) = 238.8 mg/L

The fraction of COD is therefore 238.80 (mg/L) / 394.7 (mg/L) = 60.5%. This is higher than the 35% calculated from the COD balance, indicating that aerobic heterotrophs could not oxidize the same amount of substrate using oxygen when there was current generation. With current generation, the faster reduction in the COD concentration reduced the rate of substrate consumed by aerobic heterotrophs as it was shown in open circuit tests that substrate removal was first-order with respect to COD concentration. Thus, a decrease in COD with current generation reduces the rate that substrate is lost to aerobic heterotrophs.

The reduction in COD lost to oxygen leakage at high current density compared to open circuit reactors is

[271.4 (mg/L) – 238.8 (mg/L)] / 271.4 (mg/L) = 32.6 (mg/L) / 271.4 (mg/L) = 12 %

Based on these calculations, it is concluded that part of the reduction in substrate consumption by aerobic heterotrophs (from 67% at open circuit to 35% at high current density) could partly be due to less oxygen transfer (12%) into the reactor, but the main reason was the faster COD depletion with current generation due to the increased consumption by exoelectrogens.

Appendix C

Supporting information for Chapter 5

C.1 Batch test on methane production

Methane production of the domestic wastewater was measured in batch test using serum bottles (165 mL, Wheaton, Millville, NJ, USA). Primary clarifier effluent (100 mL) and anaerobic sludge (1%, 20 mL) collected from the Pennsylvania State University Wastewater Treatment Plant, and 10g (wet weight) of GAC (DARCO® MRX, Norit activated carbon) was first added into the serum bottle, and then sparged with N_2 gas for 20 min. Deionized water (100 mL) was used instead of the primary effluent as a control to measure the methane production by the anaerobic sludge alone. All tests were conducted and analyzed in duplicate at ambient temperature. Biogas (200 μL samples) in the headspace of the serum bottle was sampled using gastight syringes (250 μL; Hamilton Samplelock Syringe), and analyzed using gas chromatographs (SRI Instruments) for H_2, N_2, and CH_4 every day until the methane content reached plateau after 7 days.

The initial tCOD of the domestic wastewater was 247 ± 7 mg/L. At the end of the batch test, the methane produced by the domestic wastewater was 3.9 ± 0.2 mL, compensated by subtracting the methane production measured (1.9 ± 0.2 mg/L) in the control bottles from that in the test bottles (5.9 ± 0.3 mg/L). Thus, the methane production of the domestic wastewater was

$$\frac{3.9\ (mL\ \text{methane})}{247\ (mg\ \text{COD}/L)\times 0.1\ (L)} = 0.16\ (mL\ \text{methane})/(mg\ \text{COD})$$

C.2 Theoretical methane production in AFMBR

The tCOD of the influent into AFMBR was 107 ± 10 mg/L. With the assumption that 50% of the tCOD could be converted into methane, the amount of methane that theoretically could be produced in the AFMBR was

$$107\ (mg\ \text{COD}/L)\times 50\%\times 0.16\ (mL\ \text{methane})/(mg\ \text{COD}) = 8.6\ (mL\ \text{methane})$$

Appendix D

Supporting information for Chapter 6

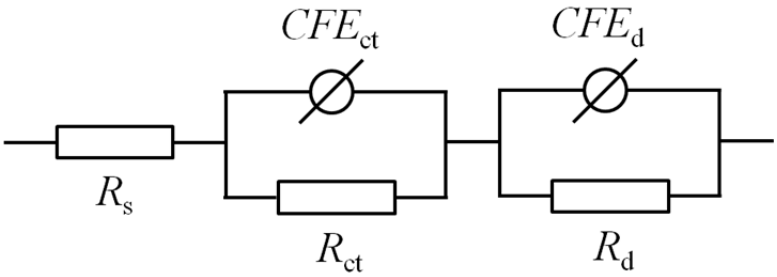

Scheme D-1 Equivalent circuit of the electrochemical half cell for EIS. The electrode process was presented by an ohmic drop resistance with the symbol R_s, a charge transfer element (charge transfer resistance R_{ct} inparallel with CPE_{ct}), and a diffusion element (diffusion resistance R_d in parallel with CPE_d) in series.

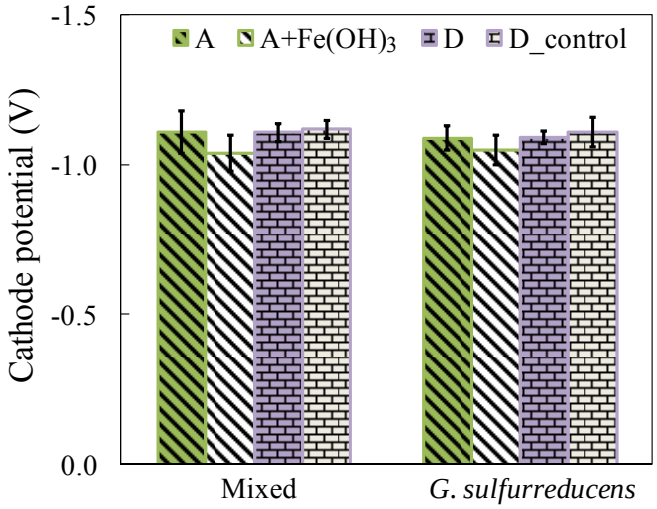

Figure D-1 Cathode potentials of mixed cultures and *G. sulfurreducens* in BBS-30 medium before and after addition of $Fe(OH)_3$. The letters A indicate results for duplicate reactors in the presence and absence of $Fe(OH)_3$, and D remained as duplicate controls (with no chemical addition).

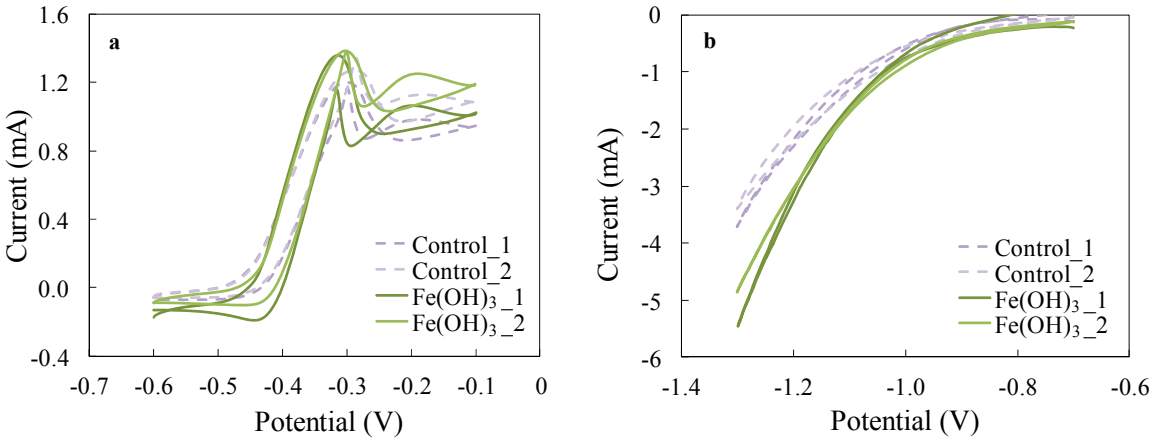

Figure D-2 Cyclic voltammetry curve of control electrodes and those with $Fe(OH)_3$ addition: (a) anode and (b) cathode.

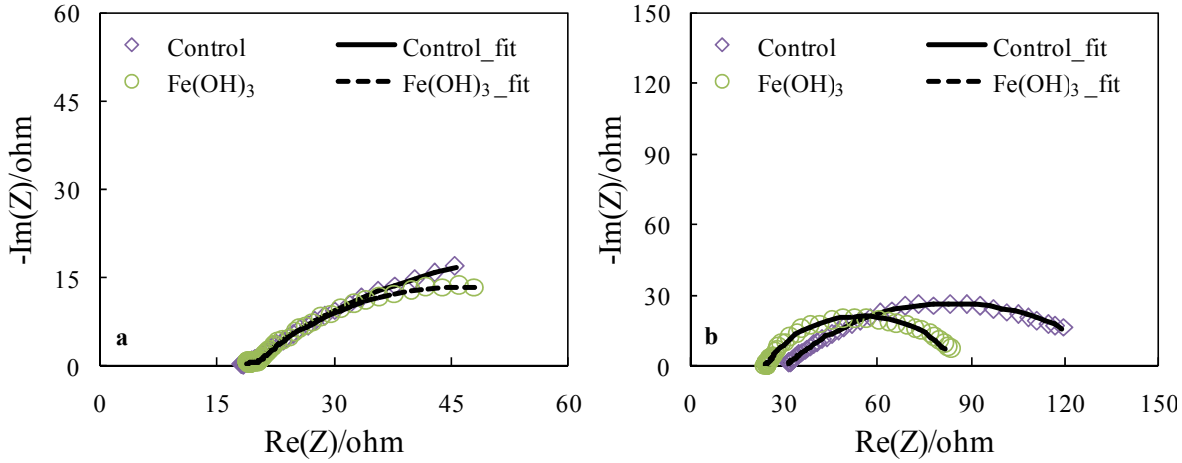

Figure D-3 EIS plots and fits of the control reactors and those with $Fe(OH)_3$ addition.

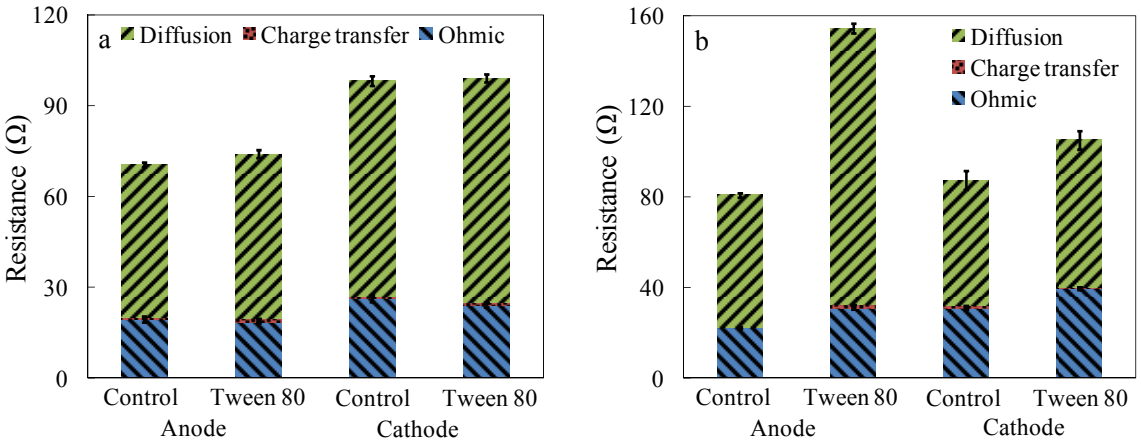

Figure D-4 Electrode resistance of mixed culture and *G. sulfurreducens* in 30 mM BBS medium with increased Tween 80 concentration. (a) mixed culture and (b) *G. sulfurreducens*.

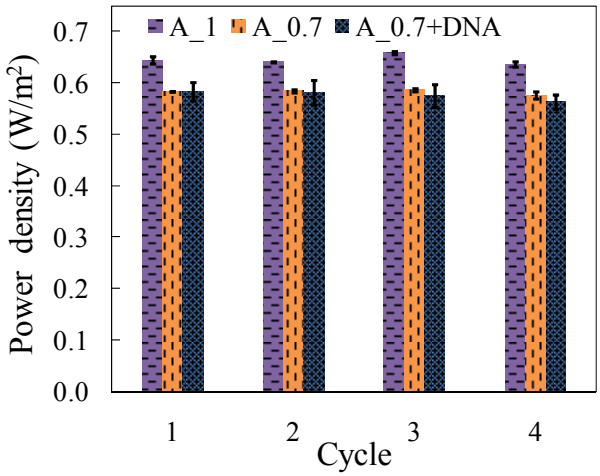

Figure D-5 Power density at 250 Ω external resistance of MFCs with 1 cm^2 anode, 0.7 cm^2 anode, and 0.7 cm^2 anode modified by DNA.

Table D-1 Conductivity and pH of mixed culture mini-MECs fed BBS-30 medium after chemical factors addition at beginning and end of the cycle.

	Conductivity (mS/cm)		**pH**	
	Beginning	End	Beginning	End
Control	7.75 ± 0.05	8.10 ± 0.10	7.48 ± 0.12	7.80 ± 0.15
$Fe(OH)_3$	7.34 ± 0.05	7.90 ± 0.07	7.33 ± 0.10	7.92 ± 0.05
Tween80	7.23 ± 0.04	7.91 ± 0.04	7.32 ± 0.09	7.73 ± 0.11
DNA	7.30 ± 0.08	8.03 ± 0.03	7.32 ± 0.11	7.83 ± 0.10

Appendix E

Supporting information for Chapter 7

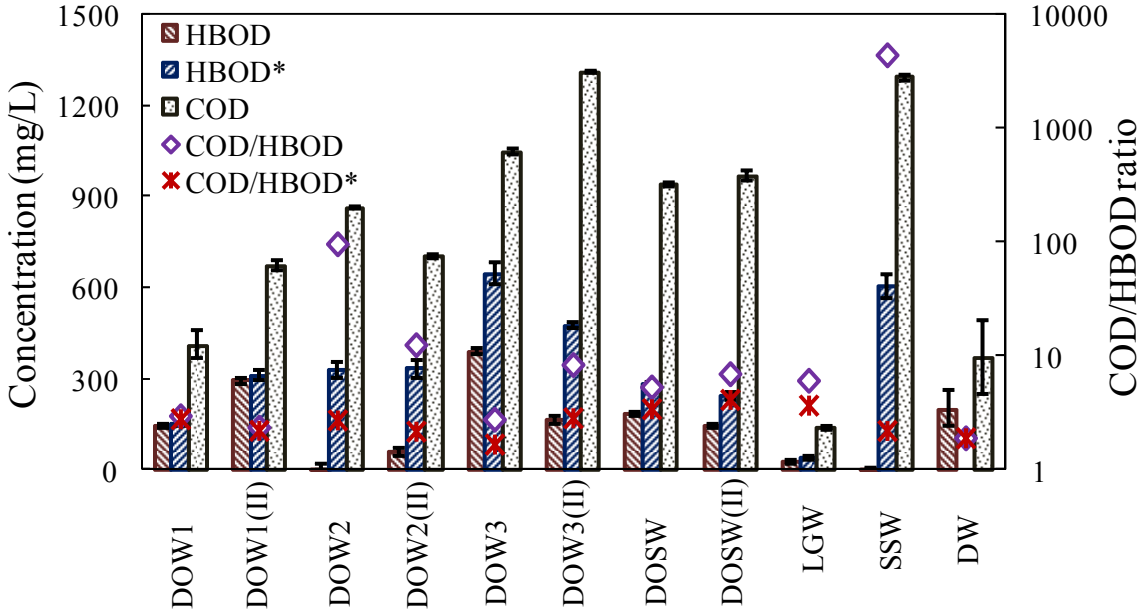

Figure E-1 COD, HBOD, HBOD*, the ratio of COD/HBOD, and the ratio of COD/HBOD* for the different refinery wastewater samples, with domestic wastewater (DW) as a positive control.

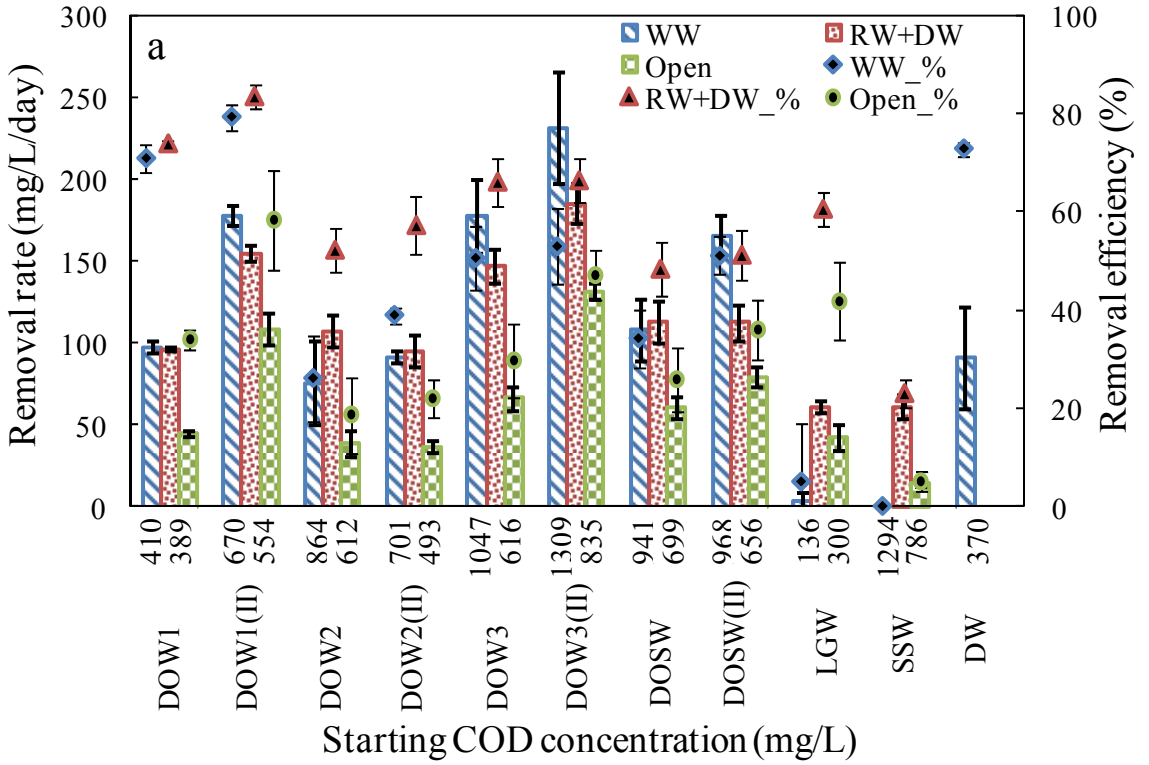
a
WW
RW+DW
Open
WW_%
RW+DW_%
Open_%
Removal rate (mg/L/day)
Removal efficiency (%)
300
250
200
150
100
50
0
100
80
60
40
20
0
410 389
670 554
864 612
701 493
1047 616
1309 835
941 699
968 656
136 300
1294 786
370
DOW1
DOW1(II)
DOW2
DOW2(II)
DOW3
DOW3(II)
DOSW
DOSW(II)
LGW
SSW
DW
Starting COD concentration (mg/L)

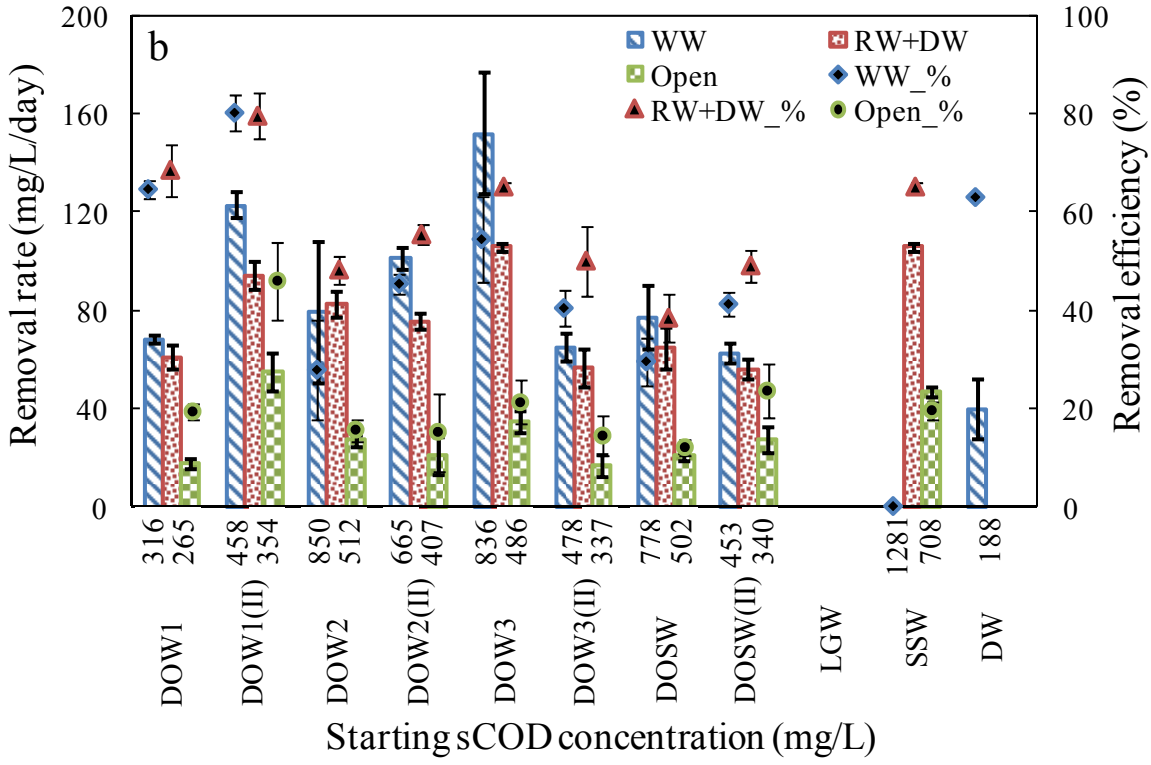
b
WW
RW+DW
Open
WW_%
RW+DW_%
Open_%
Removal rate (mg/L/day)
Removal efficiency (%)
200
160
120
80
40
0
100
80
60
40
20
0
316 265
458 354
850 512
665 407
836 486
478 337
778 502
453 340
1281 708
188
DOW1
DOW1(II)
DOW2
DOW2(II)
DOW3
DOW3(II)
DOSW
DOSW(II)
LGW
SSW
DW
Starting sCOD concentration (mg/L)

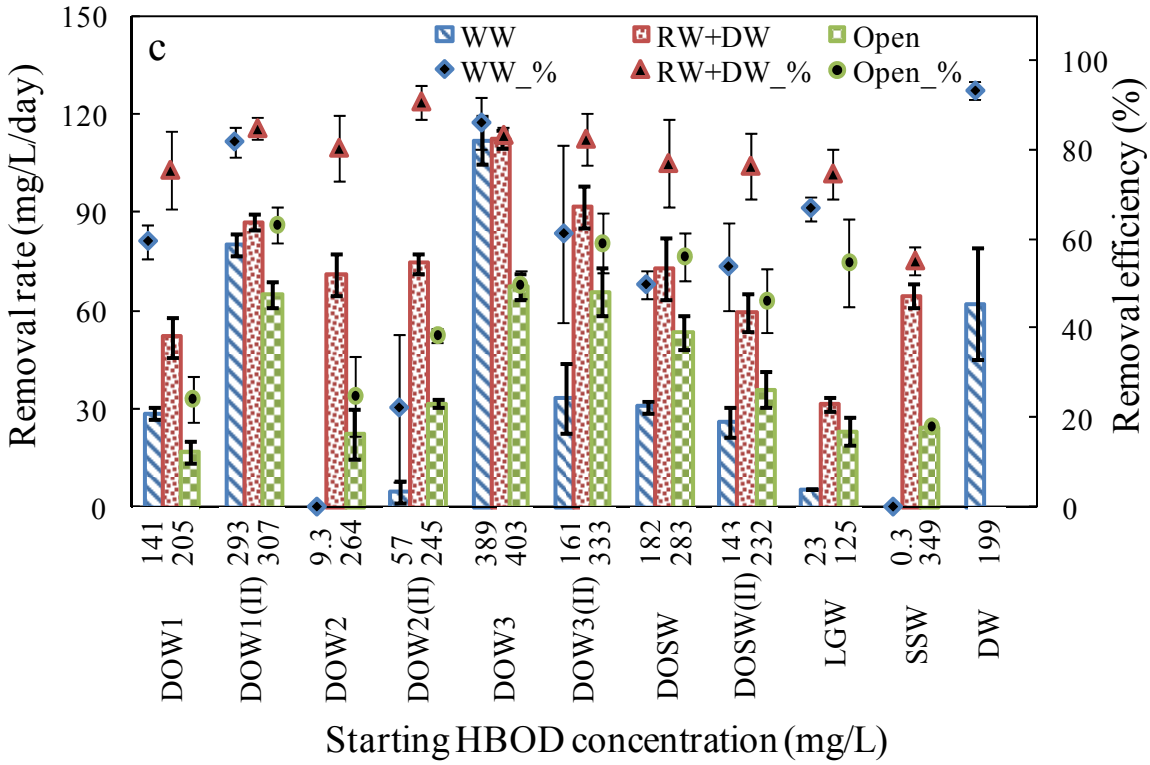

Figure E-2 COD, sCOD, and HBOD removal rate and removal efficiency of the refinery and domestic wastewaters (WW), the 50:50 refinery wastewater + demostic wastewater mixture (RW+DW), and the open circuit 50:50 mixture (Open): (a) COD; (b) sCOD; (c) HBOD.

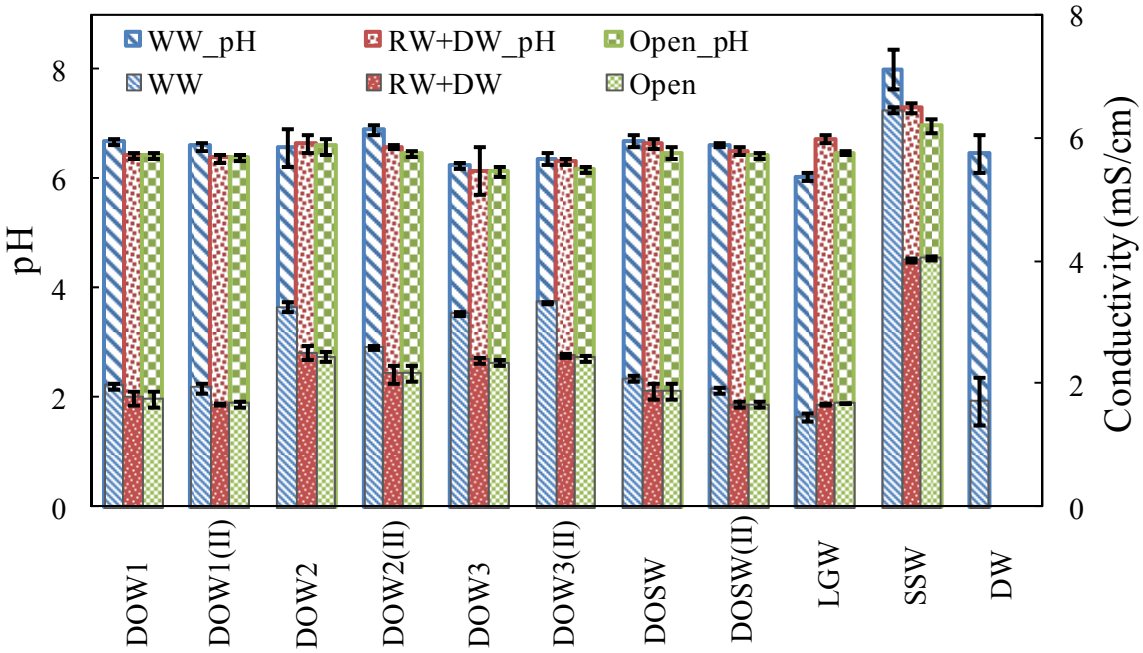

Figure E-3 Solution pH and conductivity of the refinery and the domestic wastewaters (WW), the 50:50 refinery wastewater + domestic wastewater mixture (RW+DW), and the open circuit 50:50 mixture (Open) after treatment in MECs.

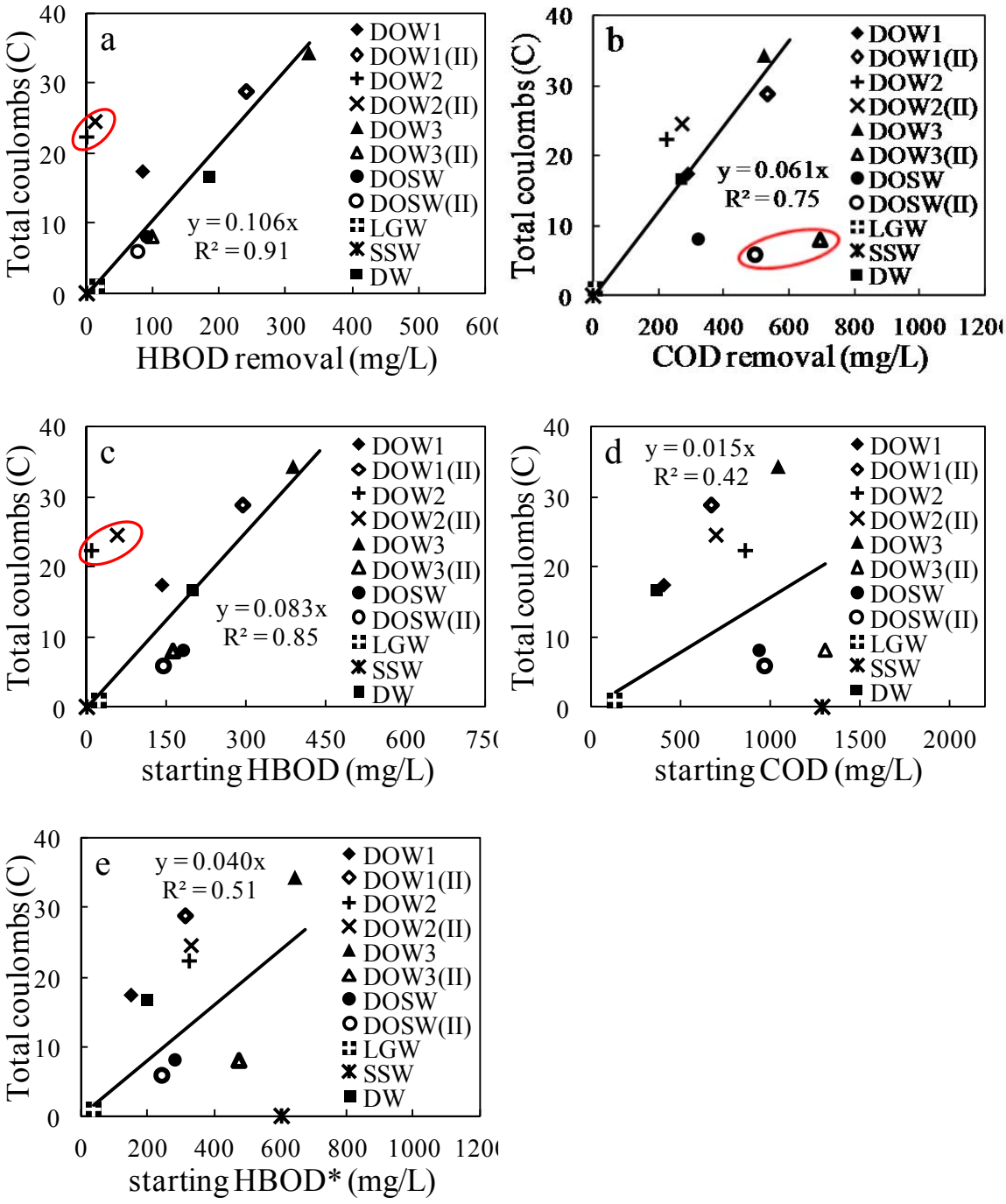

Figure E-4 Correlation between electricity production and oxygen demand. Regressions were made without those points in the red circles.

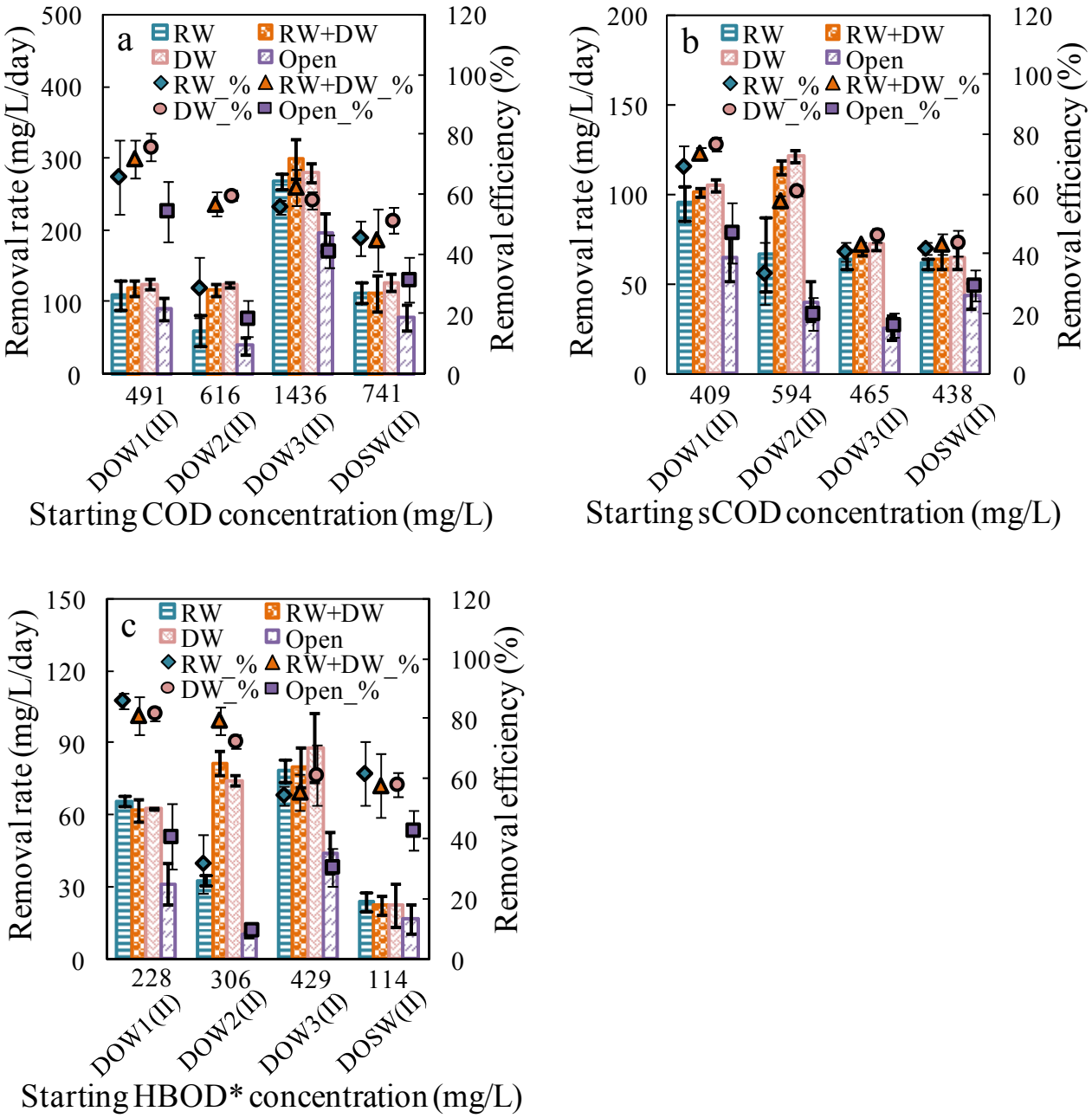

Figure E-5 COD, sCOD and HBOD removal rate and removal efficiency of the refinery wastewater samples during cross-feeding test: (a) COD; (b) sCOD; (c) HBOD. MEC reactors acclimated to only refinery wastewater was indicated by "RW", to the 50:50 refinery wastewater + domestic wastewater mixture by "RW+DW", and to only domestic wastewater by "DW". The open circuit 50:50 mixture was also fed full strength refinery wastewater and kept open circuit (Open).

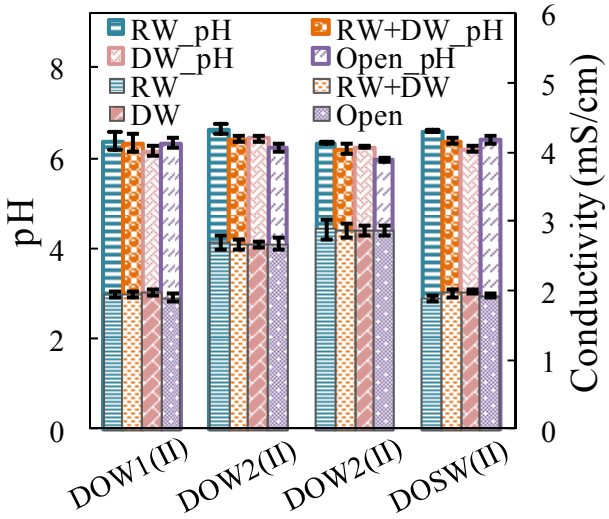

Figure E-6 Solution pH and conductivity of the refinery wastewater samples after treatment in MECs during cross-feeding test. MEC reactors acclimated to only refinery wastewater was indicated by "RW", to the 50:50 refinery wastewater + domestic wastewater mixture by "RW+DW", and to only domestic wastewater by "DW". The open circuit 50:50 mixture was also fed full strength refinery wastewater and kept open circuit (Open).

Table E-1 Abbreviation for the different refinery wastewater samples.

Sample acronym	Sample description
DOW1	De-oiled wastewater, combined source, facility 1
DOW1(II)	De-oiled wastewater, combined source, facility 1, re-sample
DOW2	De-oiled wastewater, combined source, facility 2
DOW2(II)	De-oiled wastewater, combined source, facility 2, re-sample
DOW3	De-oiled wastewater, combined source, facility 3
DOW3(II)	De-oiled wastewater, combined source, facility 3, re-sample
DOSW	De-oiled oily sewer wastewater, facility 4
DOSW(II)	De-oiled oily sewer wastewater, facility 4, re-sample
LGW	Lagoon water with algae, facility 2
SSW	Stripped sour water, facility 3

Table E-2 pH and conductivity of the refinery and the domestic wastewater samples.

Sample name	pH ± SD	Conductivity ± SD (mS/cm)
DOW1	7.4 ± 0.1	2.0 ± 0.2
DOW1(II)	8.4 ± 0.1	1.8 ± 0.1
DOW2	8.3 ± 0.2	3.1 ± 0.1
DOW2(II)	8.9 ± 0.1	2.6 ± 0.1
DOW3	7.9 ± 0.1	3.2 ± 0.1
DOW3(II)	8.8 ± 0.1	3.2 ± 0.1
DOSW	7.5 ± 0.1	2.0 ± 0.1
DOSW(II)	7.2 ± 0.1	1.9 ± 0.1
LGW	7.4 ± 0.1	1.3 ± 0.1
SSW	10.5 ± 0.2	6.4 ± 0.1
DW	7.3~7.8	1.3~1.9

LIJIAO REN

Education

B.S. Environmental Engineering (Honors School), Harbin Institute of Technology, China, 2004 – 2008

M.S. Environmental Science and Engineering, Harbin Institute of Technology, China, 2008 – 2010

Ph.D. Environmental Engineering, The Pennsylvania State University, USA, 2010 – present

Journal publications

Wang, X. H., Zhang, K., Ren, N. Q., Li, N., and **Ren, L. J.** (**2009**). Monitoring microbial community structure and succession of an A/O SBR during start-up period using PCR-DGGE. *J. Environ. Sci. (China)*, 21(2), 223-228.

Ren, L. J., Wu, Y. N., Ren, N. Q., Zhang, K. and Xing, D. F. (**2010**). Microbial community structure in an integrated A/O reactor treating diluted livestock wastewater during start-up period. *J. Environ. Sci. (China)*, 22(5), 656-662.

Ren, L. J., Tokash, J. C., Regan, J. M. and Logan, B. E. (**2012**). Current generation in microbial electrolysis cells with addition of amorphous ferric hydroxide, Tween 80, or DNA. *Int. J. Hydrogen Energy*, 37(22), 16943-16950.

Yang, F., **Ren, L. J.,** Yu, Y. P., and Logan, B. E. (**2012**). Electricity generation from fermented primary sludge using single-chamber air-cathode microbial fuel cells. *Biores. Technol.*, 128, 784-787.

Ren, L. J., Siegert, M., Ivanov, I., Pisciotta, J. M., and Logan, B. E. (**2013**). Treatability studies on different refinery wastewaters using high-throughput microbial electrolysis (MEC) reactors. *Biores. Technol.*, 136: 322-328.

Ivanov, I., **Ren, L. J.,** Siegert, M., and Logan, B. E. (**2013**). A quantitative method to evaluate microbial electrolysis cell effectiveness for energy recovery and wastewater treatment. *Int. J. Hydrogen Energy*, 38(30), 13135-14220.

Conference presentations

Simultaneous wastewater treatment and odor elimination in an integrated A/O reactor. Oral presentation in the 5th Annual International Symposium on Environment, Athens, Greece, May, **2010**.

Increased current density and self-assembled porous structure on cathode in microbial electrolysis cells by ferric hydroxide addition. Poster in the 15th Annual Environmental Chemistry Student Symposium, The Pennsylvania State University, University Park, PA, USA, April, **2012**.

Current generation in microbial electrolysis cells with addition of amorphous ferric hydroxide, Tween 80, or DNA. Poster in NA-ISMET meeting, Cornell University, Ithaca, NY, USA, October, **2012**.

Treatability studies on different refinery wastewaters using high-throughput microbial electrolysis cell (MEC) reactors. Oral presentation in the 2th International Symposium on Bioremediation and Sustainable Environmental Technologies, Jacksonville, FL, USA, June, **2013**.